

Computational Studies of Bond-Site Percolation

By

Léonard NDUWAYO

Submitted in partial fulfillment of the requirements for the degree of Doctor of
Philosophy in Physics in the School of Physics at the University of KwaZulu-Natal
Pietermaritzburg

June, 2007

Dedication

To my wife

Ida Ntawundora,

To my daughters

Ella Monia Ndemesha, Ornella Marina Girimbere, Snella Sabrina Akimana and
Diella Marthe Gateka.

Their moral support and constant patience contributed to my success.

Acknowledgments

I would like solemnly to acknowledge the incredible support of my supervisors Prof Nithaya Chetty and Dr Robert Lindebaum. They have generously supported me not only academically but also financially with a warm and personal humanism.

I thank Prof Roger Raab who kindly read and commented on my draft thesis. He showed me some key guidelines for scientific writing (for instance, 3 Cs - correct, concise, and clear).

I would also like to express my huge, sincere, and warm thanks to my wife Ida who successfully managed family matters while I was away from home.

I am indebted to the numerous people (compatriots, friends, colleagues, staff and students of UKZNP, Emaphethelweni Dominican brethren, etc.), whom I have met in South Africa (SA), for their tireless assistance in various aspects. They helped to make my student life in Pietermaritzburg much easier and friendlier, and SA has progressively become my second home.

To all people who wrote me e-mails, thank you for your wonderful moral support and understanding.

Last, but not least, I acknowledge the financial support for my studies from the Government of Burundi.

Declaration

I declare that this thesis is a result of my own research, except where specially indicated, and has not been submitted in any form for any other degree or diploma of examination to any other university.

Léonard Nduwayo

Signed:

Date:

We hereby certify that this statement is correct.

Prof Nithaya Chetty

Supervisor

Signed:

Date:

Dr Robert Lindebaum

Supervisor

Signed:

Date:

Abstract

Percolation theory enters in various areas of research including critical phenomena and phase transitions. Bond-site percolation is a generalization of pure percolation motivated by the fact that bond-site is close to many physical realities. This work relies on a numerical study of percolation in lattices. A lattice is a regular pattern of sites also known as nodes or vertices connected by bonds also known as links or edges. Sites may be occupied or unoccupied, where the concentration p_s is the fraction of occupied sites. The quantity p_b is the fraction of open bonds. A cluster is a set of occupied sites connected by opened bonds.

The bond-site percolation problem is formulated as follows: we consider an infinite lattice whose sites and bonds are at random or correlated and either allowed or forbidden with probabilities p_s and p_b that any site and any bond are occupied and open respectively. If those probabilities are small, there appears a sprinkling of isolated clusters each consisting of occupied sites connected by open bonds surrounded by numerous unoccupied sites. As the probabilities increase, reaching critical values above which there is an infinitely large cluster, then percolation is taking place. This means that one can cross the entire lattice by going successively from one occupied site connected by a opened bond to a neighbouring occupied site. The sudden onset of a spanning cluster happens at particular values of p_s and p_b , called the critical concentrations.

Quantities related to cluster configuration (mean cluster and correlation length) and individual cluster structure (size and gyration radius of clusters) are determined and compared for different models. In our studies, the Monte Carlo approach is applied while some authors used series expansion and renormalization group methods.

The contribution of this work is the application of models in which the probability of opening a bond depends on the occupancy of sites. Compared with models in which probabilities of opening bonds are uncorrelated with the occupancy of sites, in the suppressed bond-site percolation, the higher site occupancy is needed to reach percolation. The approach of suppressed bond-site percolation is extended by considering direction of percolation along bonds (directed suppressed bond-site percolation).

Fundamental results for models of suppressed bond-site percolation and directed suppressed bond-site percolation are the numerical determination of phase boundary between the percolating and non-percolating regions. Also, it appears that the spanning cluster around critical concentration is independent on models. This is an intrinsic property of a system.

Contents

Dedication	i
Acknowledgments	ii
Declaration	iv
Abstract	v
Contents	vii
List of Tables	ix
List of Figures	xii
1 Introduction	1
1.1 Definitions	1
1.2 Applications	4
1.3 Bond-site percolation	6
1.4 Directed percolation	7
1.5 Invasion percolation	9
1.6 Delimitation and context of the present work	9
2 Bond percolation	13
2.1 Reference systems	13

2.2	Size and mean cluster size	17
2.3	Gyration radius	20
2.4	Correlation length	22
2.5	Concluding remarks	26
3	Bond-site percolation	28
3.1	Partition of (p_s, p_b) plane	28
3.2	Size and mean cluster size	31
3.3	Gyration radius and correlation length	32
4	Suppressed bond-site percolation	40
4.1	Models	41
4.2	Partition of the (p_s, p_b) plane	42
4.3	Size and mean cluster size	46
4.4	Gyration radius and correlation length	48
4.5	Comparison of results of models with those of standard bond percolation	51
5	Directed suppressed bond-site percolation	63
5.1	Models and partition of the (p_s, p_b) plane	64
5.2	Size and mean cluster size	67
5.3	Gyration radius and correlation length	69
6	Conclusions	84
	Appendix	88
	References	98
	Résumé	99
	Summary in French	100

List of Tables

2.1	Lattice properties	16
2.2	Values of p_{bc} for pure bond percolation	19
3.1	Values of p_{sc} for pure site percolation	29
3.2	Numerical values of p_{bc} for various values of p_s	30
3.3	Values of parameters of the curve of the best fit a and b	30
4.1	Model 1: Numerical values of p_{bc} for various values of p_s	44
4.2	Model 2: Numerical values of p_{bc} for various values of p_s	45
4.3	Model 1: Values of the coefficients a_i for curves of best fit	45
4.4	Model 2: Values of the coefficients b_i for curves of best fit	47
5.1	Model 1: Numerical values of p_{bc} for various values of p_s for $\gamma = 0.85$, $\alpha = 1$	66
5.2	Model 2: Numerical values of p_{bc} for various values of p_s	67

List of Figures

2.1	Lattices and reference axes	14
2.2	Cluster distribution in sizes	18
2.3	Mean cluster size	19
2.4	Variation of S_s with p_b	21
2.5	Variation of S_b with p_b	22
2.6	Cluster distribution in gyration radii around critical concentration . .	23
2.7	Comparison between ξ_s and ξ_b	24
2.8	Variation of ξ_s with p_b	25
2.9	Variation of ξ_b with p_b	26
2.10	Cluster distribution in gyration radii for the case of square lattices . .	27
3.1	Variation of p_{bc} versus p_s	32
3.2	Cluster distribution in sizes for 75% site occupation	33
3.3	Mean cluster size S_s for 75% site occupation	34
3.4	Mean cluster size S_b for 75% site occupation	35
3.5	Cluster distribution in gyration radii around critical concentration for 75% site occupation	36
3.6	Comparison between ξ_s and ξ_b for 75% site occupation	37
3.7	Variation of ξ_s as function of p_b for 75% site occupation	38
3.8	Variation of ξ_b as function of p_b for 75% site occupation	39
4.1	Representations of the two models	43

4.2	Variation of p_{bc} versus p_s	46
4.3	Critical curves in model 1 for three values of α : Case of square lattice	47
4.4	Critical curves in model 2 for three values of β : Case of triangular lattice	48
4.5	Model 1: Cluster distribution in sizes around critical concentration .	49
4.6	Model 2: Cluster distribution in sizes around critical concentration .	50
4.7	Model 1: Mean cluster size S_s	51
4.8	Model 1: Mean cluster size S_b	52
4.9	Model 2: Mean cluster size S_s	53
4.10	Model 2: Mean cluster size S_b	54
4.11	Model 1: Cluster distribution in gyration radii	55
4.12	Model 2: Cluster distribution in gyration radii	56
4.13	Model 1: Comparison between ξ_s and ξ_b	57
4.14	Model 2: Comparison between ξ_s and ξ_b	58
4.15	Model 1: Variation of ξ_s with p_b	59
4.16	Model 2: Variation of ξ_s with p_b	60
4.17	Model 1: Variation of ξ_b with p_b	61
4.18	Model 2: Variation of ξ_b with p_b	62
5.1	Variation of p_{bc} versus p_s for three values of γ	68
5.2	Variation of p_{bc} versus p_s in models 1 and 2 for $\gamma = 0.85$. Solid curve is model 1, dashed curve is model 2	69
5.3	Model 1: Cluster distribution in sizes	70
5.4	Model 2: Cluster distribution in sizes	71
5.5	Model 1: Mean cluster size S_s	72
5.6	Model 1: Mean cluster size S_b	73
5.7	Model 2: Mean cluster size S_s	74

5.8	Model 2: Mean cluster size S_b	75
5.9	Model 1: Cluster distribution in gyration radii around critical concentration	76
5.10	Model 2: Cluster distribution in gyration radii around critical concentration	77
5.11	Model 1: Comparison between ξ_s and ξ_b	78
5.12	Model 2: Comparison between ξ_s and ξ_b	79
5.13	Model 1: Variation of ξ_s with p_b	80
5.14	Model 2: Variation of ξ_s with p_b	81
5.15	Model 1: Variation of ξ_b with p_b	82
5.16	Model 2: Variation of ξ_b with p_b	83

Chapter 1

Introduction

In the following sections, general considerations about percolation theory are presented and basic notions of the applications are developed. The outline of the work developed in this thesis is also sketched.

1.1 Definitions

In general, percolation theory is a simple geometric description of a phase transition. A phase transition is defined as a phenomenon where a system shows a qualitative change while one defined parameter is modified gradually[1, 2]. Actually, criticality is observed in a subset of systems showing phase transitions, as in studies of diffusion, conductivity in composite materials, spread of forest fires and diseases[3], etc. The fundamental difference between percolation theory and other phase transition modes is the absence of a Hamiltonian in the former. The theory is based mainly on probabilistic assumptions[4].

In critical phenomena, there are many concepts and ideas which should be developed. Systems show second-order phase transitions. By a second-order phase

transition, one understands that a system continuously approaches a new state and some response functions of the system become unbounded. Quantities may either vanish or diverge as the transition point is approached[5]. Percolation problems present a similar situation to that of phase transitions. In both cases, critical exponents and scaling laws are defined. Critical exponents that are linked to critical behaviour of a second-order phase transition depend on fundamental parameters like Euclidean dimensions, symmetries and potential range parameters such as the strength of an interaction in a given system[6].

Originally, percolation was defined as a process of displacement and filtering of fluids through porous materials[7]. Broadbent introduced the theory of percolation as a branch of statistical physics in 1954 while he was modelling masks for protecting mine workers from toxins contained in coal. The masks were formed by a tube in which granular particles of carbon were packed together. By the effect of pressure on the particles, the porosity of the medium changed. Breathing through the masks was made easier when a proportion of pores was opened[8].

An analogy to the percolation theory would be illustrated by a regular pattern or lattice on which sites (described in the literature also as vertices or nodes) and bonds (also named links or edges) between sites play a key role[9]. In the following chapters we will use the terms lattice, site and bond. Two types of percolation (site percolation and bond percolation) and their hybrid (bond-site percolation) are the most studied in percolation systems.

Site percolation, also called Bernoulli percolation[10], uses lattice vertices as entities occupied with a given probability p_s while bond percolation considers lattice edges opened with a probability p_b . The structure and the size of clusters depend

on the values of p_s , and p_b . Clusters are defined as occupied sites connected by open bonds. Two occupied sites belong to the same cluster if there is between the two a path of nearest neighbour occupied sites connected by opened bonds. The key aspect of percolation arises with the emergence of an infinite cluster corresponding to the minimum concentration of occupied sites and open bonds. The minimum value of the probability for this to happen is named the threshold probability or critical probability and determines a second-order phase transition[11]. The critical probability depends on the geometry and dimension of lattice, and the nature of percolation[12]. The behaviour of percolation systems near the threshold contains singularities, which are similar to those of systems under thermodynamic phase transitions[13].

For the finite samples of lattices which we consider in our numerical studies, the percolating cluster is a cluster that connects one side of the system to the opposite side[14]. This cluster can extend from the top to the bottom or from the right to the left of the lattice. The size of a cluster is defined as a measure involving both the number of bonds and sites[15].

Zallen formulated percolation theory by associating a non-geometric property (a state) with each of the sites (vertices) or bonds of a regular periodic geometric lattice[1]. Here bonds are connections between sites limited to pairs of sites which are nearest neighbours. The non-geometric property is assumed to have only two exclusive values as likely as a site is occupied or empty while a bond is either opened or closed.

Pure percolation refers to site percolation (or bond percolation) corresponding to values of p_s (or p_b) varying from 0 to 1, while p_b (or p_s) is maintained at the value of 1.

1.2 Applications

The concept of percolation occurs in many different contexts. It has been applied in the domain of physical chemistry[16, 17], computer programming, mining engineering, solid state physics and theoretical physics to describe systems essentially involving a mixture of exclusive states [18].

Kirkpatrick applied percolation theory to study the role of the percolation threshold in hopping conduction and thus to provide a macroscopic theory in conductivity[3]. Electrons were treated as a fluid subject to electrostatic constraints.

Nakanishi and Stanley established an analogy between thermodynamic functions and an equation of state for percolation[19]. They confirmed the scaling hypothesis for the two-dimensional bond percolation problem by using a Monte Carlo method. Thus the Gibbs free energy corresponds to the mean number of finite clusters per site, while the analogue of the spontaneous magnetization in a ferromagnet is the probability that an occupied site belongs to the percolating (infinite) cluster. In this analogy, the isothermal susceptibility is associated with the mean number of sites contained in a finite cluster[20].

Percolation models were successful in simulation of multi-fragmentation reactions[21]. Fragmentation is described by distributing a set of sites, each of which represents a nucleon on a three-dimensional lattice with bonds inbetween sites. Some lattice bonds are broken. Remaining bonds connecting clusters are identified with fragments of the reaction and the bond-breaking probability is associated with the

excitation energy per nucleon.

Percolation theory explains and models a wide range of phenomena in basic sciences and industry, as discussed in the book by Sahimi in 1994 [22]. It is effective in the prediction and improvement in the production of natural gas and oil wells. The flow of electricity through random networks of resistors, the chromatography in chemistry and the formation of a crack in ceramics constitute examples where percolation theory is applied[23]. This theory is useful for predicting evolution in biological and ecological systems[24]. Goldenberg and his co-authors applied the theory to the diffusion of innovation in economic and social systems [25]. This theory has also been applied to random elastic central-force networks to obtain an understanding of the geometrical aspects of elasticity when the focal interest is on rigidity[26]. Kikuchi developed a method of approximations which allows the study of the percolation problem for non-interacting and interacting systems[27].

Katori used percolation transitions to construct a theory of non-equilibrium statistical mechanics. By considering the discrete time version of contact processes, he developed a representation on the spatio-temporal plane of a given parameter[28]. Contact process is an approach describing steady-state properties in a range of desorption rates involving interactions[29].

Vidal-Beaudet and Charpentier studied the effects of loading on intrinsic permeability of urban soils using percolation theory[30], in terms of which they were able to explain the variation of porosity. The loading of soils acts on flow paths because during the compression the number of pores per unit area decreases. Urban soils can be designed in different ways to improve their physical properties, such as permeability.

Percolation theory allows one to study dynamical systems which exhibit a phase transition around a critical limit. Subsequently, it is essential to define the order parameter associated with each transition. For example, the magnetic field and the temperature are determinants for macroscopic effects of superconductivity and superfluidity. Liquid helium acquires frictionless super-flow properties as its temperature is decreased. In a similar way, superconducting materials are capable of carrying resistanceless current once they are cooled below a critical temperature[31].

1.3 Bond-site percolation

Bond-site percolation is a generalization of the pure percolation that has been developed in many studies where bond percolation (site percolation) is analysed by assuming that sites (bonds) are occupied (opened) with probability 1 [32, 33]. The generalization is motivated by the fact that bond-site percolation more closely describes physical reality. It has been applied to treat the gelation of polymers[34, 35], and anti-ferromagnetic and ferromagnetic interactions[36]. In the statistical description of condensation and cross-linking of linear polymers, open bonds, occupied sites, and empty sites can represent chemical bonds, monomers, and solvent molecules respectively. This description predicts interactions between particles (solvents and monomers) in the system by including effects of van der Waals interactions and bonding energy[37, 38]. Hammersley and Welsh used bond-site percolation to model the spreading of disease in a biological population where sites and bonds represent susceptibility and infectability of individuals [39].

The basic idea in our algorithm is to create sample lattices by occupying randomly

a percentage of sites, to which bond percolation is then applied. A bond can only be added if it connects the two nearest sites which are already occupied. Systematically these sites are identified by a cluster to which they belong. Once a bond establishes a bridge between two different clusters, a recursive subroutine is used to relabel the cluster with fewer sites. Bond-site percolation systems are treated under two categories – the uncorrelated and correlated ones.

Uncorrelated bond-site percolation handles randomly occupied sites and randomly opened bonds which connect these sites[40]. Consequently there is no relationship between p_s and p_b . During site (bond) percolation, the number of opened (occupied) bonds (sites) is fixed and these are randomly distributed on the lattice. This is similar to the canonical statistical ensemble where the number of particles is fixed [41, 42].

In correlated bond-site percolation, p_s and p_b are related with local or global values depending on which short-range or global-range correlation model is used[43]. This correlation induces changes in critical concentrations and the order of transition of its corresponding uncorrelated model. In the models (seen in Chapters 4 and 5), p_s is fixed to generate configurations of occupied sites. Then, p_b becomes a specific parameter for each model. The minimum requirement is that a bond is opened between two nearest occupied sites.

1.4 Directed percolation

In this model, bonds are classified according to the properties with which one is dealing. They can be considered as diodes, resistors or conductors. The terminology of

directed percolation (DP) refers to the flow of information in a particular direction [44, 45, 46]. Here information has the sense of direction of connectivity[47]. Thus, a given bond has two opposite directions corresponding to two types of connectivity between bonds.

There is an analogy between DP and spatiotemporal intermittency(STI). STI may be loosely described as patches of ordered and disordered states fluctuating randomly in space and time [48, 49]. DP is a process modelled by a probabilistic cellular automation with two states associated with laminar and chaotic patches in the case of STI. One of the features of DP is the presence of an absorbing state corresponding to a laminar state. Its role is to prevent the nucleation of chaotic domains within the laminar state. The fraction of chaotic domains increases greatly near criticality.

DP is relevant in explaining many interesting topics such as Reggeon field theory, population dynamics, epidemics, forest fires, catalysis, galactic evolution, branching Markov processes that occur in biology and irreversible chemical reactions, diffusion and conduction in systems under an external bias [50, 51]. Gingl and his co-authors suggested the biased-percolation form of DP for studying the degradation and noise properties of electronic devices[52]. During the simulation of DP, where phenomena of breaking, recombination, and absorption are observed[53], it requires a prior definition of an activation probability p .

DP is a dynamic process with an absorbing state where p is the order parameter. A small p corresponds to a stationary state, whereas a large p means an active phase – “*a system which refuses to die*” [54, 55]. Dynamical particle systems, which involve extinction-survival phase transitions, belong to an universal percolation class defined by critical exponents.

1.5 Invasion percolation

In 1983, Wilkinson and Willemsen developed invasion percolation(IP) by analysing a fluid transportation process [56]. In a medium, the network of pores and throats is viewed as a regular lattice in which sites and bonds between sites stand respectively for pores and throats. IP introduces the modelling of the slow immiscible displacement of a wetting fluid by a non-wetting one in a porous medium.

A network is initially filled by a fluid, named the defender, that needs to be displaced. A displacing fluid, known as the invader, is injected and moves the defender. Two situations are possible [57, 58]. On the one hand, the defender is incompressible. This leads to a situation where a blob of the defender fluid can be trapped by the invader. On the other hand, the defender is compressible. It means that a blob can be penetrated by the invader. Thus IP describes the behaviour of an interface between an invading fluid and a defending fluid through a porous medium. Shepard and his co-authors used IP to characterise paths and domain walls in disorder media [59, 60]. They also simulated the Ising model at the critical temperature, finding that IP is a model which exhibits a self-organised criticality [61]. Compared to standard percolation, IP has the advantage of describing dynamical evolution.

1.6 Delimitation and context of the present work

This thesis is an extension of a previous MSc study. Algorithms inspired by that of Newman and Ziff[42] are used. A set of percolation states is created by adding sites or bonds one by one to a lattice starting with an empty one. The fundamental steps in our algorithm were firstly to list, in meaningful order, sites and bonds by

giving them a label. Secondly, at the j^{th} step of the algorithm, a site (bond) was chosen randomly from the list of unoccupied(unopened) sites(bonds). Lastly, the site (bond) is then occupied (opened) and its label is swapped with the j^{th} label in the list. Each occupied (opened) site (bond) belongs to a cluster. The use of recursive subroutines allowed the characterisation of the clusters.

In [62] we considered lattices in 2-dimensions (honeycomb, square and triangular lattices), and determined numerically the cluster-number scaling function (f in (1.1) below) related to the size distribution proposed by Stauffer [63] as

$$n_s(p) = s^{-\tau} f[(p - p_c)s^\sigma]. \quad (1.1)$$

Here p and p_c are, respectively, the probability of occupying (opening) sites (bonds) and the critical probability in case of pure percolation, and $n_s(p)$ is the number of clusters of size s per lattice site (or lattice bond). The critical exponents τ and σ were determined numerically from which $f(z)$ with $z = (p - p_c)s^\sigma$ was found. The calculated values of p_c were consistent with those reported in the literature[64]. We found that, for a fixed value of s , $f(z)$ has a maximum for a value of p below p_c , and vanishes as p approaches its extreme values 0 and 1. This universal behaviour of $f(z)$ had also been noted. Concepts of scaling and universality are useful for understanding the behaviour of the percolation transition at the critical point[65].

The present work employed a set of codes written in Fortran 90. A dual-AMD-processor PC having 3.7 GB of RAM and running at 2.8 GHz per processor was used to produce our data. In our codes we used a random number generator found on the website <http://www.math.keio.ac.jp/matsumoto/emt.html> coded in C by Takuji Nishimura and Makoto Matsumoto, and converted into Fortran by Josi Rui Faustino de Sousa. The Monte Carlo approach was used to treat bond-site percolation as-

pects instead of series expansion or renormalisation group methods applied by many authors [66, 67, 68, 69]

In Chapter 2, we analyse the case of pure bond percolation where in each cluster we take simultaneously into account the number of sites and bonds. Quantities of interest in this work are cluster size, mean cluster size, radius of gyration, and correlation length. Here the probability of occupying a site becomes 1 when it is an end of an opened bond.

Chapter 3 outlines some aspects of bond-site percolation as an alternative way to deal with percolation problems in a general manner. It shows up the partition in the (p_s, p_b) plane between non-percolating and percolating regions. The bond percolation is analysed on lattice samples where only a fraction of sites is occupied randomly, since then there is not a correlation between p_s and p_b . This treats the case of uncorrelated bond-site percolation. The various quantities determined in the previous chapter for $p_s = 1$ are now discussed for values of $p_s < 1$.

In Chapter 4 we consider the bond site percolation in the case of a relationship between p_s and p_b through suitable models. This relationship affects the structure of the non-percolating and percolating regions mentioned in Chapter 3. Particular attention is focused on a correlated bond-site percolation that we name the suppressed bond-site percolation. This is a new model and has not been considered in the literature before.

Chapter 5 investigates the directed suppressed bond site percolation. Aspects of directed percolation are put together with those of suppressed bond percolation. Here directed percolation is treated as a percolation with a preferential direction

in which an activity can flow one way but not the other. Thus a bond is assigned to two different directions opened with different probabilities, thereby affecting the connectivity of clusters in general and particularly their size.

Finally, concluding remarks appear in Chapter 6.

Chapter 2

Bond percolation

In this chapter we present aspects of the standard theory of bond percolation, where we count up simultaneously the number of sites and bonds in a cluster. Once a bond is chosen, its end sites are occupied with probability 1.

Quantities of interest are cluster size, mean cluster size, radius of gyration, and correlation length. They are determined for three 2-dimensional lattices (triangular, square, and honeycomb). Modifications are made to the usual definitions[70, 71] of the above quantities by referring them simultaneously to the number of bonds and the number of sites that each cluster contains.

These quantities are useful to describe clusters. They give an insight to the geometrical structure of clusters while cluster concept is the central point in percolation theory[72].

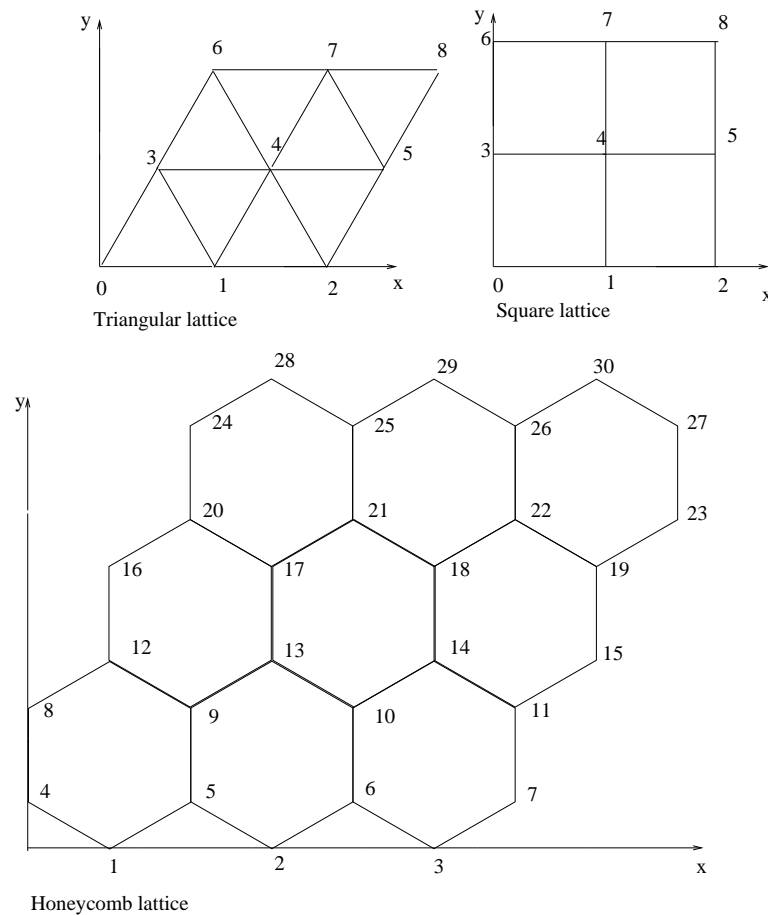
2.1 Reference systems

The calculation of the above quantities involves the notion of distance between two points for different lattices, and requires a reference system of axes for each type of

lattice sample. The unit of distance is defined as the distance between two nearest-neighbour sites. In defining distance as it relates to bonds, we present a bond as a point in the middle of its end sites.

With respect to Cartesian x,y axes, different systems of coordinates are adopted

Figure 2.1: Lattices and reference axes



for specifying sites, depending on the lattice type shown in Figure 2.1. The x axis passes through the bottom row of sites in the lattice sample. The y axis passes through the site of label 0 for square and triangular lattices, while for a honeycomb lattice the y axis passes through the sites of labels $N + 1$ and $2(N + 1)$, where N has the value 3 in Figure 2.1. For computational reasons, sites of triangular and square lattices have their label starting from zero, while those for the honeycomb lattice

begin with one[62].

The x and y coordinates of a site are uniquely determined by two parameters: the number N of sites on the x axis, and the label q as the site number in Figure 2.1. Then for the three lattices considered:

- Square lattice

$$y = y' \text{ with } y' \text{ equal to the integer part of the fraction } \frac{q}{N}.$$

$$x = q - yN$$

- Triangular lattice

$$y = y' \sin\left(\frac{\pi}{3}\right); \text{ where } y' \text{ is the integer part of the fraction } \frac{q}{N}$$

$$x = q - Ny' + y' \cos\left(\frac{\pi}{3}\right).$$

- Honeycomb lattice

Every site labelled by q is located on a row t which is the integer part of the fraction $\frac{q}{N+1}$. Rows are numbered from 0. Two other parameters t' and t'' , defined respectively as the integer parts of the fractions $\frac{t}{2}$ and $\frac{t+1}{2}$, are used in the determination of x,y coordinates . Thus,

$$y = (t + t') \sin\left(\frac{\pi}{6}\right)$$

$$x = 2(q - t(N + 1)) \cos\left(\frac{\pi}{6}\right) + (t'' - 1) \cos\left(\frac{\pi}{6}\right).$$

Table 2.1 gives some properties of the the lattice types considered for general values of N .

Due to the limitation of our computational resources, some calculations are done for $N = 100$ in the case of square and triangular lattices, and $N = 90$ for a honeycomb lattice. Thus the square lattice sample contains 10000 sites and 19800 bonds, the triangular one has 10000 sites and 29601 bonds, and the honeycomb one counts 16560 sites and 24559 bonds.

For coming discussions, we define for lattice samples a parameter Δ which is the distance between two parallel planes passing by the bottom and top rows of sites for each sample. Δ is expressed in the nearest-integer units of a distance between the two nearest-neighbour sites (this the distance is the unit adopted). It depends on the lattice type and on the parameter N defined above. Thus Δ has values of 86 and 99 for the triangular and square lattices for $N = 100$, while $\Delta = 136$ for the honeycomb lattice for $N = 90$.

Table 2.1: Lattice properties

	Lattice type		
	Triangular	Square	Honeycomb
Number of sites along the bottom edge of the lattice	N	N	N
Number of sites	N^2	N^2	$2(N + 1)^2 - 2$
Number of bonds	$(3N - 1)(N - 1)$	$2N(N - 1)$	$3N^2 + 4N - 1$
Generic number of nearest neighbours of a site	6	4	3
Generic number of nearest neighbours of a bond	10	6	4
Range of variation of the ratio $s:b$	2:1 - 1:3	2:1 - 1:2	2:1 - 2:3
Area of the sample	$\sqrt{3}(N - 1)^2$	$(N - 1)^2$	$\frac{3\sqrt{3}}{2}N^2$

2.2 Size and mean cluster size

The size of a cluster, also termed mass of the cluster, is defined in terms of the number of sites s and bonds b that it contains. A hybrid size represented by $\sqrt{s \times b}$ may be considered but this does not have a physical meaning. The density of a cluster may be defined in terms of the ratio between s and b . It gives an idea of the connectivity of occupied sites by opened bond, and on the geometrical aspect of a cluster. The larger the ratio $s:b$ in a cluster, the fewer the inside loops contained in it. The ratio shown in Table 2.1 ranges for each lattice type from a value for two sites and one bond to a value for an infinite cluster. As an example of determining the ratio for an infinite cluster, that for a honeycomb lattice is

$$\lim_{N \rightarrow \infty} \frac{2(N+1)^2 - 2}{3N^2 + 4N - 1} = \frac{2}{3}. \quad (2.1)$$

Referring to the definition of the mean cluster size as described by Stauffer and Aharony[70], we consider in an analogous way the mean cluster size S_s for sites for clusters with b bonds and s sites by

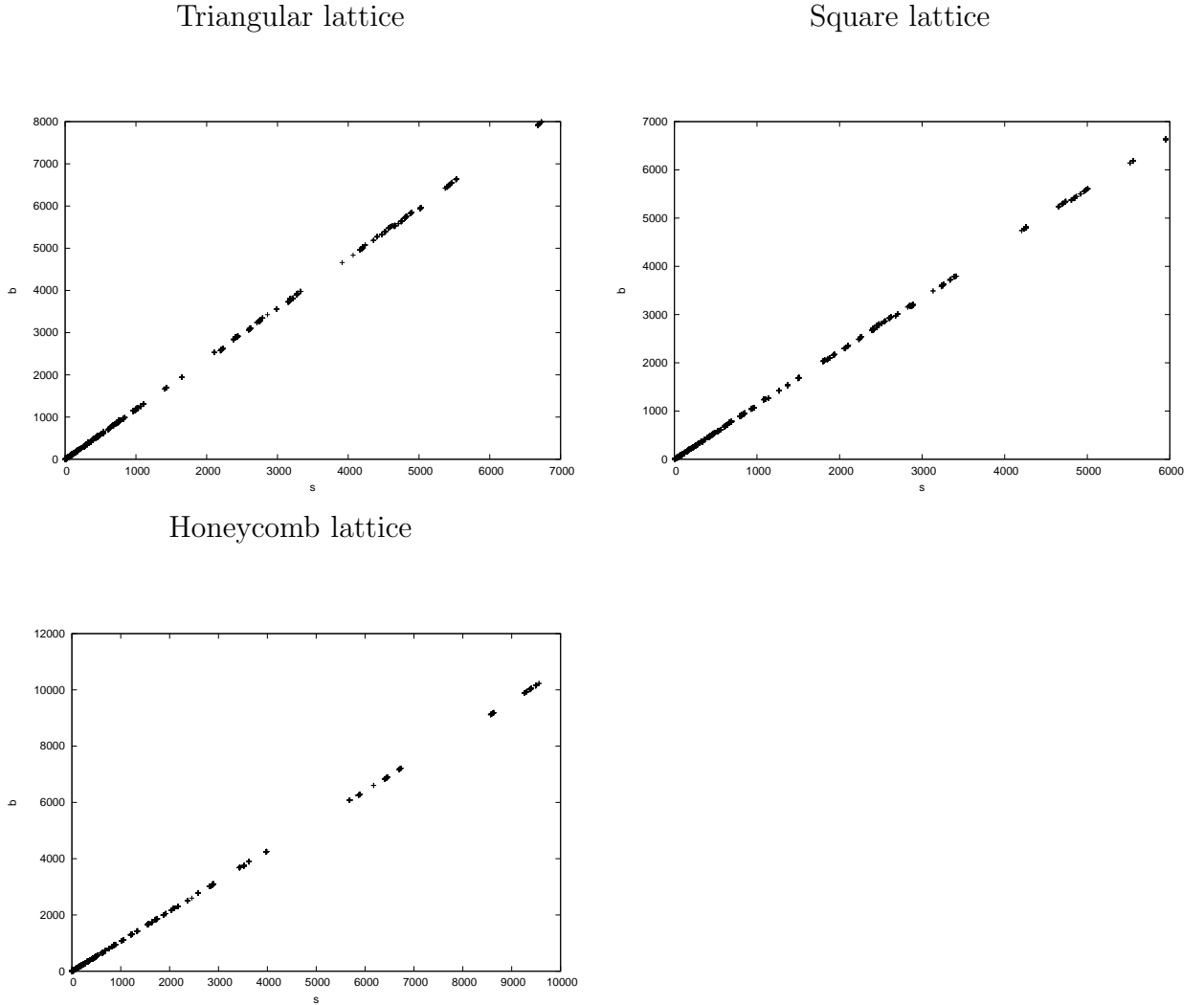
$$S_s = \frac{\sum_{sb} s^2 n_{sb}}{\sum_{sb} s n_{sb}}, \quad (2.2)$$

where n_{sb} is the number of clusters containing s sites and b bonds. Similarly, we define the mean cluster size S_b for bonds by,

$$S_b = \frac{\sum_{sb} b^2 n_{sb}}{\sum_{sb} b n_{sb}}. \quad (2.3)$$

In Figure 2.2, we have analysed how clusters are distributed according to the numbers of sites and bonds that they contain for pure bond percolation, where $p_s = 1$ and p_b can vary from 0 to 1. For each cluster we plot the number of bonds b versus the number of sites s . The values plotted in Figure 2.2 correspond in each case to the value of p_b close to the critical concentration p_{bc} , also termed the threshold

Figure 2.2: Cluster distribution in sizes

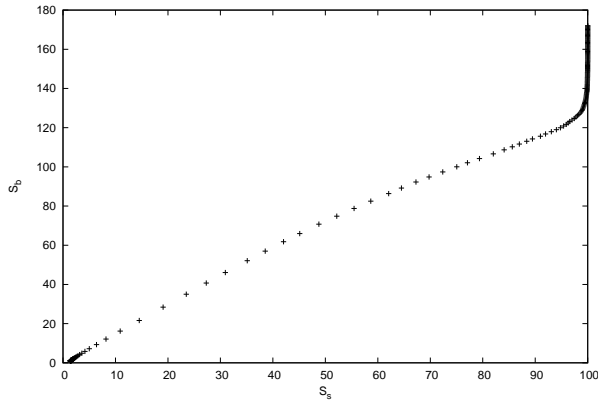


probability, values of which are given in Table 2.2 [70]. Ranges for p_b of $[0.345 - 0.349]$, $[0.498 - 0.502]$, and $[0.651 - 0.655]$ about these p_{bc} values were considered for triangular, square, and honeycomb lattices, respectively. The largest cluster contains a number of sites comprised between 27 and 40 % of the total number of sites of the entire system. Its number of bonds is in ranges of 57 and 65 % of the global number of bonds for different types of lattices.

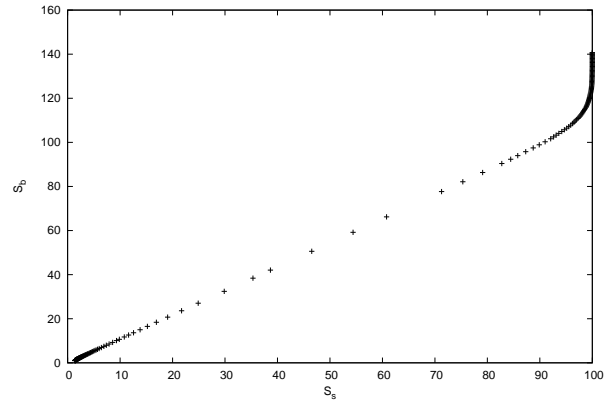
We compare in Figure 2.3 the mean cluster sizes for sites S_s and bonds S_b for

Figure 2.3: Mean cluster size

Triangular lattice



Square lattice



Honeycomb lattice

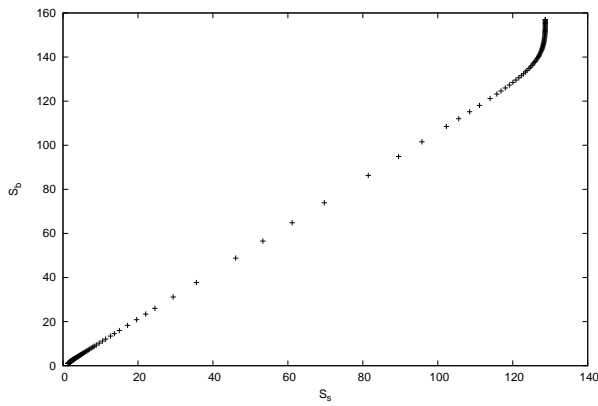


Table 2.2: Values of p_{bc} for pure bond percolation

	p_{bc}
Triangular lattice	0.34729
Square lattice	0.50000
Honeycomb lattice	0.65271

the whole range of values of p_b . Similarities and differences arise between Figures 2.2 and 2.3 for our lattice samples. The differences are due mainly to the fact that the three lattices do not have the same value of p_{bc} as shown in Table 2.2. Secondly, the process of merging of clusters into large ones causes clusters of intermediate size to disappear. Except for small fluctuations, it appears that some quantities can be referred to sites or bonds – there is no significant difference between Figures 2.2 and 2.3 below critical concentration. This leads us to assume that for a given cluster, the number of bonds and the number of sites are related by a simple linear function. Figures 2.4 and 2.5 show how the mean cluster size changes with p_b , and they allow one to localise the critical concentration p_{bc} . Mean cluster sizes S_s and S_b display a phase transition around critical concentration.

2.3 Gyration radius

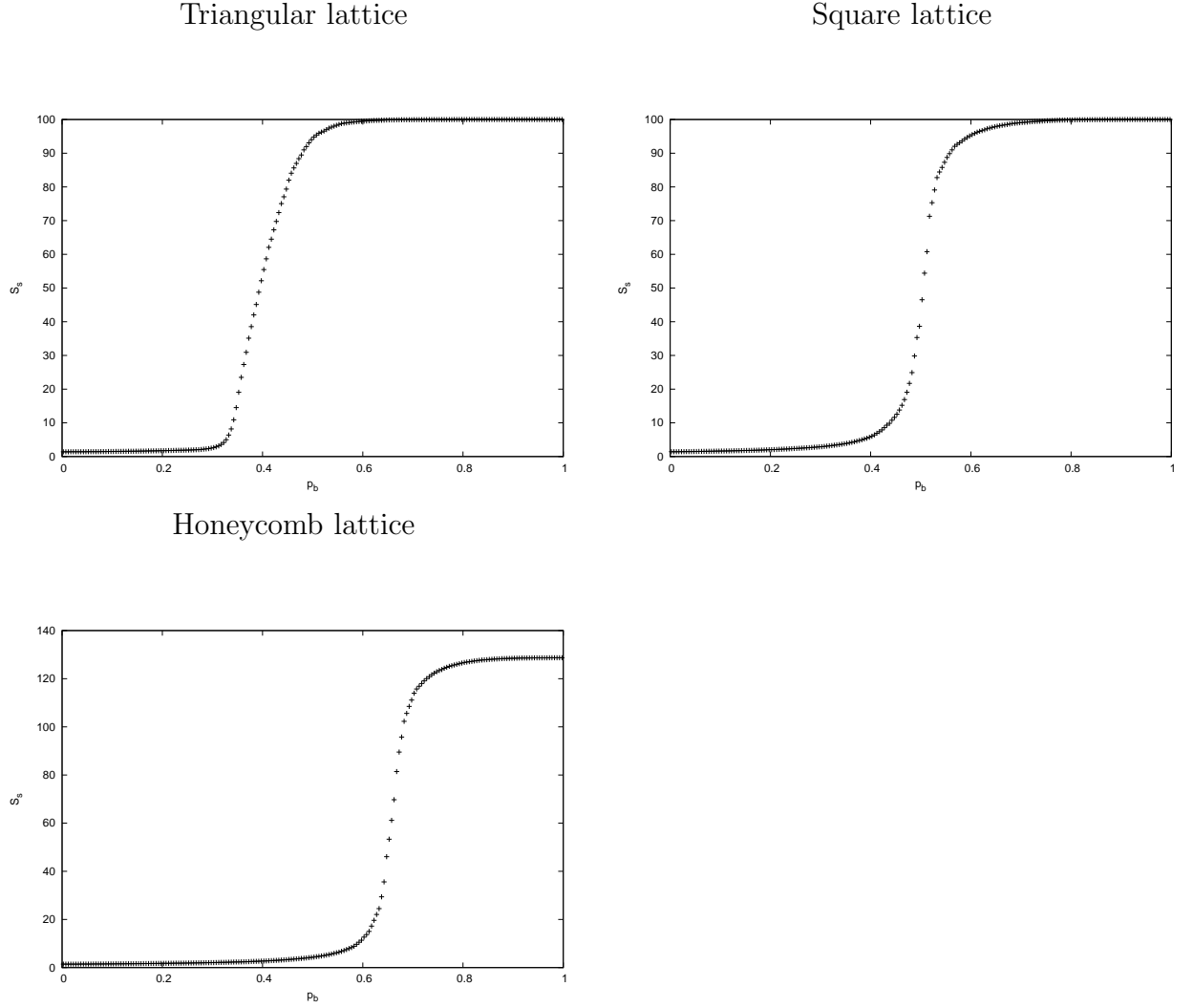
In a cluster, the centre of mass is placed at the position \vec{r}_o given by Equation (2.4) for a given system of reference[70]. The average distance between this centre and any site or bond of the cluster, named the gyration radius R_g of the cluster, is expressed by Equation (2.5). The size of a cluster s or b is the number of sites or bonds. The quantity \vec{r}_i stands for the position of the individual site or bond i in the cluster.

$$\vec{r}_o = \frac{\sum_i^s \vec{r}_i}{s} \quad (2.4)$$

$$R_g = \sqrt{\frac{\sum_i^s |\vec{r}_i - \vec{r}_o|^2}{s}} \quad (2.5)$$

R_g can be calculated in terms of Cartesian components (x_i, y_i) of the i^{th} site or bond in the (x, y) plane. Equation (2.5) yields to Equation (2.6) after some mathematical manipulations.

Figure 2.4: Variation of S_s with p_b

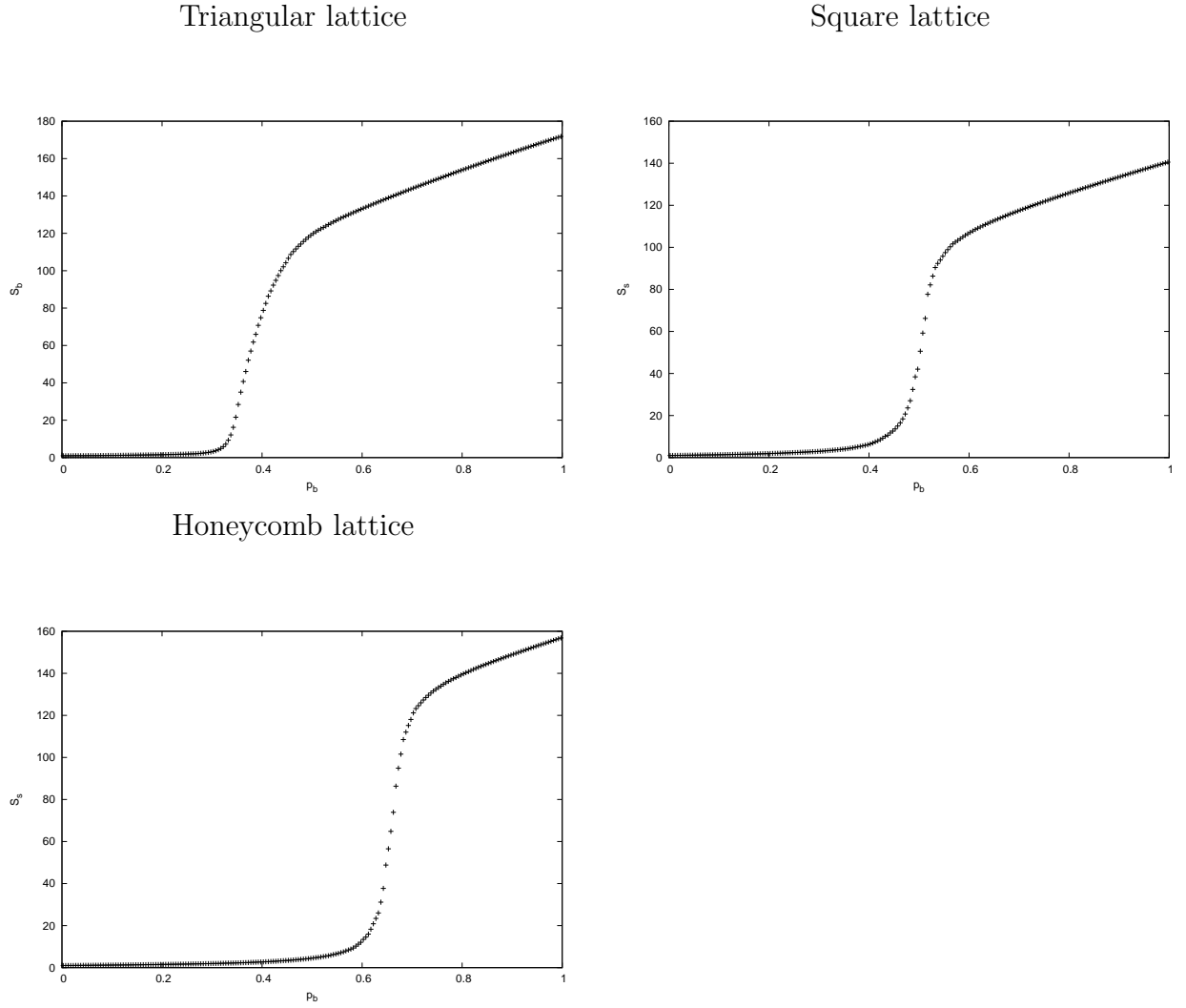


$$R_g = \sqrt{\frac{s \sum_i^s (x_i^2 + y_i^2) - [(\sum_i^s x_i)^2 + (\sum_i^s y_i)^2]}{s^2}} \quad (2.6)$$

In the following steps, we will make a distinction between the gyration radius related to sites and the one referred to bonds by noting them differently respectively as R_{gs} and R_{gb} .

The distribution of clusters in gyration radii for a range of values of p_b close to the critical concentration is given in Figure 2.6. The whole values of R_{gs} and R_{gb}

Figure 2.5: Variation of S_b with p_b

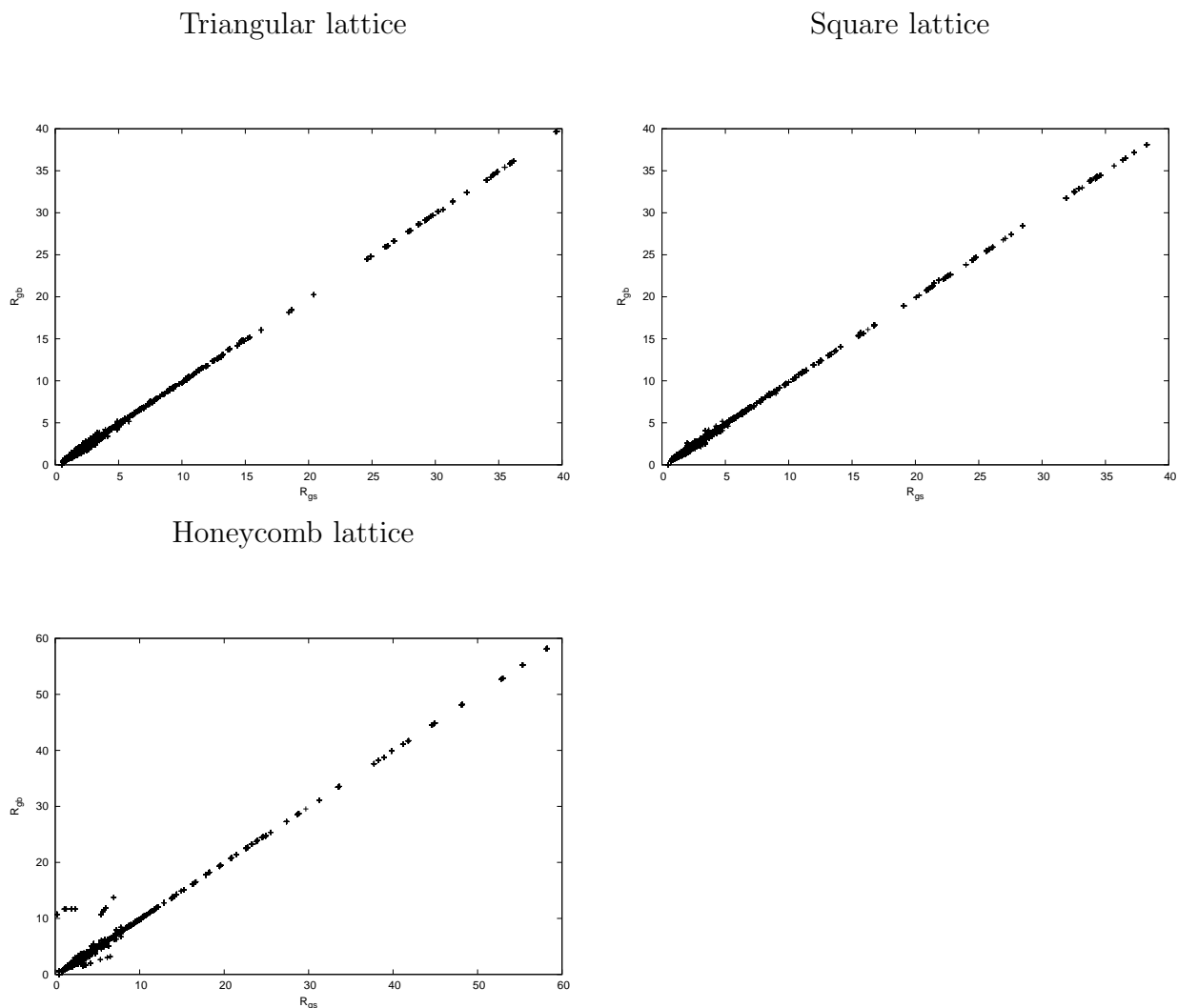


are less than a half of Δ for each type of lattices.

2.4 Correlation length

The correlation length is the measure of the average gyration radius of clusters. Its expression in Equations (2.7) and (2.8) is related to gyration radii for the whole system, in our case the lattice sample for given probabilities of occupied and opened

Figure 2.6: Cluster distribution in gyration radii around critical concentration



sites and bonds respectively.

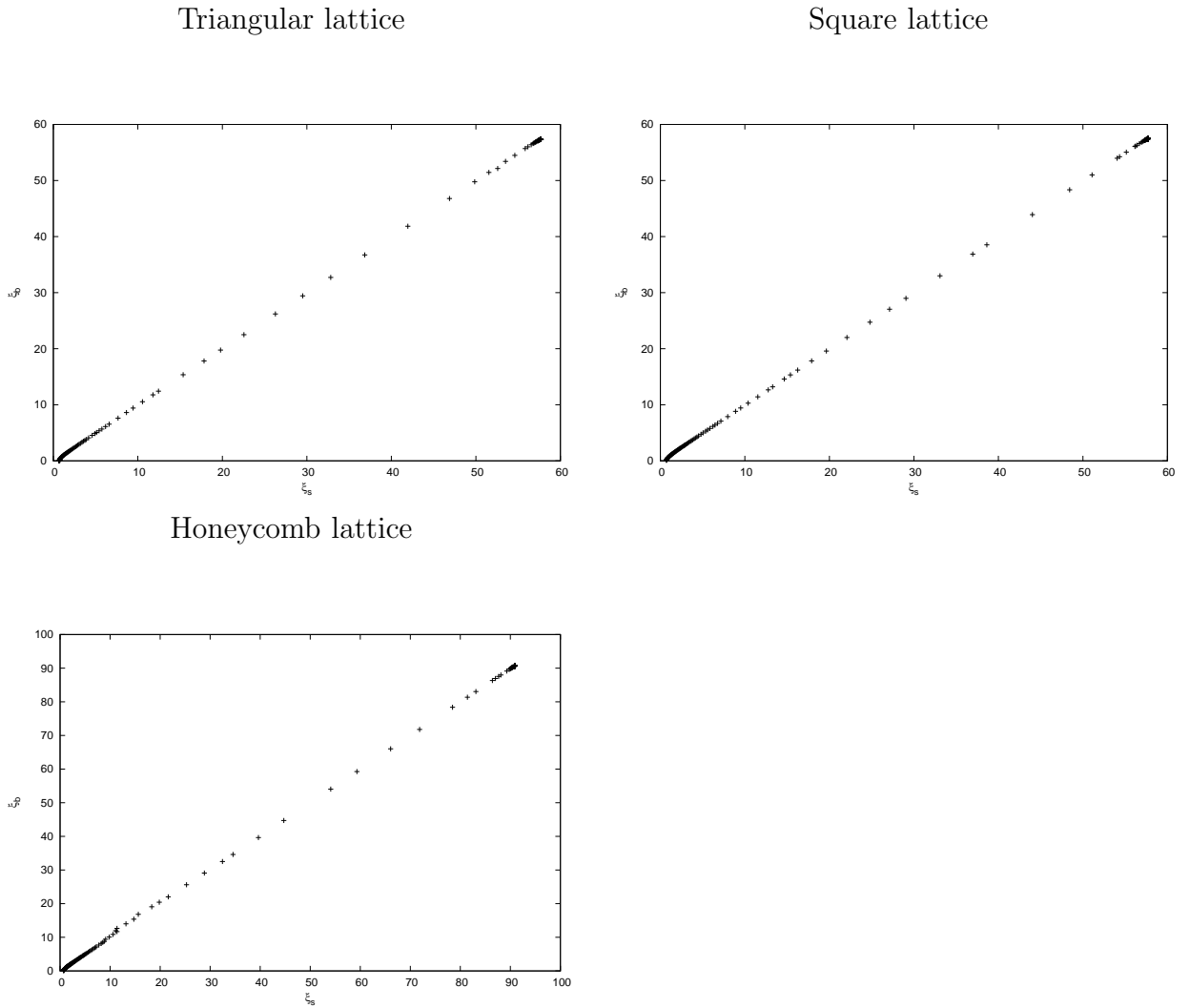
$$\xi_s = \sqrt{\frac{2 \sum_{sb} R_{gs}^2 s^2 n_{sb}}{\sum_{sb} s^2 n_{sb}}} \quad (2.7)$$

In Equation (2.7) the correlation length ξ_s given is related to the sites where n_{sb} and R_{gs} are respectively the number of clusters with s sites and b bonds, and the gyration radius of clusters of s sites. A similar expression of correlation length ξ_b related to bonds is used and represented by the Equation (2.8).

$$\xi_b = \sqrt{\frac{2 \sum_{sb} R_{gb}^2 b^2 n_{sb}}{\sum_{sb} b^2 n_{sb}}} \quad (2.8)$$

In Figure 2.7, we have compared the average values of ξ_s and ξ_b for 100 iterations for all values of p_b . In Figures 2.8 and 2.9, we show how the correlation length

Figure 2.7: Comparison between ξ_s and ξ_b



(associated with sites and bonds respectively) varies as the probability of opening bonds changes. It is important to note that above critical concentration all cluster properties are dominated by those attached to the spanning cluster. As a function

of p_b , the graph of the correlation length allows roughly to detect in which range of values of p_b , a system reaches percolation.

Below p_{bc} , values of ξ_s and ξ_b are less than a quarter of Δ while above p_{bc} they are greater than 58 % of Δ .

Figure 2.8: Variation of ξ_s with p_b

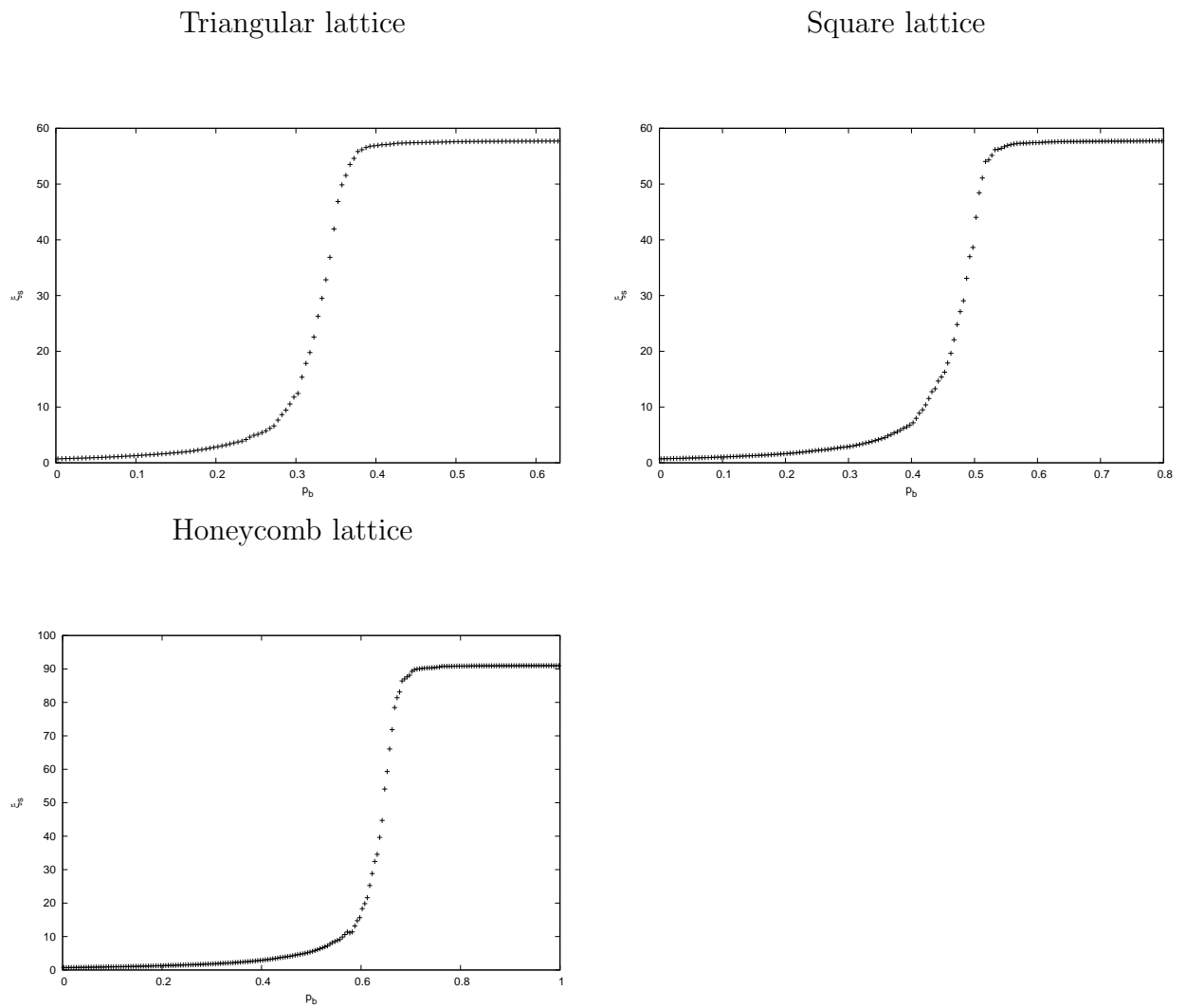
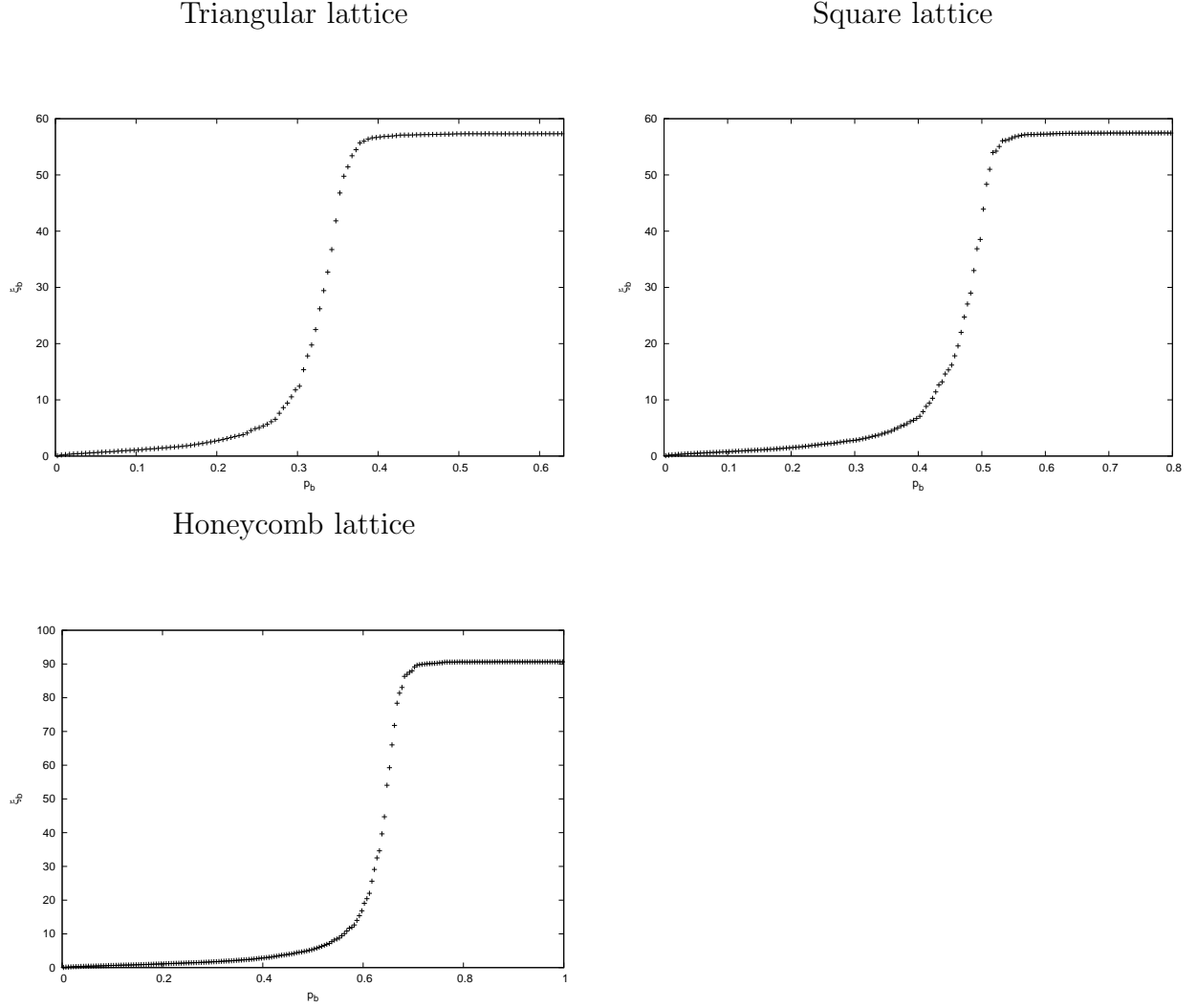


Figure 2.9: Variation of ξ_b with p_b



2.5 Concluding remarks

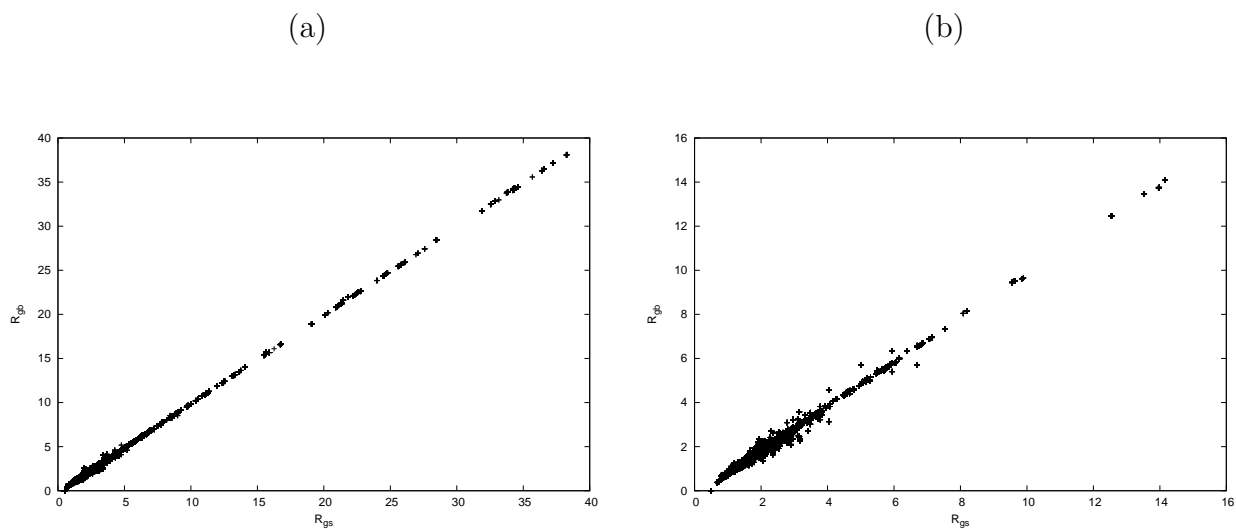
One important feature is that for each cluster, the number of sites and bonds that it contains are comparable. This feature is also observed when we plot R_{gb} versus R_{gs} as it is plotted in Figure 2.6. The straight line of best fit has a slope approximately 1.

In our discussions on the quantities that we plotted from Figure 2.2 till Figure

2.9, finite size effects impact on the lattice samples. One may get rid of these effects by considering only clusters which do not touch samples edges. In Figure 2.10, we compare the distribution of cluster gyration radii for the case of square lattices when p_b is near p_{cb} for the pure bond percolation. The range $[0.495 - 0.505]$ of p_b is considered. The part (a) of Figure 2.10 contains the whole number of clusters in the considered range while (b) has only clusters which do not touch edges in the same range of values of p_b . It appears that by eliminating the clusters which touch edges we get rid of most clusters with large sizes. These clusters may merge and evolve into the spanning cluster.

In the following chapter, we will analyse the effect of changing the parameter

Figure 2.10: Cluster distribution in gyration radii for the case of square lattices



p_s into a value less than 1 on the above determined quantities, i.e. we will consider bond-site percolation.

Chapter 3

Bond-site percolation

We consider our lattice samples as given in Figure 2.1 where a percentage of sites is occupied and upon which bond percolation is applied. A bond contributes to the connectivity of clusters if it is confined between two occupied nearest neighbour sites.

The (p_s, p_b) plane is subdivided into regions of percolating and non-percolating phases. Quantities determined in Chapter 2 are also calculated in the percolating area. They keep their definition. Our attention in this stage is focussed on changes made by the modification of the parameter p_s .

3.1 Partition of (p_s, p_b) plane

By varying the percentage of occupied sites from 0 to 100%, in bond percolation, a spanning cluster appears at a particular value of p_s which is greater than the known critical concentration of pure site percolation p_{sc} as given in Table 3.1 [70]. Above that value, as p_s increases, the value of the critical concentration for bond percolation p_{bc} decreases from a value close to 1 to its lowest value which is the critical concentration for pure bond percolation, as listed in Table 2.2.

Table 3.2 gives average values of p_{bc} determined numerically for various values

Table 3.1: Values of p_{sc} for pure site percolation

	p_{sc}
Triangular lattice	0.50000
Square lattice	0.592746
Honeycomb lattice	0.6962

of p_s and equivalent to 1000 iterations. The hyphens in the table mean that for the corresponding value of p_s , the system does not percolate. At $p_s = 1$, the obtained values of p_{bc} are in perfect concordance with the known critical concentrations for bond percolation. In Figure 3.1, data in Table 3.2 are plotted. The curve of the best fit has the form,

$$p_{bc} = \frac{1}{a p_s + b} \quad (3.1)$$

and corresponds to the dashed curve in Figure 3.1. The parameters a and b as shown in Table 3.3 depend on the nature of the lattice. The correlation matrix of these fit parameters shows that they are strongly negatively correlated[73].

Values in Table 3.2 are in harmony with the formula of Yanuka and Englman[23, 74] in the limits of numerical calculations. They suggested that points on the critical curve separating the percolation zone to the non-percolating one satisfy,

$$\frac{\log(p_s)}{\log(p^*_{sc})} + \frac{\log(p_b)}{\log(p^*_{bc})} = 1; \quad (3.2)$$

Table 3.2: Numerical values of p_{bc} for various values of p_s

p_s	p_{bc}		
	Triangular lattice	Square lattice	Honeycomb lattice
0.50	–	–	–
0.55	$0.85383 \pm 1.43616\text{E-}003$	–	–
0.60	$0.74644 \pm 1.14628\text{E-}003$	$0.97481 \pm 8.56525\text{E-}004$	–
0.65	$0.65611 \pm 9.73058\text{E-}004$	$0.88043 \pm 9.69804\text{E-}004$	–
0.70	$0.58298 \pm 7.89305\text{E-}004$	$0.79768 \pm 8.49874\text{E-}004$	$0.98884 \pm 4.33712\text{E-}004$
0.75	$0.52595 \pm 6.83189\text{E-}004$	$0.72613 \pm 7.43757\text{E-}004$	$0.92451 \pm 7.30453\text{E-}004$
0.80	$0.47643 \pm 5.72630\text{E-}004$	$0.66728 \pm 6.39509\text{E-}004$	$0.85435 \pm 9.61437\text{E-}004$
0.85	$0.43655 \pm 5.05983\text{E-}004$	$0.61490 \pm 5.50951\text{E-}004$	$0.79148 \pm 2.85572\text{E-}004$
0.90	$0.40251 \pm 4.25567\text{E-}004$	$0.57158 \pm 5.04533\text{E-}004$	$0.73658 \pm 8.59709\text{E-}004$
0.95	$0.37277 \pm 3.79538\text{E-}004$	$0.53360 \pm 4.73049\text{E-}004$	$0.69273 \pm 3.82068\text{E-}004$
1.00	$0.34742 \pm 3.47673\text{E-}004$	$0.49904 \pm 4.03624\text{E-}004$	$0.65273 \pm 3.38435\text{E-}004$

Table 3.3: Values of parameters of the curve of the best fit a and b

Lattices	a	b
Triangular	3.78048 ± 0.04113	-0.924846 ± 0.02851
Square	2.44134 ± 0.01237	-0.447102 ± 0.008706
Honeycomb	1.7618 ± 0.003868	-0.229772 ± 0.003094

where p^*_{cs} and p^*_{bc} are the thresholds for pure site percolation and for pure bond percolation respectively. The frontier between percolating and non-percolating regions was also investigated by Ziff and Sapoval[75].

The parameters a and b allow one to estimate p^*_{sc} and p^*_{bc} through expressions (3.3) and (3.4).

$$p^*_{sc} = \frac{1-b}{a} \quad (3.3)$$

$$p^*_{bc} = \frac{1}{a+b} \quad (3.4)$$

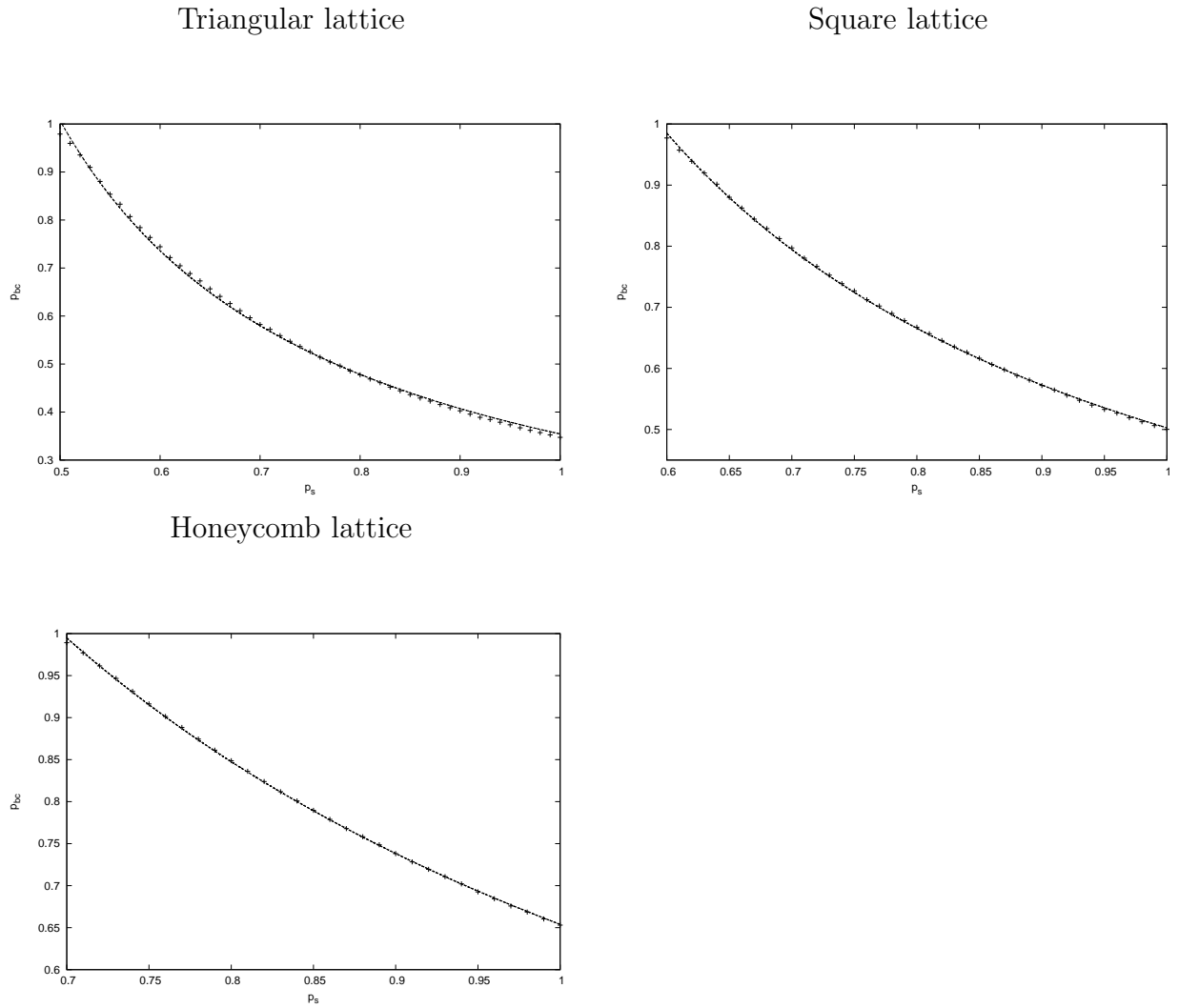
3.2 Size and mean cluster size

Referring to Table 3.2 and Figure 3.1, we look only at cluster sizes around the critical concentration p_{bc} .

In Figure 3.2, we plot the distribution of all clusters according to their number of sites s and bonds b around critical concentration when 75 % of sites in the sample are occupied. In the (s,b) plane, each cluster is represented by a plus sign (+). As the critical concentration depends on the type of the lattices, the ranges of p_b [0.510:0.524], [0.718:0.728] and [0.910:0.919] are considered for triangular, square, and honeycomb lattices respectively. The largest cluster contains a number of sites comprised between 64 and 76% of the fraction of occupied sites in the entire system, while the number of bonds in the largest cluster is in the ranges of 25 and 45% of the total number of bonds for various lattices.

As seen in Chapter 2, S_s and S_b are defined for a given value of p_b . Equations (2.2) and (2.3) are applied to calculate S_s and S_b . As functions of the values of p_b , S_s and S_b are plotted in Figures 3.3 and 3.4. It is important to note that above the

Figure 3.1: Variation of p_{bc} versus p_s

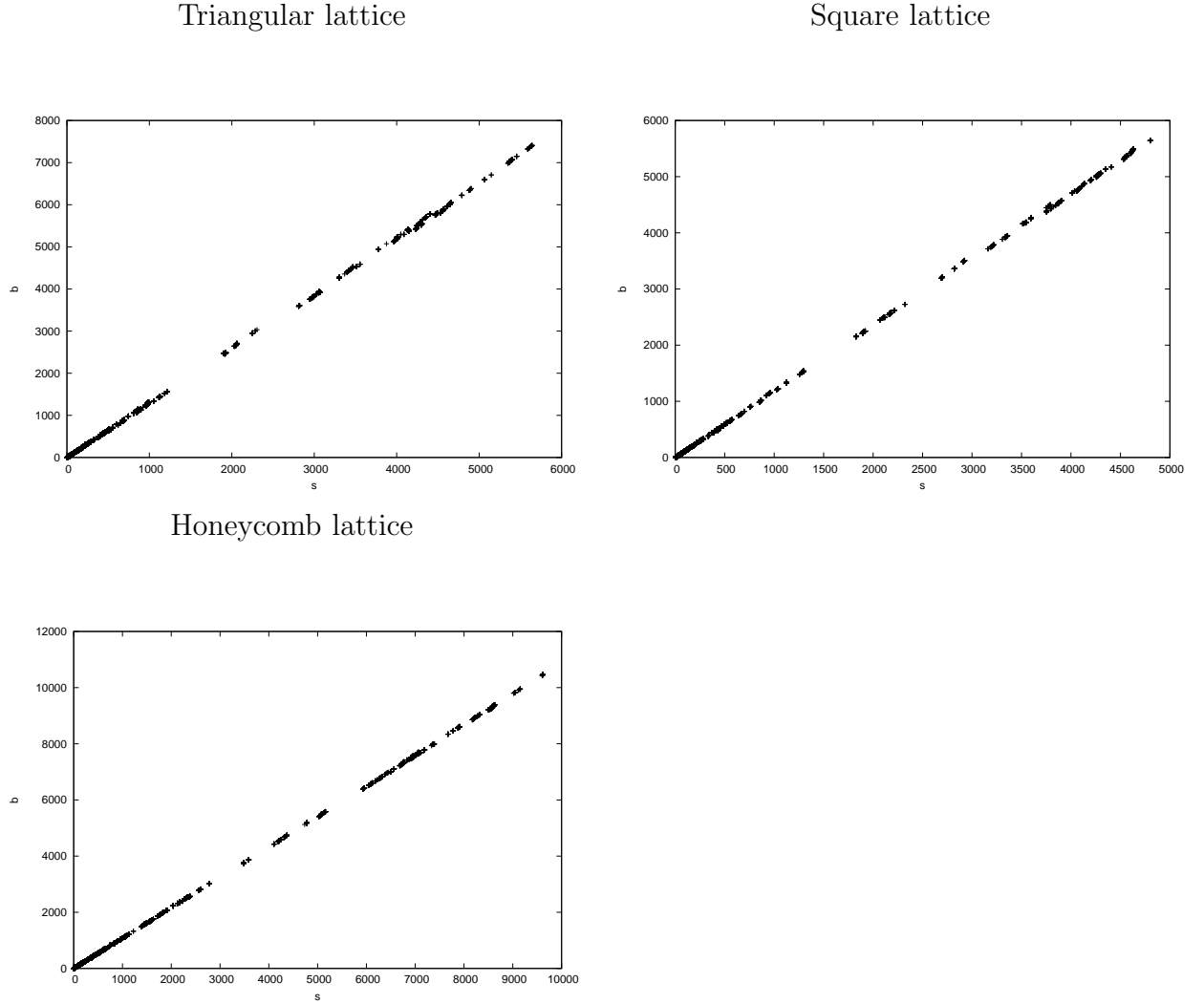


critical concentration, the spanning cluster dominates.

3.3 Gyration radius and correlation length

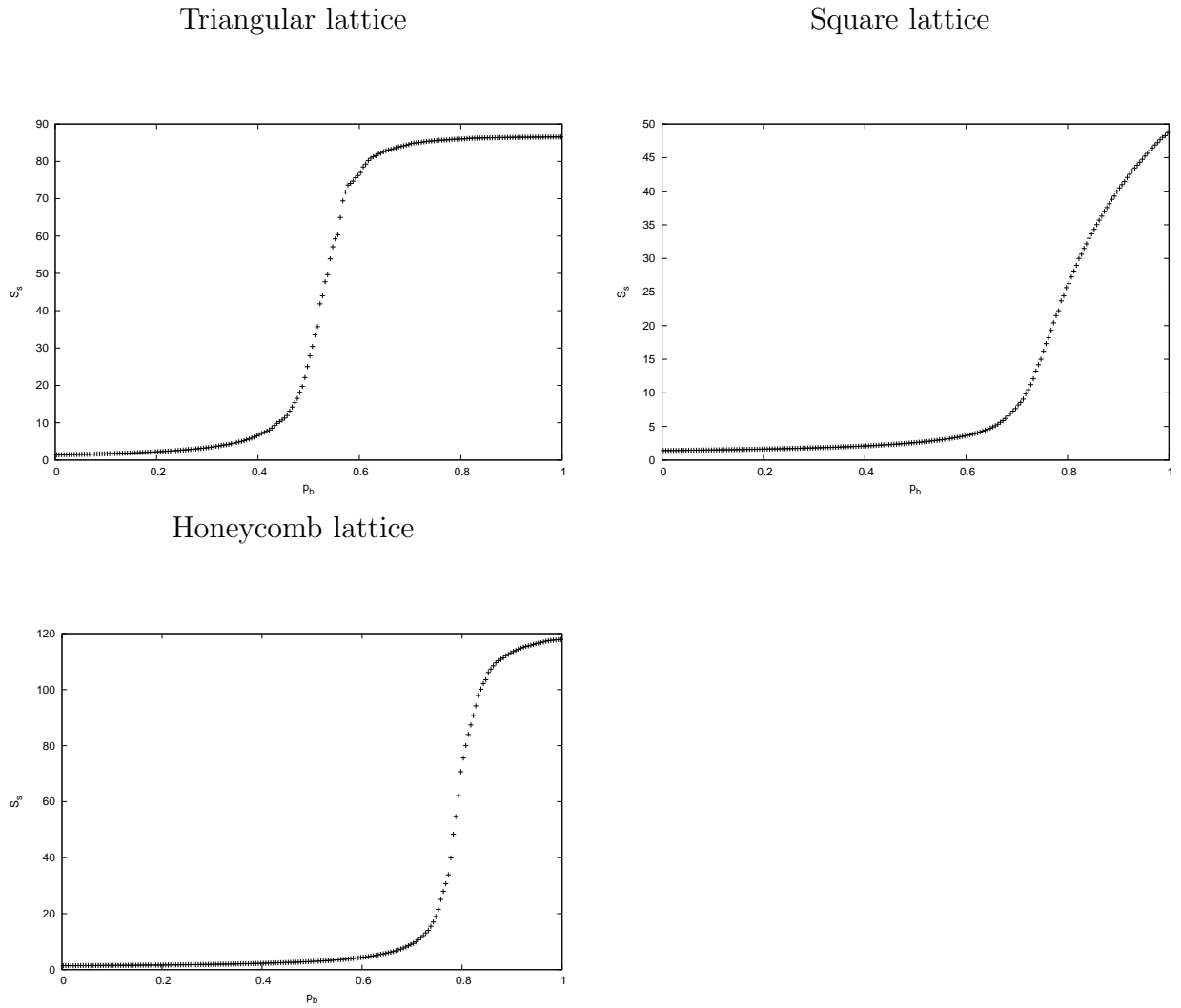
Equations (2.6) to (2.8) are applied to determine the radius of gyration and the correlation length. These quantities are presented from Figure 3.5 to Figure 3.8.

Figure 3.2: Cluster distribution in sizes for 75% site occupation



These figures display similar behaviour as what we found in the previous chapter. The first difference appears in the shifting up of the value of p_{bc} and in the change of the magnitude of the property envisaged. The second difference is observed by finding some clusters where the number of bonds is higher compared to the number of sites that they contain. This fact shows that most of clusters have inside loops – the ratio $b : s$ is greater than 1 mainly for the largest cluster. All values of R_{gs} and R_{gb} are less than a half of Δ (defined in chapter 2).

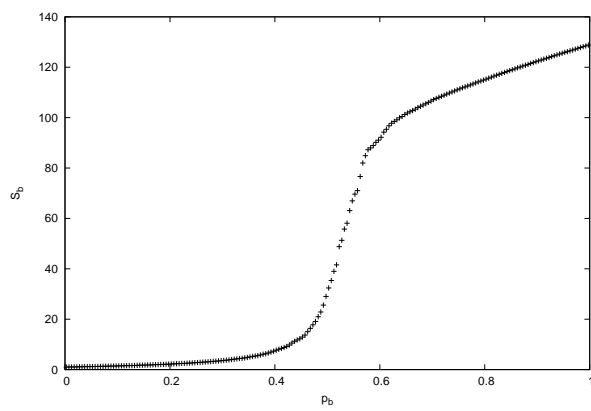
Figure 3.3: Mean cluster size S_s for 75% site occupation



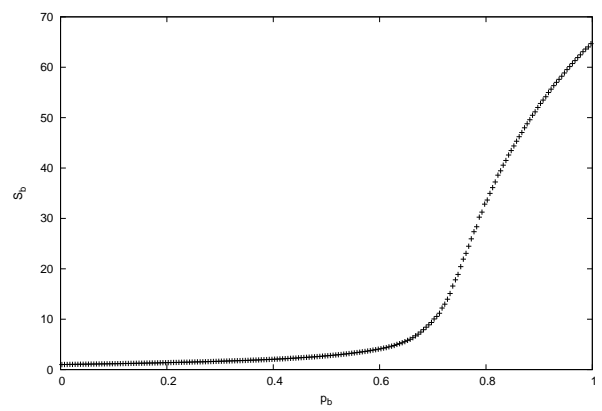
The variation of ξ_s or ξ_b as a function of p_b once p_s is fixed localises roughly the percolation threshold. Its graph looks like a smoothed step function around the critical concentration p_{bc} which starts and ends as a plateau function.

Figure 3.4: Mean cluster size S_b for 75% site occupation

Triangular lattice



Square lattice



Honeycomb lattice

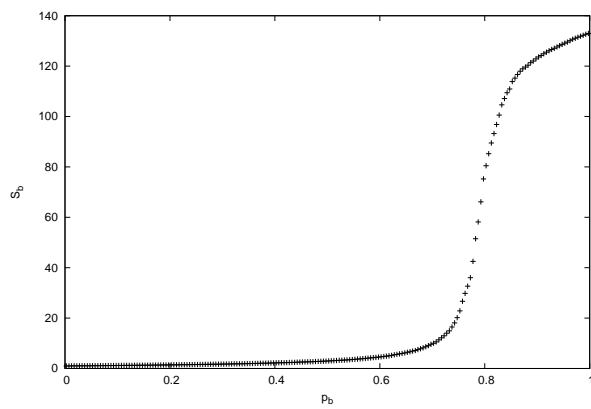
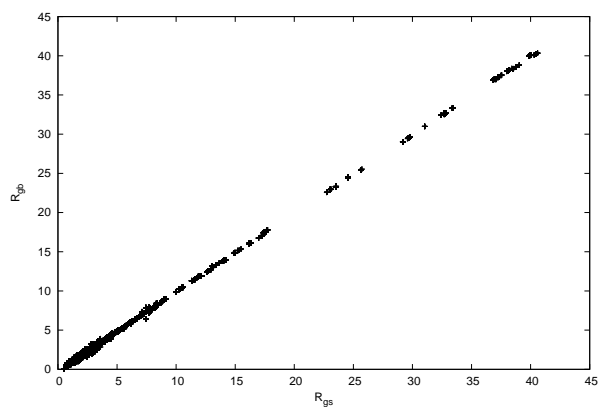
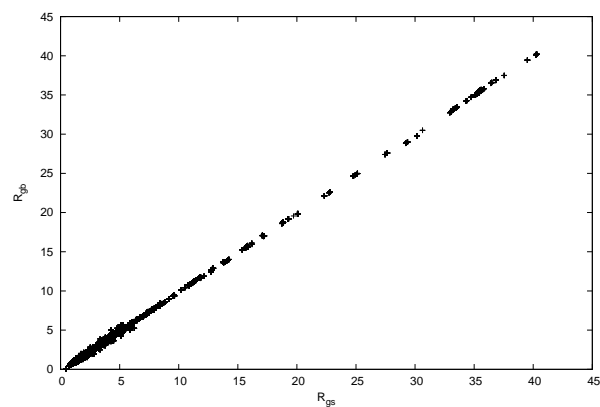


Figure 3.5: Cluster distribution in gyration radii around critical concentration for 75% site occupation

Triangular lattice



Square lattice



Honeycomb lattice

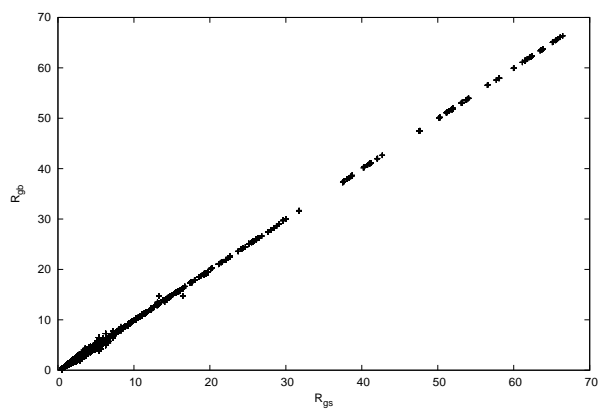
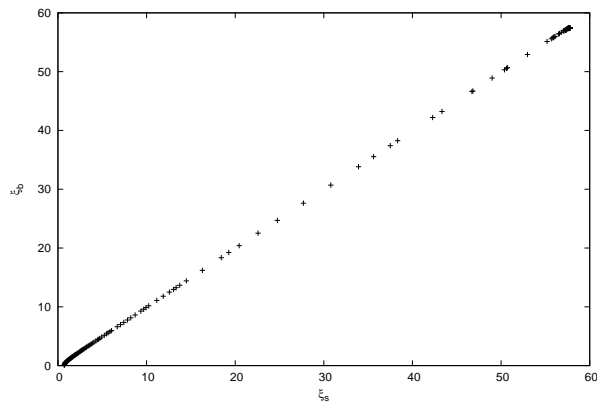
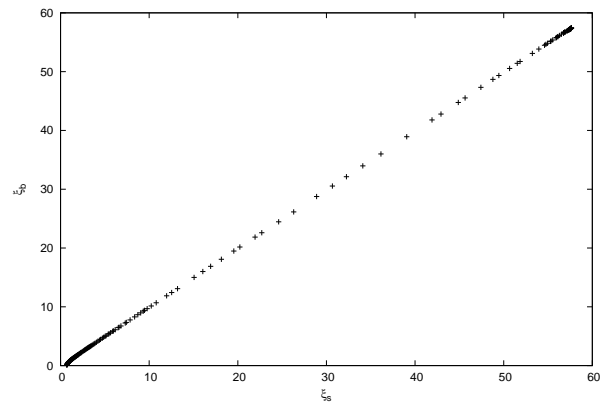


Figure 3.6: Comparison between ξ_s and ξ_b for 75% site occupation

Triangular lattice



Square lattice



Honeycomb lattice

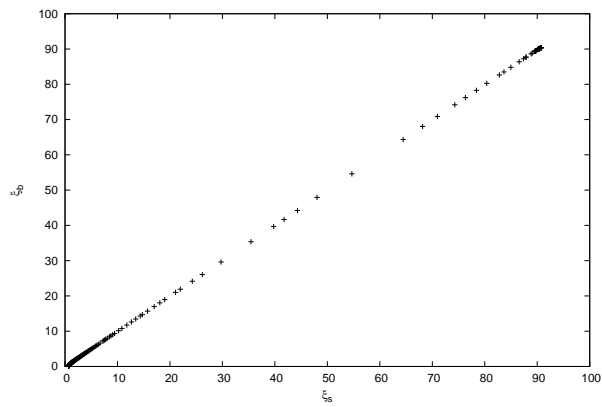
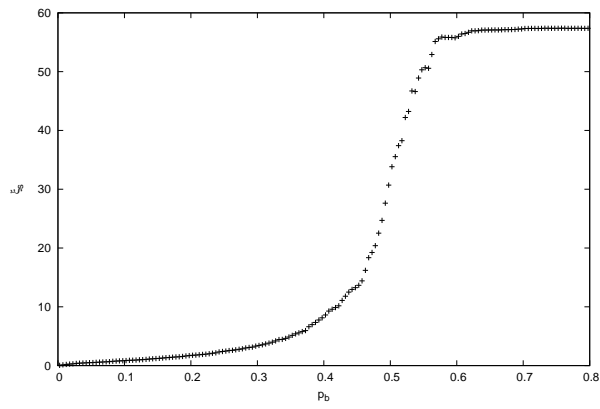
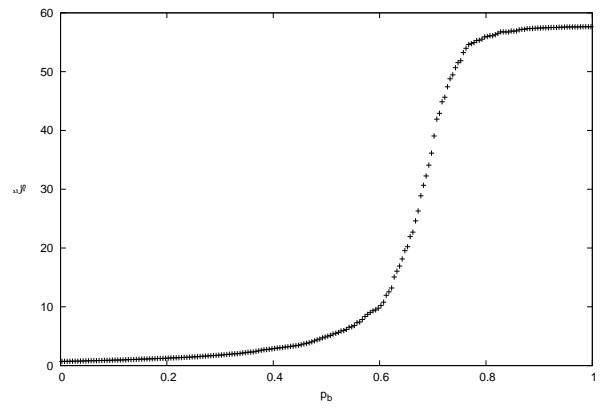


Figure 3.7: Variation of ξ_s as function of p_b for 75% site occupation

Triangular lattice



Square lattice



Honeycomb lattice

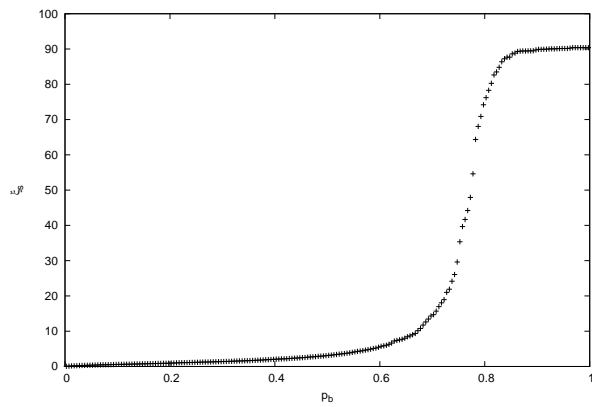
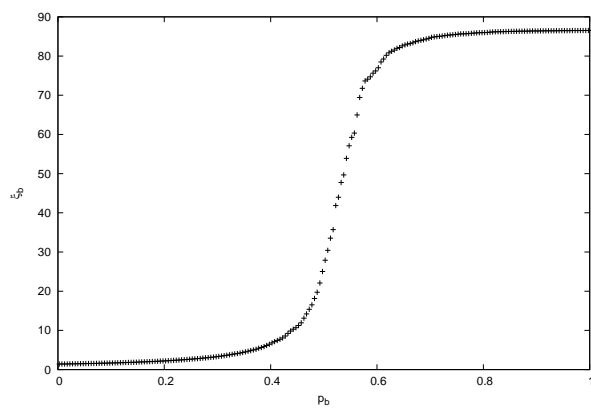
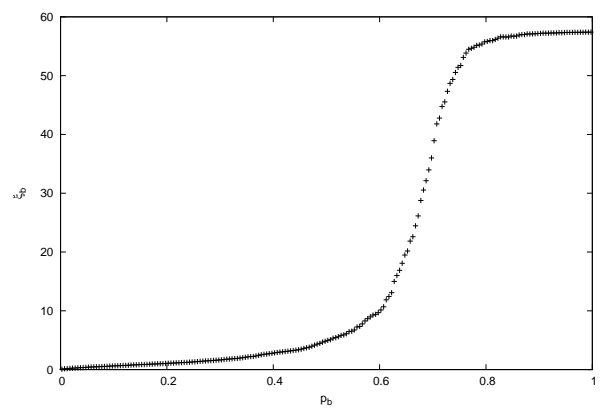


Figure 3.8: Variation of ξ_b as function of p_b for 75% site occupation

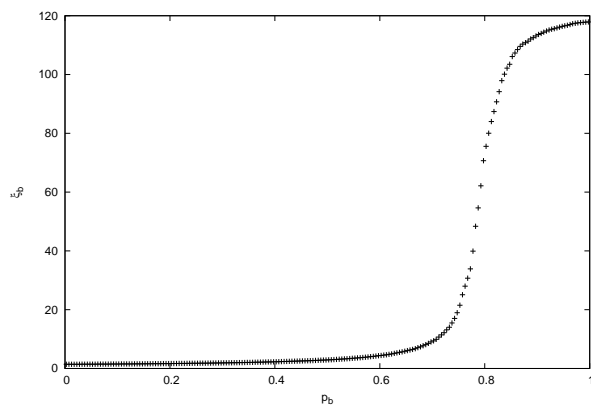
Triangular lattice



Square lattice



Honeycomb lattice



Chapter 4

Suppressed bond-site percolation

In the previous chapters, we considered the opening of a chosen bond, once its end sites were occupied, for the two cases: with probability 1 or randomly. At this stage, a relationship is introduced between the occupying probability of sites and the probability of opening bonds. A percentage of sites is occupied randomly on a lattice sample. Then bonds between nearest-neighbour occupied sites are opened according to the local density of sites, where we take into account the number of next nearest-neighbour sites of a given bond. By next nearest sites of a bond we mean the nearest neighbour sites of its origin and end. We keep track of the connectivity of a cluster. Thus the opening of a bond is related to local and global features of the percolation system. It appears that the critical concentration for bond percolation is higher compared to its value in the case of pure bond-site percolation. The introduction of a relationship between the opening probability of bonds and the occupancy probability of sites restrains the system from reaching percolation as rapidly. This property explains the use of the description *suppressed bond-site percolation*.

In physical systems such as polymers, the suppression factor can be associated with

the steric and entropic factors in the formation of gels, that is, in the arrangement of atoms in the constituent molecules .

The steric factor is an expression used in collision theory in formation of molecules in which the more complex the reactant molecules are, the lower is the steric factor[76]. This is important as in collision theory, a reaction probability depends on certain mutual orientations of reactant molecules[77], thus molecules will have various geometries different from the spherical one.

4.1 Models

First of all, the end sites of a bond have to be occupied before defining the probability of opening the bond. As detailed below, two models are adopted for this, which involves one or the other of the parameters α and β . Both these parameters represent the fraction of the total number of end sites of a bond plus their occupied nearest neighbours. This fraction depends on the type of lattice. It varies between $\frac{2}{10}$ to $\frac{10}{10}$ for the triangular, $\frac{2}{8}$ to $\frac{8}{8}$ for the square, and $\frac{2}{6}$ to $\frac{6}{6}$ for the honeycomb lattices. In general, sites are occupied randomly with probability p_s . Once the end sites of a bond are occupied, this bond is opened with probability p_b .

The models are defined in terms of the site fraction f_s . The site fraction is defined as the ratio between its nearest-neighbour sites which are occupied and the maximum number of its nearest-neighbour sites, which is allowed locally in order to avoid finite size effects.

Model 1 is defined by

$$p_{bl} = \alpha f_s.$$

If a bond is selected, in order to open a bond at least its end sites must be occupied. The above relation gives the probability that a selected bond will be opened. Thus the maximum number of nearest and next nearest sites of a bond depends on the lattice properties as mentioned in Table 2.2 and illustrated by Figure 2.1. It has a value of 10, 8 and 6 for triangular, square, and honeycomb lattices respectively.

Model 2 is defined by

$$p_{bl} = \begin{cases} \frac{1}{\beta} f_s & , f_s \leq \beta \\ \frac{1}{\beta-1} f_s + \frac{1}{1-\beta} & , f_s > \beta. \end{cases}$$

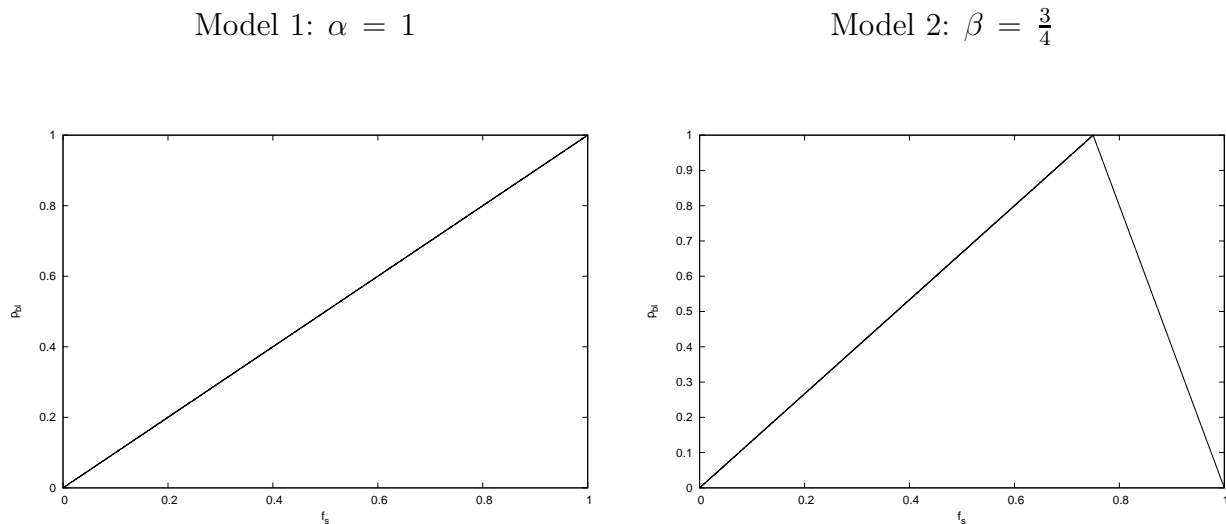
Here β is a parameter. Regarding the lattice samples used, if α and β are less than 0.5, systems were not able to reach percolation.

Examples of the relationship between f_s and p_{bl} are illustrated in Figure 4.1 for the two models with $\alpha = 1$ and $\beta = \frac{3}{4}$, respectively. Remember p_b is the probability of a bond being selected. Once selected we use p_{bl} as the probability of opening that bond.

4.2 Partition of the (p_s, p_b) plane

By varying the percentage of opened sites and considering the above relationships, there is also a partition of the (p_s, p_b) plane into percolating and non-percolating zones as found in Chapter 3.

Figure 4.1: Representations of the two models



Tables 4.1 and 4.2 give numerical values of the critical p_b i.e. p_{bc} , corresponding to the two models when $\alpha = 1$, and β having the values $\frac{3}{5}$, $\frac{3}{4}$, and $\frac{5}{6}$ for triangular, square, and honeycomb lattices, respectively. These data are plotted in Figure 4.2. The three different curves for each lattice correspond respectively to $p_{bl} = 1$ (continuous line); $p_{bl} = f_s$ (dashed line representing model 1) ; and $p_{bl} = \frac{1}{\beta} f_s$ for $f_s \leq \beta$ and $p_{bl} = \frac{1}{\beta-1} f_s + \frac{1}{1-\beta}$ for $f_s > \beta$ (alternated dot-dash line representing model 2). One notes that the curve corresponding to $p_{bl} = 1$ is that obtained in Chapter 3 and plotted in Figure 3.1. This critical curve constitutes our reference and allows us to see the effects of the relationship introduced between f_s and p_{bl} through the models.

The curves in Figure 4.2 of p_{bc} as a function of p_s in models 1 and 2 seem to follow (4.1) and (4.2) respectively.

Table 4.1: Model 1: Numerical values of p_{bc} for various values of p_s

	p_{bc}		
p_s	Triangular lattice	Square lattice	Honeycomb lattice
0.50	–	–	–
0.55	–	–	–
0.60	–	–	–
0.65	$0.98412 \pm 7.91572\text{E-}04$	–	–
0.70	$0.83333 \pm 1.13333\text{E-}03$	–	–
0.75	$0.70039 \pm 8.95893\text{E-}04$	$0.96666 \pm 8.38599\text{E-}04$	–
0.80	$0.59635 \pm 7.25626\text{E-}04$	$0.83236 \pm 8.08934\text{E-}04$	–
0.85	$0.51457 \pm 5.68151\text{E-}04$	$0.72481 \pm 6.67994\text{E-}04$	$0.99875 \pm 6.04137\text{E-}04$
0.90	$0.44648 \pm 5.03112\text{E-}04$	$0.63497 \pm 5.46426\text{E-}04$	$0.88718 \pm 1.77994\text{E-}03$
0.95	$0.39284 \pm 4.15183\text{E-}04$	$0.56181 \pm 4.79306\text{E-}04$	$0.75107 \pm 1.36774\text{E-}03$
1.00	$0.34736 \pm 3.36191\text{E-}04$	$0.49953 \pm 3.93257\text{E-}04$	$0.65232 \pm 1.10091\text{E-}03$

$$p_{bc} = \frac{1}{a_1 (p_s)^2 + a_2 p_s + a_3} \quad (4.1)$$

$$p_{bc} = b_1 (p_s)^2 + b_2 p_s + b_3 \quad (4.2)$$

The coefficients a_i , b_i in these equations, corresponding to the curve of best fit of our numerical values of p_{bc} as given in Tables 4.1 and 4.2, are listed in Tables 4.3 and 4.4. They depend on the nature of the lattices.

In Figures 4.3 and 4.4 we show how the critical curves in models 1 and 2 are modified when the values of the parameters α and β change. In Figure 4.3 α has the

Table 4.2: Model 2: Numerical values of p_{bc} for various values of p_s

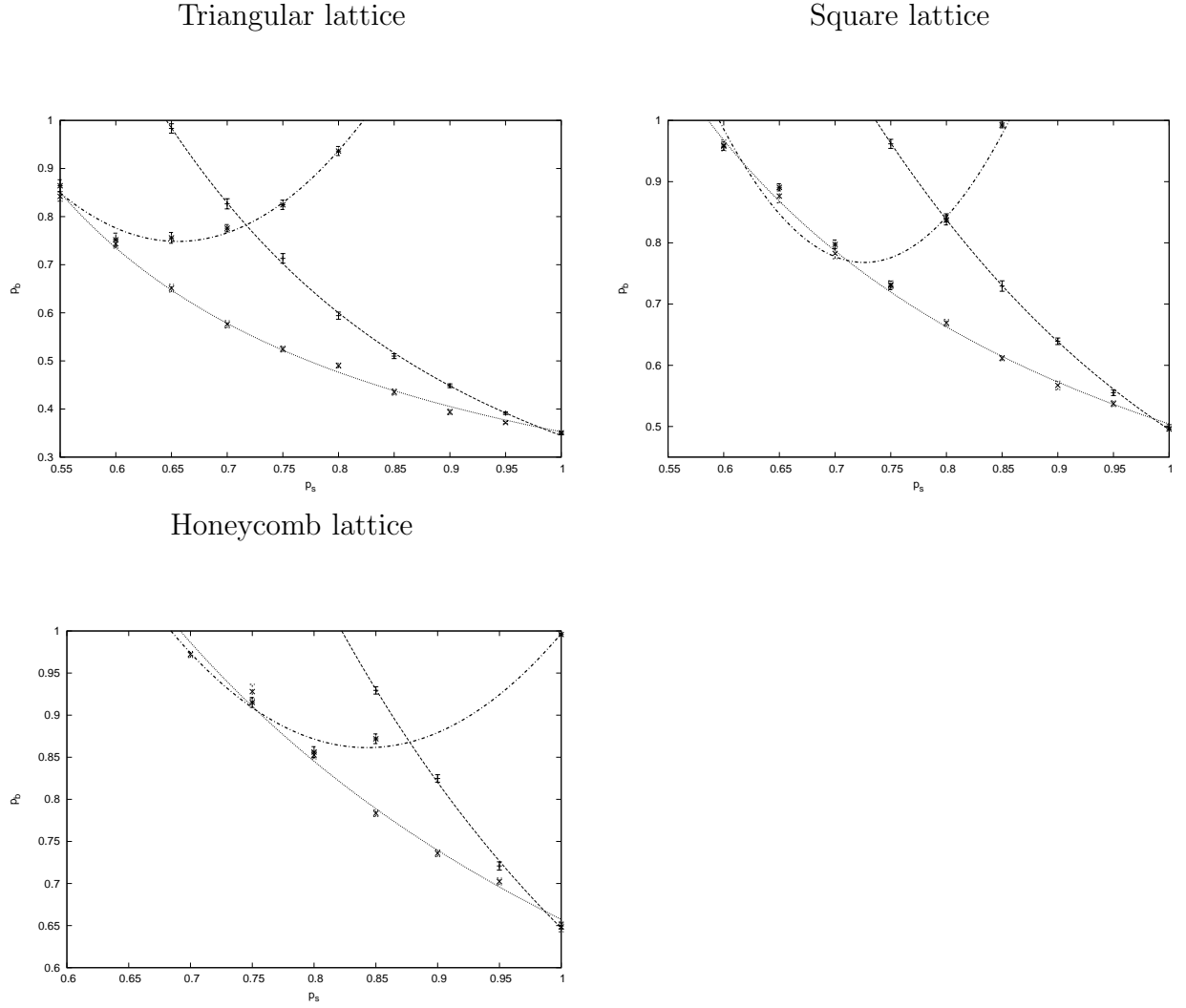
p_s	p_{bc}		
	Triangular lattice	Square lattice	Honeycomb lattice
0.50	$0.96478 \pm 6.86346\text{E-}03$	–	–
0.55	$0.86411 \pm 1.26384\text{E-}03$	–	–
0.60	$0.75190 \pm 1.37856\text{E-}03$	$0.95801 \pm 6.66087\text{E-}03$	–
0.65	$0.75585 \pm 1.12289\text{E-}03$	$0.89070 \pm 5.86915\text{E-}03$	–
0.70	$0.77591 \pm 7.51854\text{E-}03$	$0.79746 \pm 7.10466\text{E-}03$	–
0.75	$0.82447 \pm 9.67839\text{E-}03$	$0.73038 \pm 6.99559\text{E-}03$	$0.91511 \pm 5.83910\text{E-}03$
0.80	$0.93637 \pm 9.37847\text{E-}03$	$0.83684 \pm 7.54920\text{E-}03$	$0.85615 \pm 6.39551\text{E-}03$
0.85	–	$0.99239 \pm 4.55773\text{E-}03$	$0.87193 \pm 5.77509\text{E-}03$
0.90	–	–	–
0.95	–	–	–
1.00	–	–	–

Table 4.3: Model 1: Values of the coefficients a_i for curves of best fit

Lattice	a_1	a_2	a_3
Triangular	5.22275 ± 0.6584	-3.23454 ± 1.009	0.912044 ± 0.3842
Square	4.12429 ± 0.6595	-3.29094 ± 1.117	1.18671 ± 0.4733
Honeycomb	2.45979 ± 2.699	-1.4118 ± 4.939	0.497373 ± 2.262

values 0.75(stars), 0.85(crosses) and 0.95(plus), while in Figure 4.4 β has the values 0.60(plus), 0.75(crosses) and 0.85(stars). When α and β are close to 1, a system

Figure 4.2: Variation of p_{bc} versus p_s



reaches percolation rapidly.

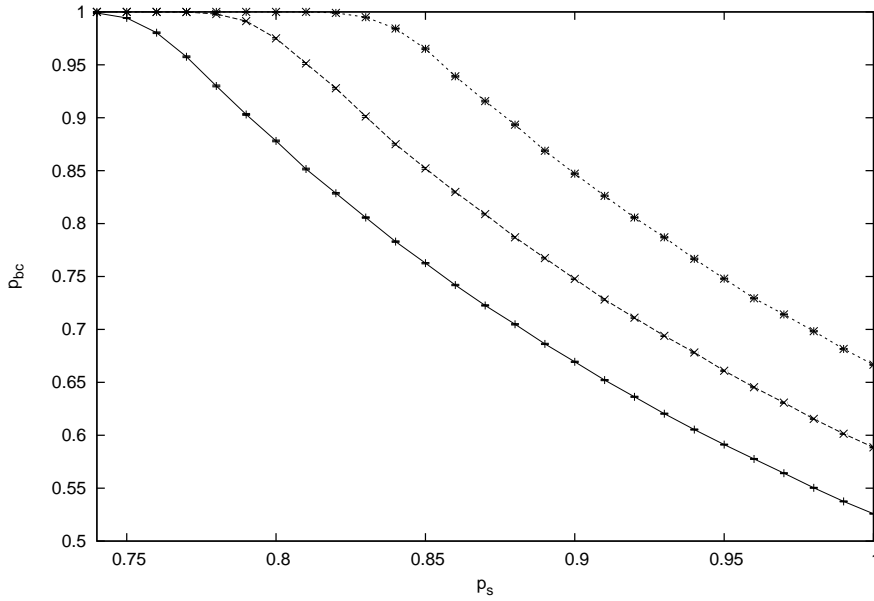
4.3 Size and mean cluster size

These quantities are determined in the model 1 for $p_s = 0.85$, $\alpha = 1$. In the model 2, we consider $p_s = 0.85$ and β equal to $\frac{3}{5}$, $\frac{3}{4}$ and $\frac{5}{6}$ for triangular, square, and

Table 4.4: Model 2: Values of the coefficients b_i for curves of best fit

Lattice	b_1	b_2	b_3
Triangular	9.27879 ± 1.176	-12.184 ± 1.59	4.74702 ± 0.5304
Square	13.6651 ± 2.767	-19.8468 ± 4.017	7.9742 ± 1.442
Honeycomb	14.9492 ± 0.538	-24.3506 ± 0.715	10.7691 ± 0.185

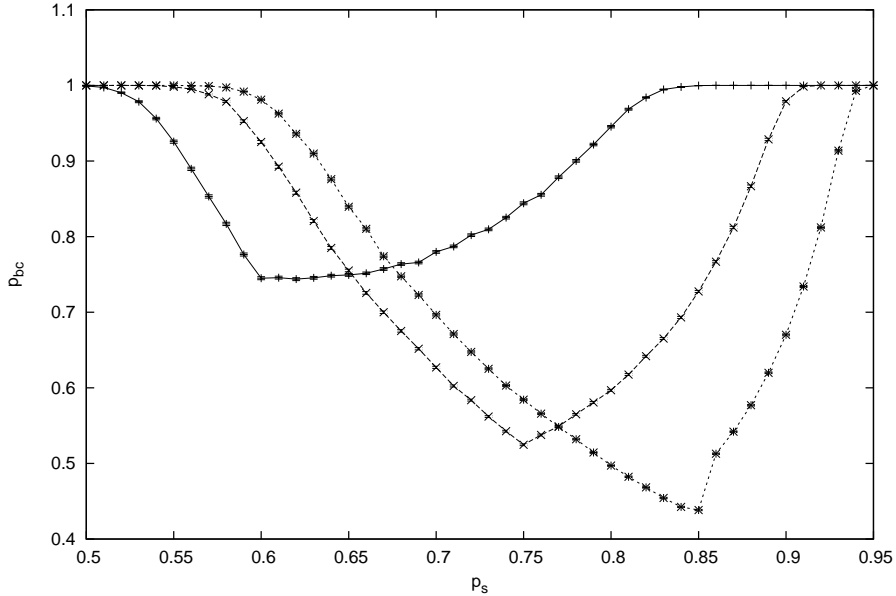
Figure 4.3: Critical curves in model 1 for three values of α : Case of square lattice



honeycomb lattices respectively.

In Figures 4.5 and 4.6, the distribution of clusters in sizes is shown for a range of values of p_b close to the respective critical concentration. We will compare our models with standard pure percolation in section 4.5.

Figure 4.4: Critical curves in model 2 for three values of β : Case of triangular lattice



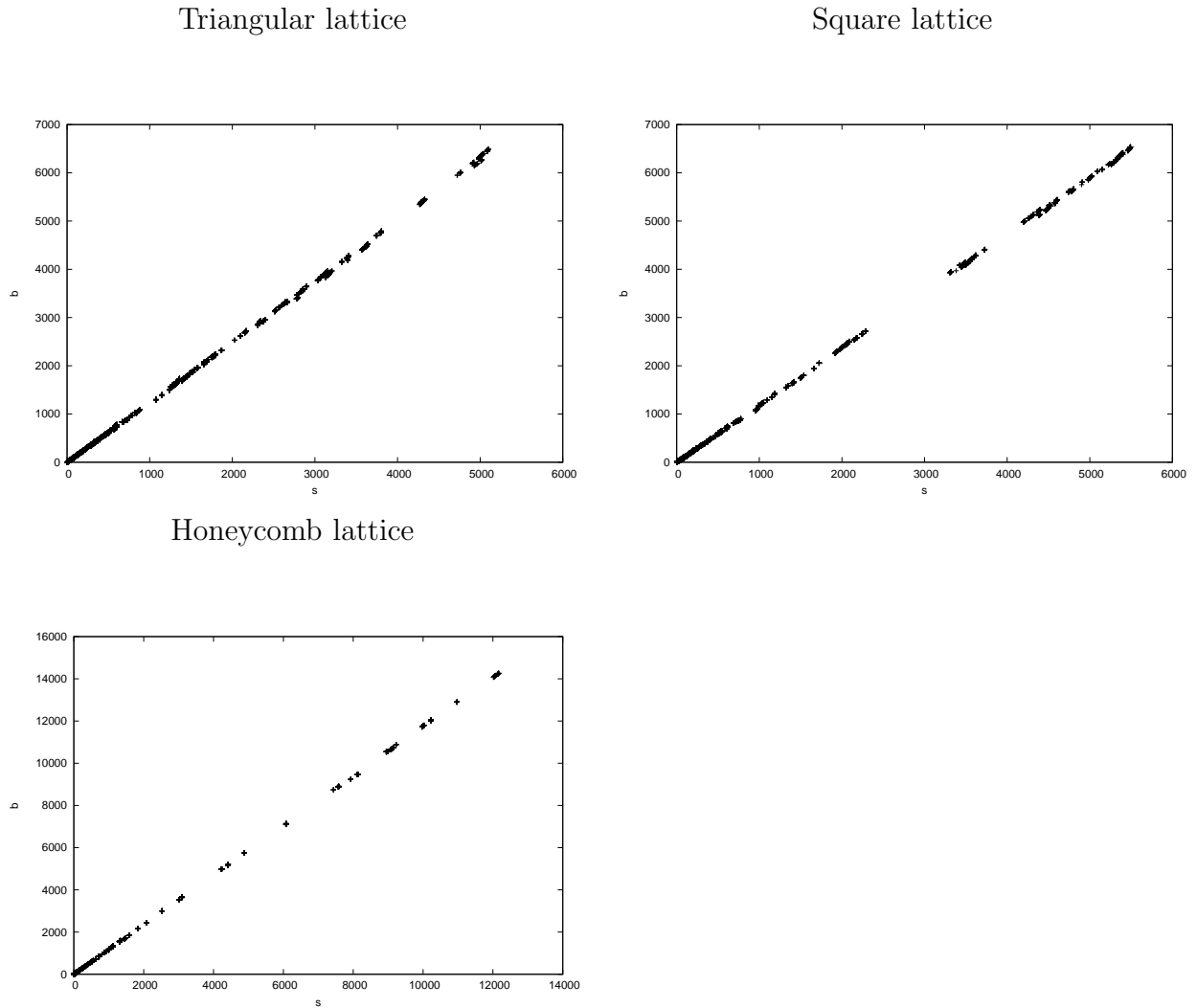
Considering models 1 and 2, for large sizes, clusters have more bonds compared to the number of sites that they contain. This is also observed from Figure 4.7 to Figure 4.10, where S_s and S_b can be compared for the whole range of values of p_b . This is due to the higher values of the critical concentration in this model.

4.4 Gyration radius and correlation length

Figures 4.11 and 4.12 show the distribution of the radius of gyration of clusters using the same range of values of p_b as is considered in the above distribution of clusters in sizes given in the previous section. Small clusters present more inside loops than do large ones.

In Figures 4.13 and 4.14, a comparison is made between the correlation length

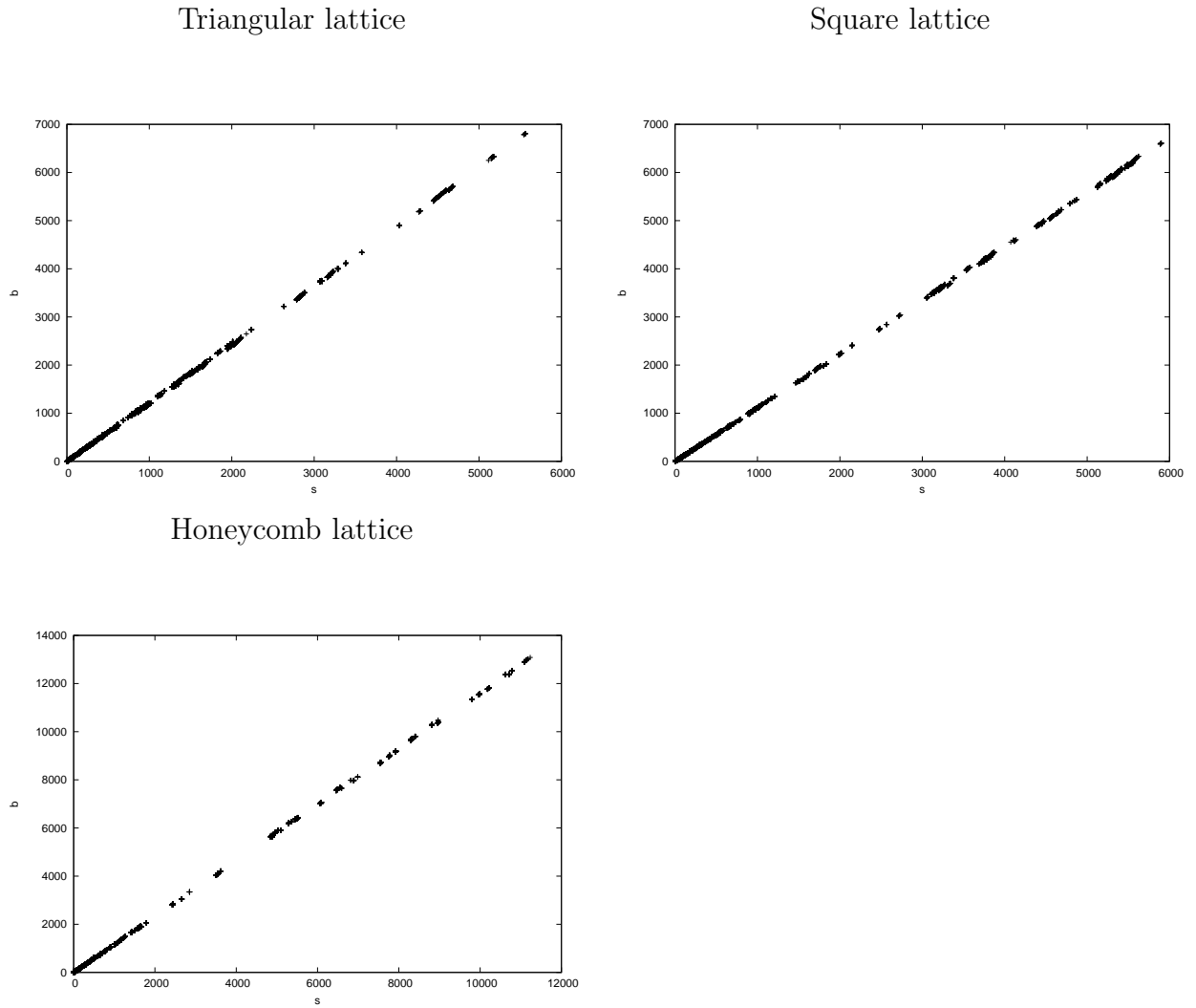
Figure 4.5: Model 1: Cluster distribution in sizes around critical concentration



due to the sites and that due to the bonds. For large clusters, ξ_b is a linear function of ξ_s . This indicates that large clusters contain fewer inside loops.

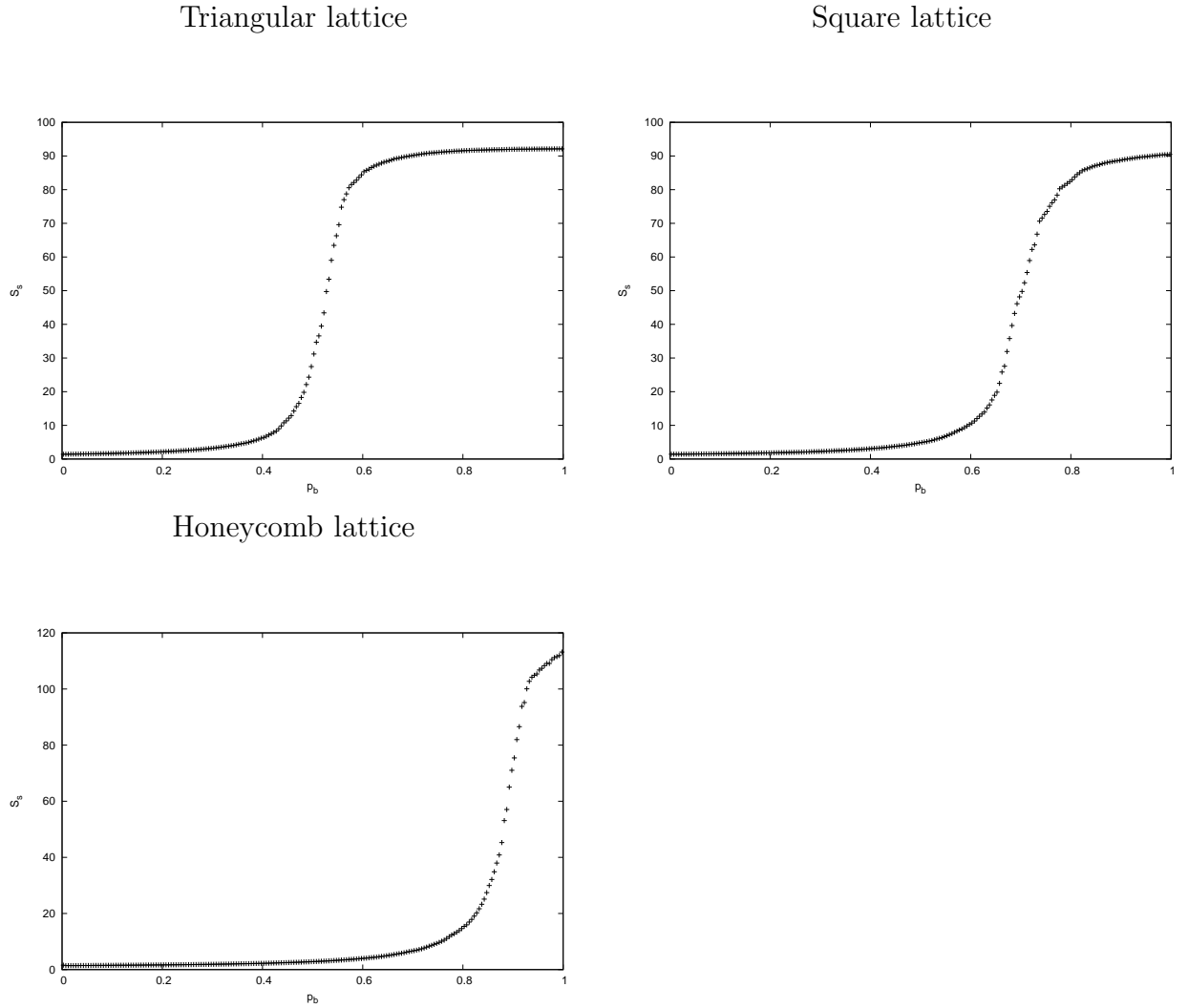
Figures 4.15 to 4.18 show the variation of correlation length as a function of p_b . By analyzing each curve, one can detect roughly the position of the determined critical concentration. The critical concentration is associated with a drastic change in the behaviour of the correlation length as a function of p_b over a small range of its values.

Figure 4.6: Model 2: Cluster distribution in sizes around critical concentration



This drastic change is observed also if one is looking at how the mean cluster size varies with p_b .

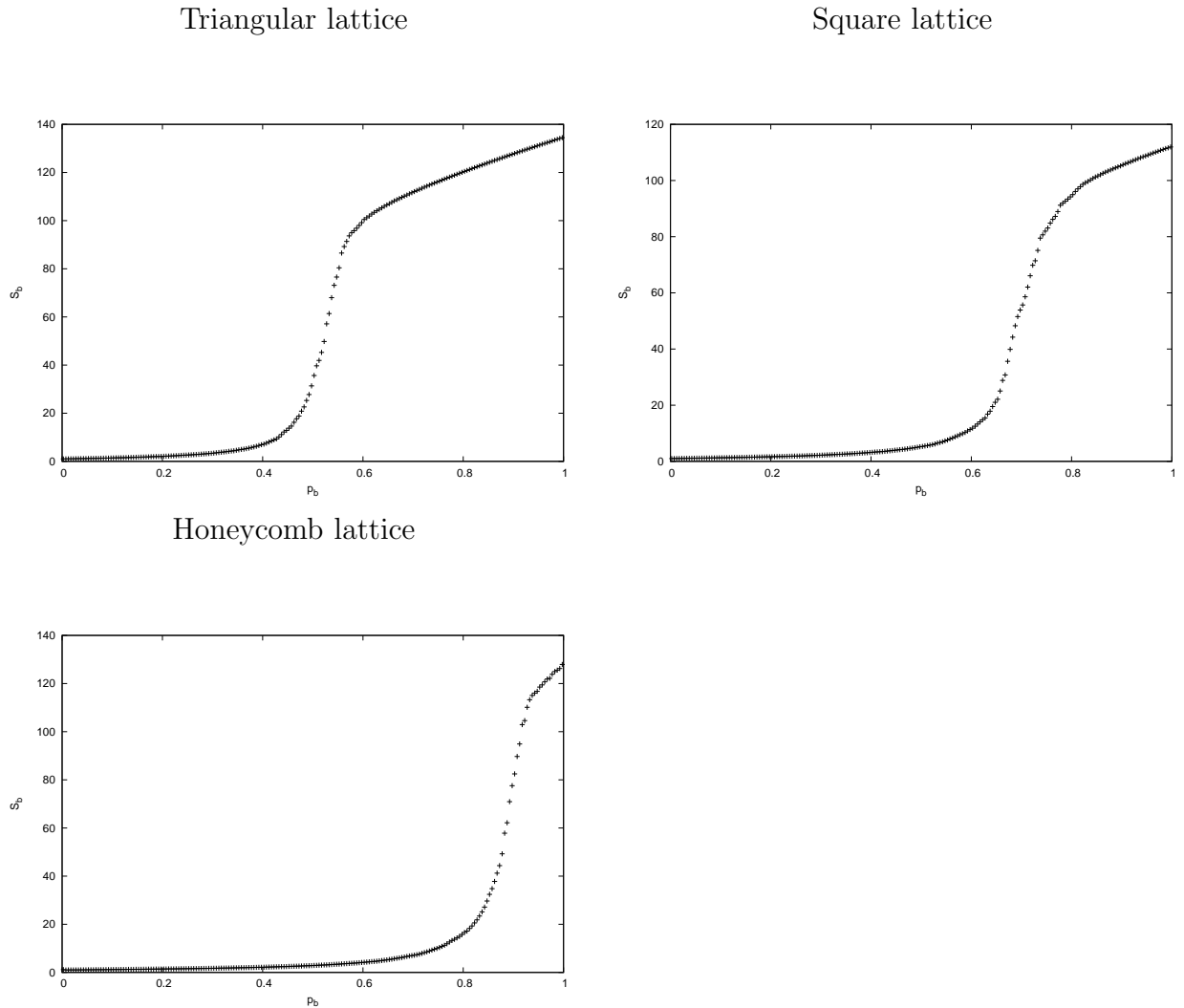
Figure 4.7: Model 1: Mean cluster size S_s



4.5 Comparison of results of models with those of standard bond percolation

In the limit of numerical simulation through Figures 2.2, 4.5, and 4.6 the spanning cluster in a system has the same size in different models related to suppressed bond-site percolation as well in pure bond percolation when the system is around criticality. The same behaviour is also observed by looking at the gyration radius

Figure 4.8: Model 1: Mean cluster size S_b

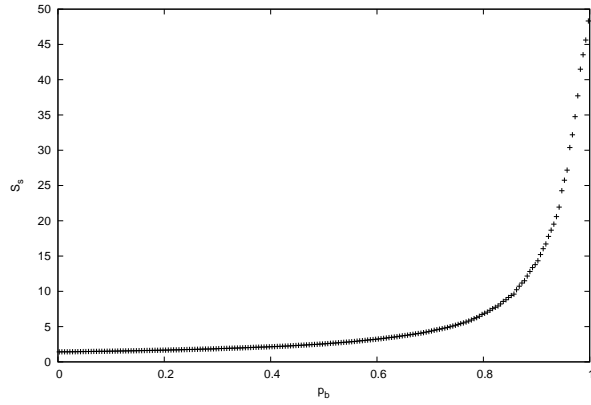


of the largest cluster around the critical concentration through Figures 2.6, 4.11, and 4.12. This fact suggests that the size of a spanning cluster around the critical concentration is an intrinsic property of a system.

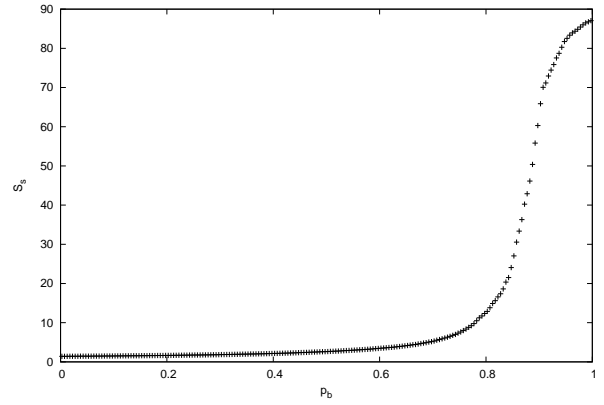
Mean cluster size and correlation length as functions of p_b for both pure bond percolation and suppressed bond-site percolation display a phase transition around critical concentration. Their magnitudes are modulated by the values of p_s and by the rela-

Figure 4.9: Model 2: Mean cluster size S_s

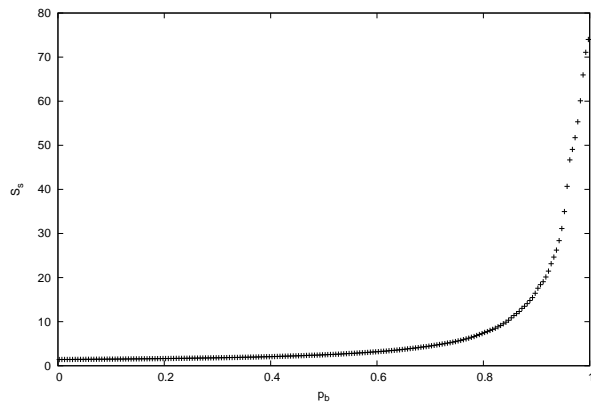
Triangular lattice



Square lattice



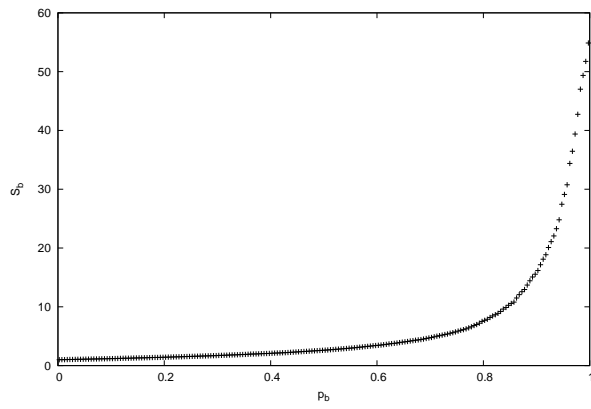
Honeycomb lattice



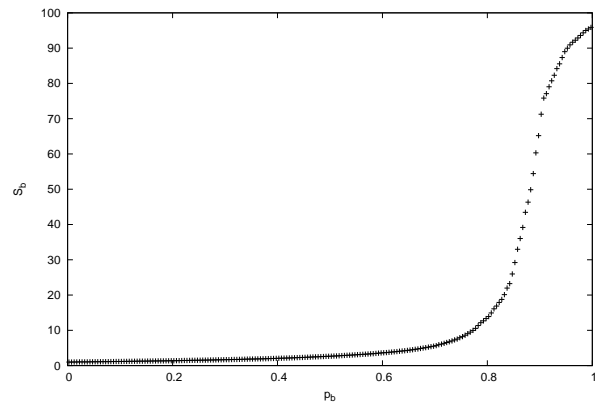
tionship between f_s and p_{bl} (expressed in terms of parameters α and β). Parameters f_s , α , and β fix in which range of values of p_b , there is the critical concentration p_{bc} .

Figure 4.10: Model 2: Mean cluster size S_b

Triangular lattice



Square lattice



Honeycomb lattice

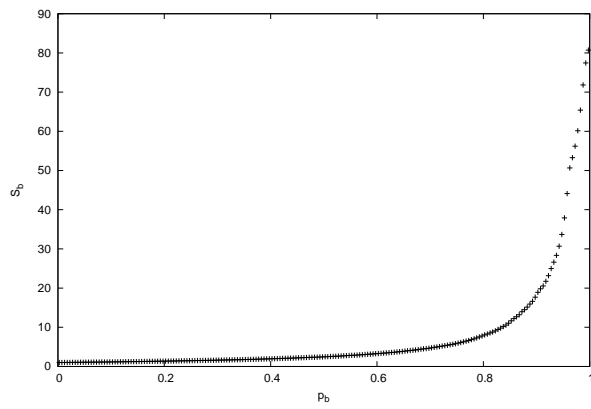
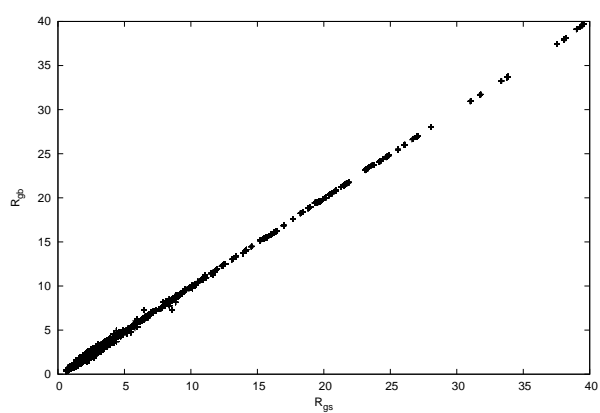
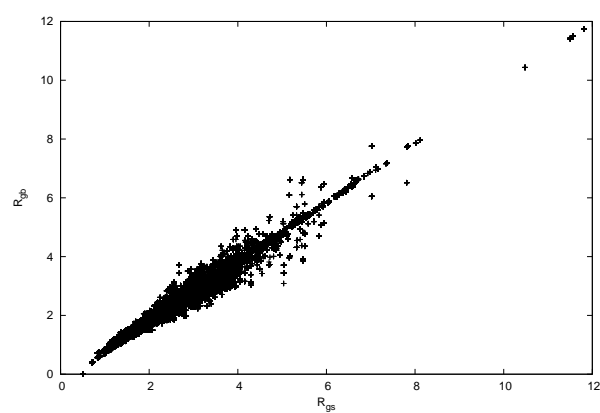


Figure 4.11: Model 1: Cluster distribution in gyration radii

Triangular lattice



Square lattice



Honeycomb lattice

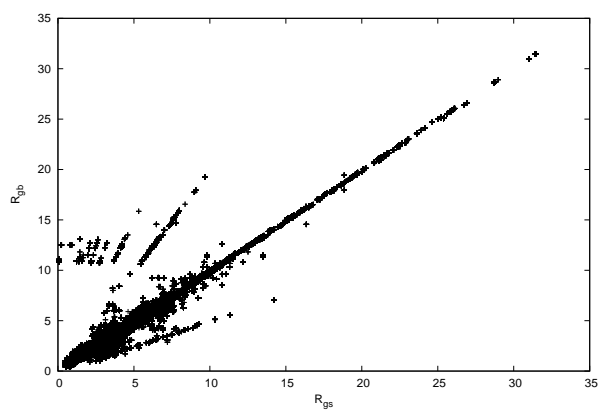
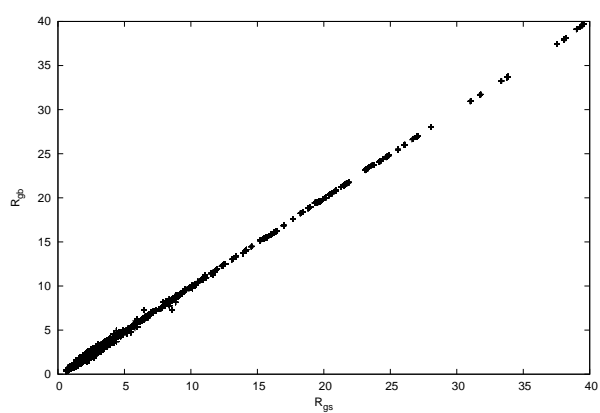
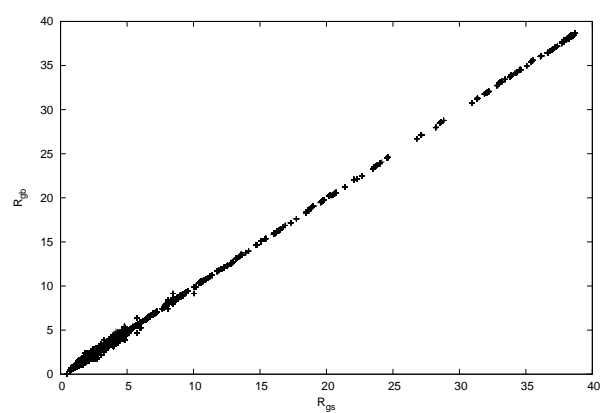


Figure 4.12: Model 2: Cluster distribution in gyration radii

Triangular lattice



Square lattice



Honeycomb lattice

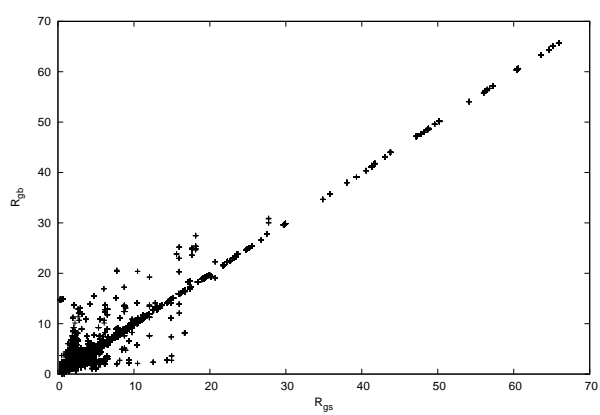
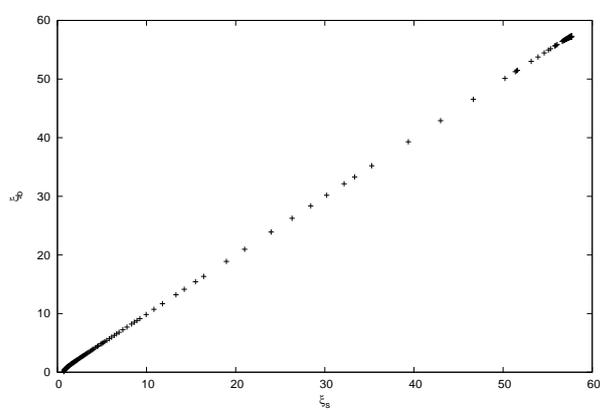
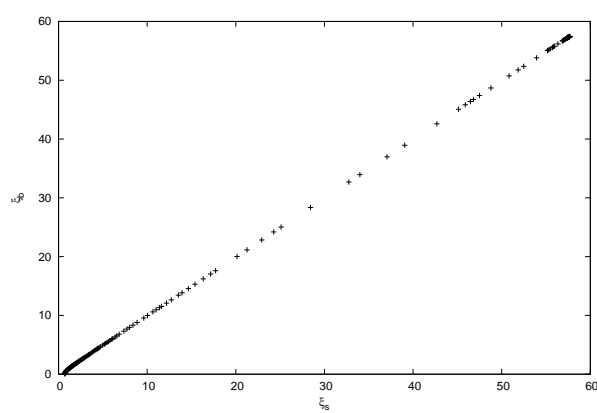


Figure 4.13: Model 1: Comparison between ξ_s and ξ_b

Triangular lattice



Square lattice



Honeycomb lattice

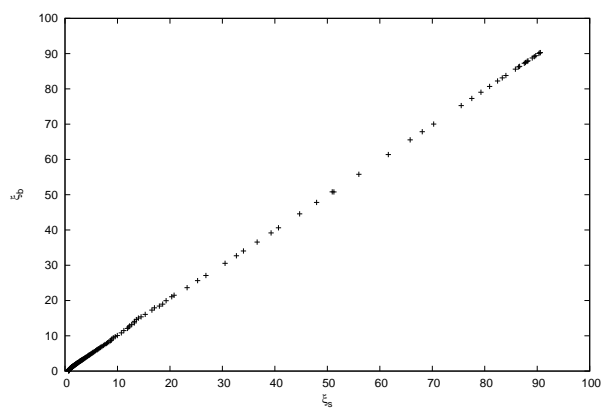
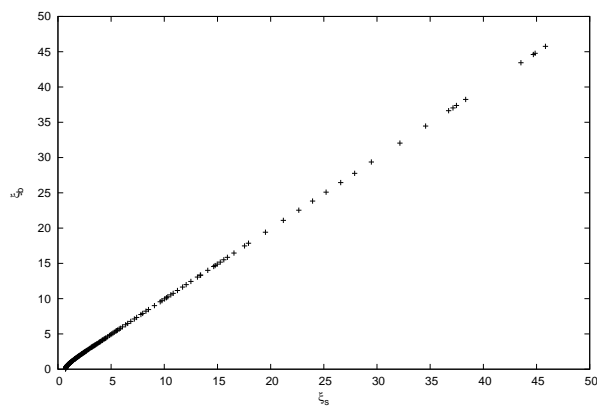
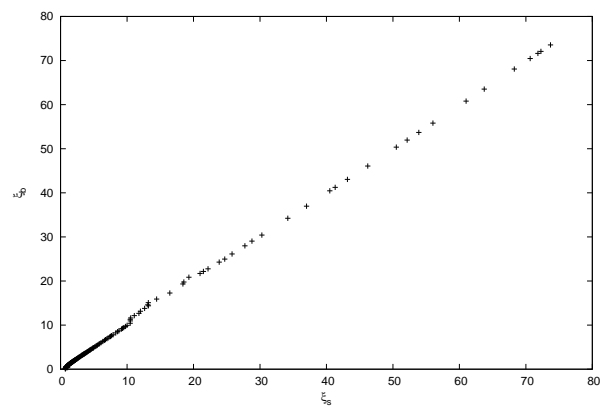


Figure 4.14: Model 2: Comparison between ξ_s and ξ_b

Triangular lattice



Square lattice



Honeycomb lattice

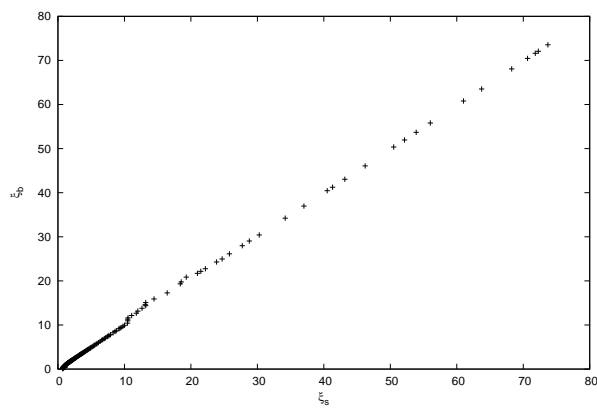
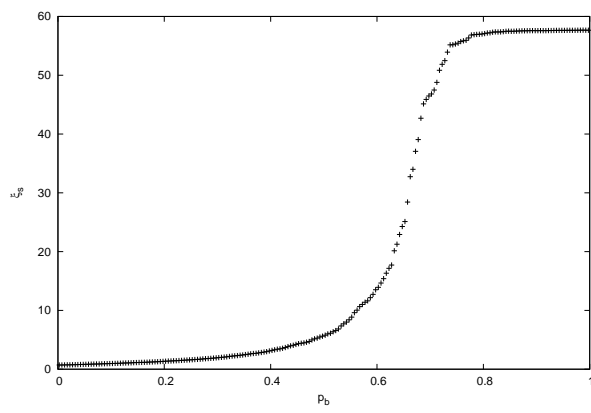
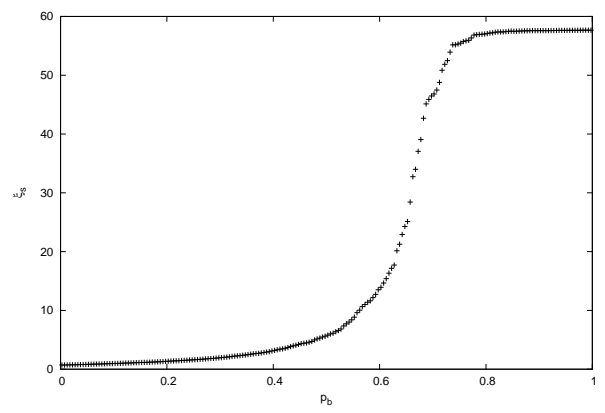


Figure 4.15: Model 1: Variation of ξ_s with p_b

Triangular lattice



Square lattice



Honeycomb lattice

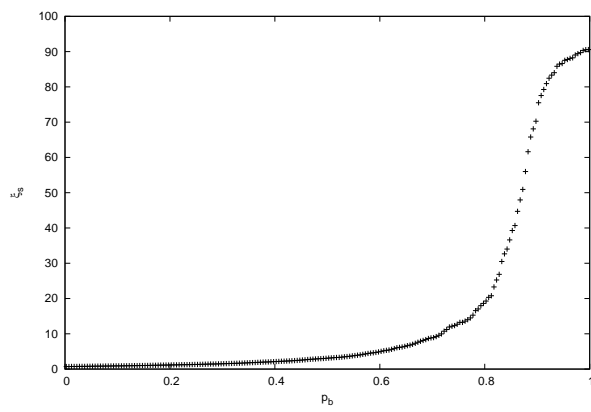
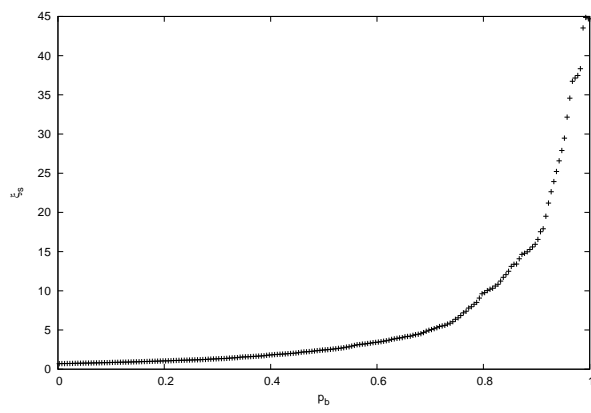
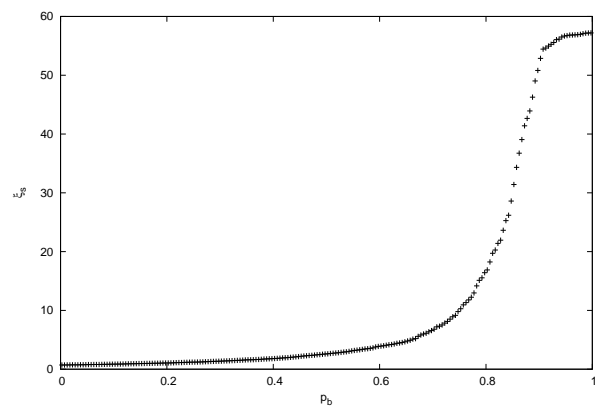


Figure 4.16: Model 2: Variation of ξ_s with p_b

Triangular lattice



Square lattice



Honeycomb lattice

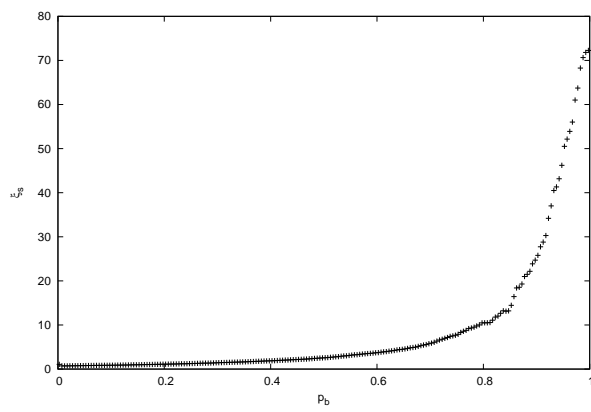
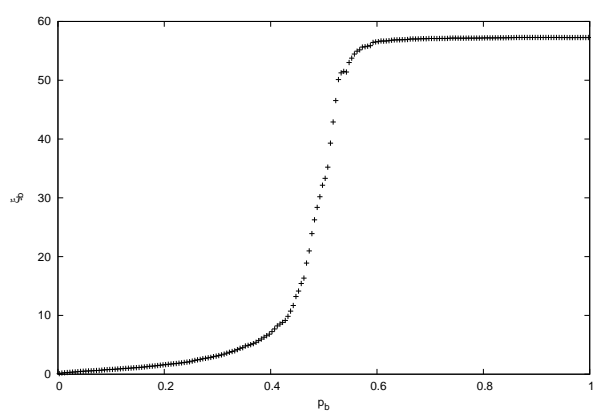
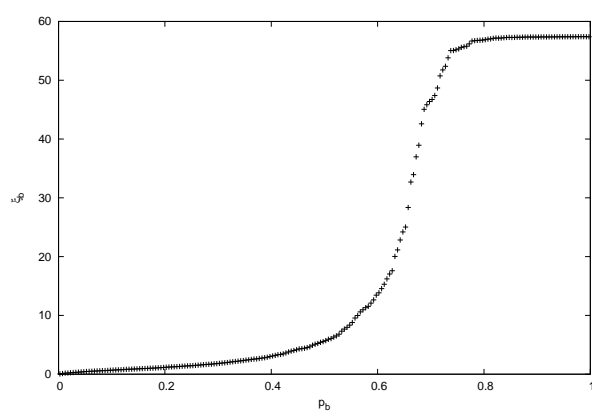


Figure 4.17: Model 1: Variation of ξ_b with p_b

Triangular lattice



Square lattice



Honeycomb lattice

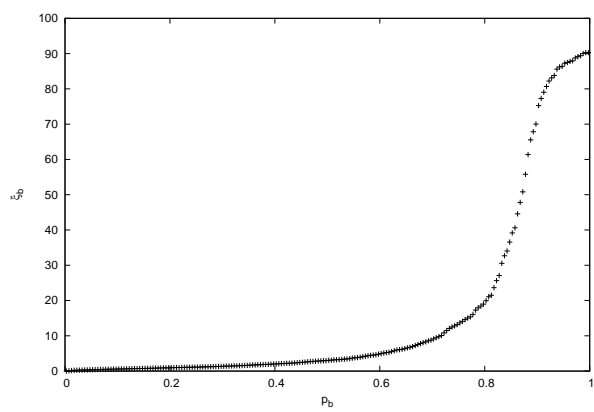
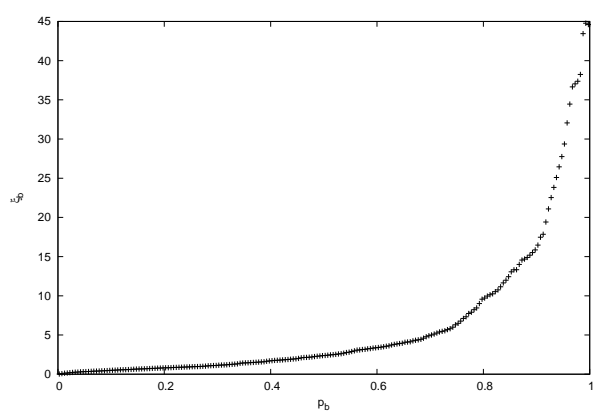
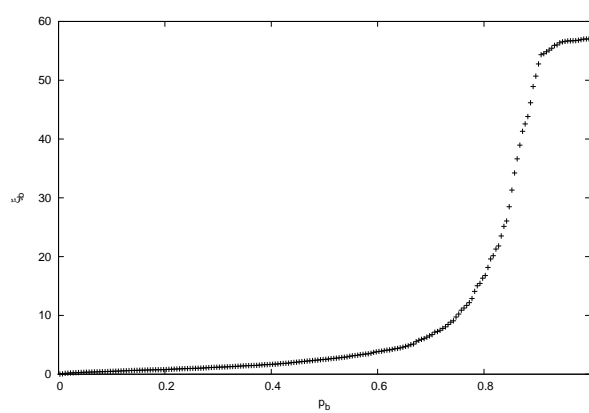


Figure 4.18: Model 2: Variation of ξ_b with p_b

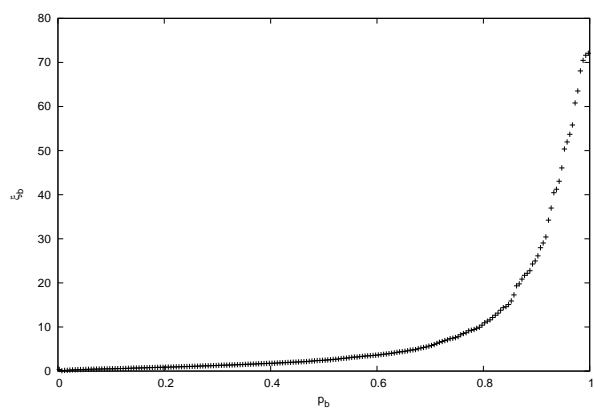
Triangular lattice



Square lattice



Honeycomb lattice



Chapter 5

Directed suppressed bond-site percolation

In this chapter we make a fundamental change to how we consider a bond from the approach in previous chapters. Any bond has two directions which affect the connectivity in cluster distribution. The size also of a cluster depends on the properties in consideration.

Each direction of a bond is chosen with a certain probability. In a square lattice for example, four types of connectivity can be adopted, up, down, left or right.

In this step we combine the effects of changes in three parameters - the percentage of occupied number of sites p_s , the probability of selecting a bond p_b , and the probability of taking one of the two directions on a given bond, let it be called γ . Consequently, a site could belong to different clusters depending on the connectivity introduced by the directionality of a bond.

The effect of the percentage of occupied sites has been observed in bond-site per-

colation – as p_s increases, the value of the critical concentration p_{bc} decreases. In chapter 4 we selected a bond according a probability p_b , but opened the bond according to the probability p_{bl} and its relationship to f_s which describes the fraction of occupied sites in the neighbourhood of the given bond. Since $p_b \leq 1$, the system either does not reach percolation or does so at a threshold value very close to the limit value of $p_{bc} = 1$.

Due to the limitation of our resources, calculations for different quantities are run for systems reduced to $N = 50$ (N gives an indication on the size of systems by referring it to Table 2.1). This is mainly due to the fact that depending on bond directions, a single site can belong to multiple clusters unlike the previous models where a site could only belong to one cluster. The storage of a file containing data needed in the determination of various properties demands a space of 1GB just for only one iteration, and the running time is in the order of one hour.

5.1 Models and partition of the (p_s, p_b) plane

In our model we look at the flow of information from the top to the bottom of our system. Each bond direction is chosen randomly with probability γ . For all lattices, γ corresponds to the bond direction from the higher to lower site label (see Figure 2.1). For the square lattice as an example, vertical bonds are chosen with probability γ down and horizontal bonds with probability γ to the left. Clearly the up and right probabilities will be $1 - \gamma$.

If γ is varied from 1 to 0.5 according to the model used, the critical concentration changes from a low value to high one if the system can reach percolation in the given circumstances. With our lattice samples, the system does not reach percola-

tion if a bond has a 50 % chance to be taken in one of the two directions. The two connectivities down-left and up-right present a certain symmetry.

Figure 5.1 illustrates how the partition of the (p_s, p_b) plane in percolating and non-percolating zones is modified for three high values of probability connectivity of bonds in one privileged direction (γ taking values 1.00, 0.95, and 0.85), combined with the respective low values of probability ($1 - \gamma$ taking values 0.00, 0.05, and 0.15) of having connectivity of bonds in the opposite direction. We choose different models for the different lattice types to show the general variation of the curves with γ .

The diagram for the triangular lattice corresponds to the case of correlated bond site percolation where $p_{bl} = f_s$. The model 2 is given in the case of a honeycomb lattice where the parameter $\beta = 0.85$. In the square lattice we consider the pure bond percolation where once the end sites of a bond are occupied, the bond is opened with probability one. For each type of lattice, the low curve (curve with stars) corresponds to the highest value of γ (equal to 1), while the up one (curve with plus) is related to $\gamma = 0.85$.

Tables 5.1 and 5.2 give average values of p_{bc} determined numerically for various values of p_s for models 1 and 2 on which the directivity of bonds has been added and expressed in terms of the parameter γ . These data are plotted in Figure 5.2 and correspond to $\alpha = 1$ and $\gamma = 0.85$. The parameter β is taking values $\frac{3}{6}$, $\frac{3}{4}$, and $\frac{5}{6}$ for triangular, square, and honeycomb lattices respectively.

As p_s varies, it appears that there are some values for which we do not have perco-

Table 5.1: Model 1: Numerical values of p_{bc} for various values of p_s for $\gamma = 0.85$, $\alpha = 1$

p_s	p_{bc}		
	Triangular lattice	Square lattice	Honeycomb lattice
0.50	–	–	–
0.55	$0.98837 \pm 1.16285\text{E-}03$	–	–
0.60	$0.98043 \pm 1.22289\text{E-}03$	–	$0.99835 \pm 5.21938\text{E-}04$
0.65	$0.95108 \pm 1.52139\text{E-}03$	–	$0.98849 \pm 2.24472\text{E-}03$
0.70	$0.83709 \pm 2.15131\text{E-}03$	–	$0.96896 \pm 2.39930\text{E-}03$
0.75	$0.72832 \pm 1.37536\text{E-}03$	$0.99867 \pm 2.05700\text{E-}04$	$0.94814 \pm 2.89797\text{E-}04$
0.80	$0.67311 \pm 1.57970\text{E-}03$	$0.96529 \pm 9.39541\text{E-}04$	$0.91657 \pm 2.25209\text{E-}03$
0.85	$0.60956 \pm 1.06682\text{E-}03$	$0.89474 \pm 1.02558\text{E-}03$	$0.88031 \pm 1.72819\text{E-}03$
0.90	$0.55110 \pm 1.16155\text{E-}03$	$0.82811 \pm 8.68724\text{E-}04$	$0.85655 \pm 1.20441\text{E-}03$
0.95	$0.51604 \pm 5.96525\text{E-}04$	$0.77257 \pm 7.71500\text{E-}04$	$0.84198 \pm 1.08899\text{E-}03$
1.00	$0.49211 \pm 1.10786\text{E-}03$	$0.72083 \pm 7.09638\text{E-}04$	$0.81678 \pm 1.21141\text{E-}03$

lation due to the simultaneous effect of our parameters. In Figure 5.1 where γ has three different values, the relation between p_s and p_{bc} looks like a transcendental function.

For Figure 5.2 there is a plateau at $p_b = 1$, for lower values of p_s whose can be shifted left or right depending on the parameter β defined in model 2.

Table 5.2: Model 2: Numerical values of p_{bc} for various values of p_s

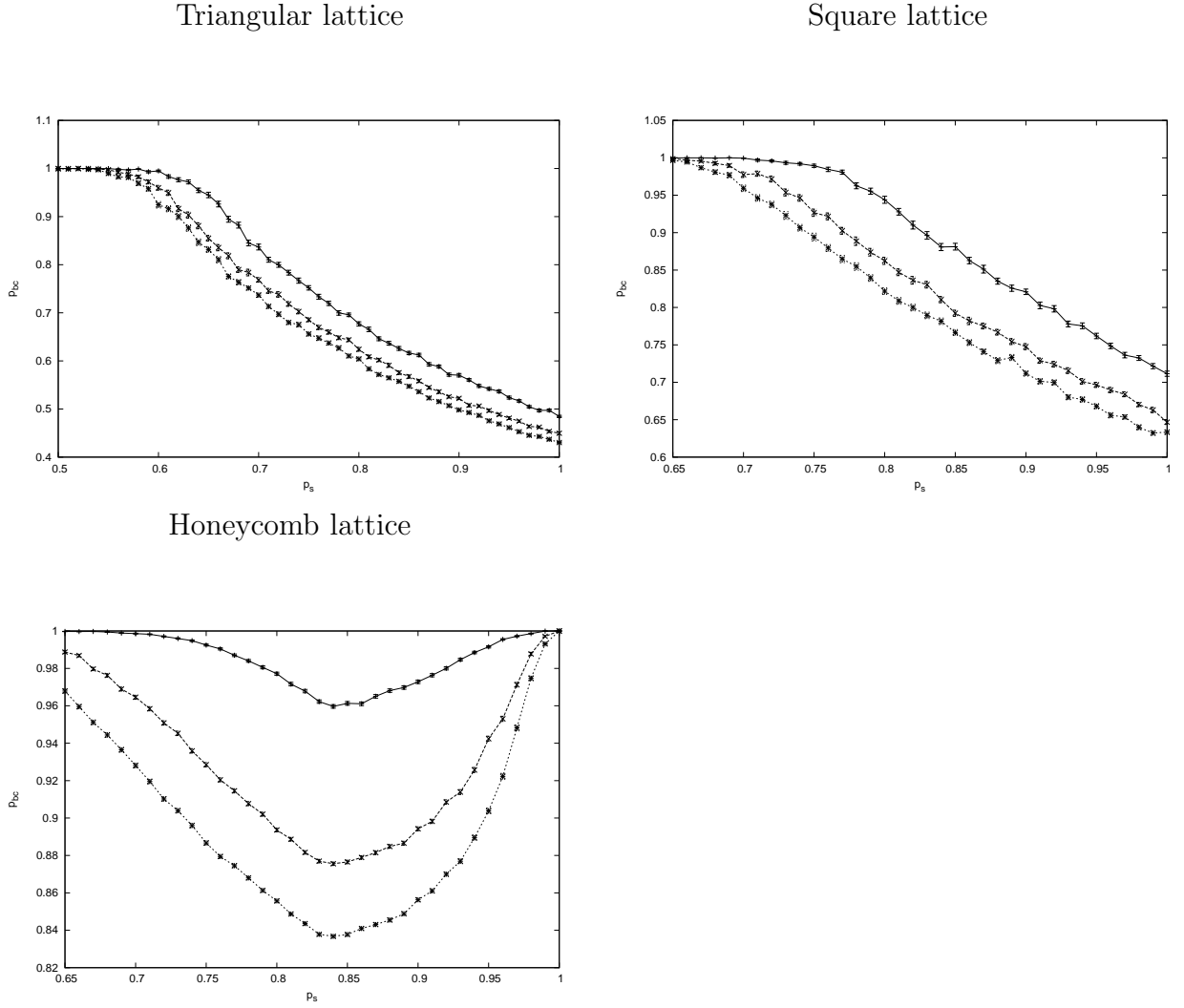
p_s	p_{bc}		
	Triangular lattice	Square lattice	Honeycomb lattice
0.50	–	–	–
0.55	$0.99716 \pm 2.83523\text{E-}04$	–	–
0.60	$0.98984 \pm 7.51098\text{E-}04$	–	–
0.65	$0.86316 \pm 1.12836\text{E-}03$	–	$0.98423 \pm 1.87625\text{E-}03$
0.70	$0.84064 \pm 1.70115\text{E-}03$	$0.99997 \pm 2.35192\text{E-}05$	$0.93423 \pm 2.19445\text{E-}03$
0.75	$0.74775 \pm 1.45864\text{E-}03$	$0.99655 \pm 3.33572\text{E-}04$	$0.92583 \pm 2.29930\text{E-}03$
0.80	$0.74647 \pm 1.08853\text{E-}03$	$0.96640 \pm 9.85848\text{E-}04$	$0.88451 \pm 2.40910\text{E-}03$
0.85	$0.71259 \pm 1.69867\text{E-}03$	$0.91991 \pm 1.12976\text{E-}03$	$0.87321 \pm 1.30076\text{E-}03$
0.90	$0.68155 \pm 1.50769\text{E-}03$	$0.88841 \pm 1.30576\text{E-}03$	$0.88716 \pm 1.29975\text{E-}03$
0.95	$0.75443 \pm 4.72189\text{E-}03$	$0.90756 \pm 1.89467\text{E-}03$	$0.89789 \pm 3.77930\text{E-}03$
1.00	–	–	–

5.2 Size and mean cluster size

In Figures 5.3 and 5.4, for each cluster we compare its number of bonds and sites for systems around critical concentration. A site can belong to different clusters due to aspects of connectivity induced by the directionality of bonds. It appears that most clusters contain more bonds than sites.

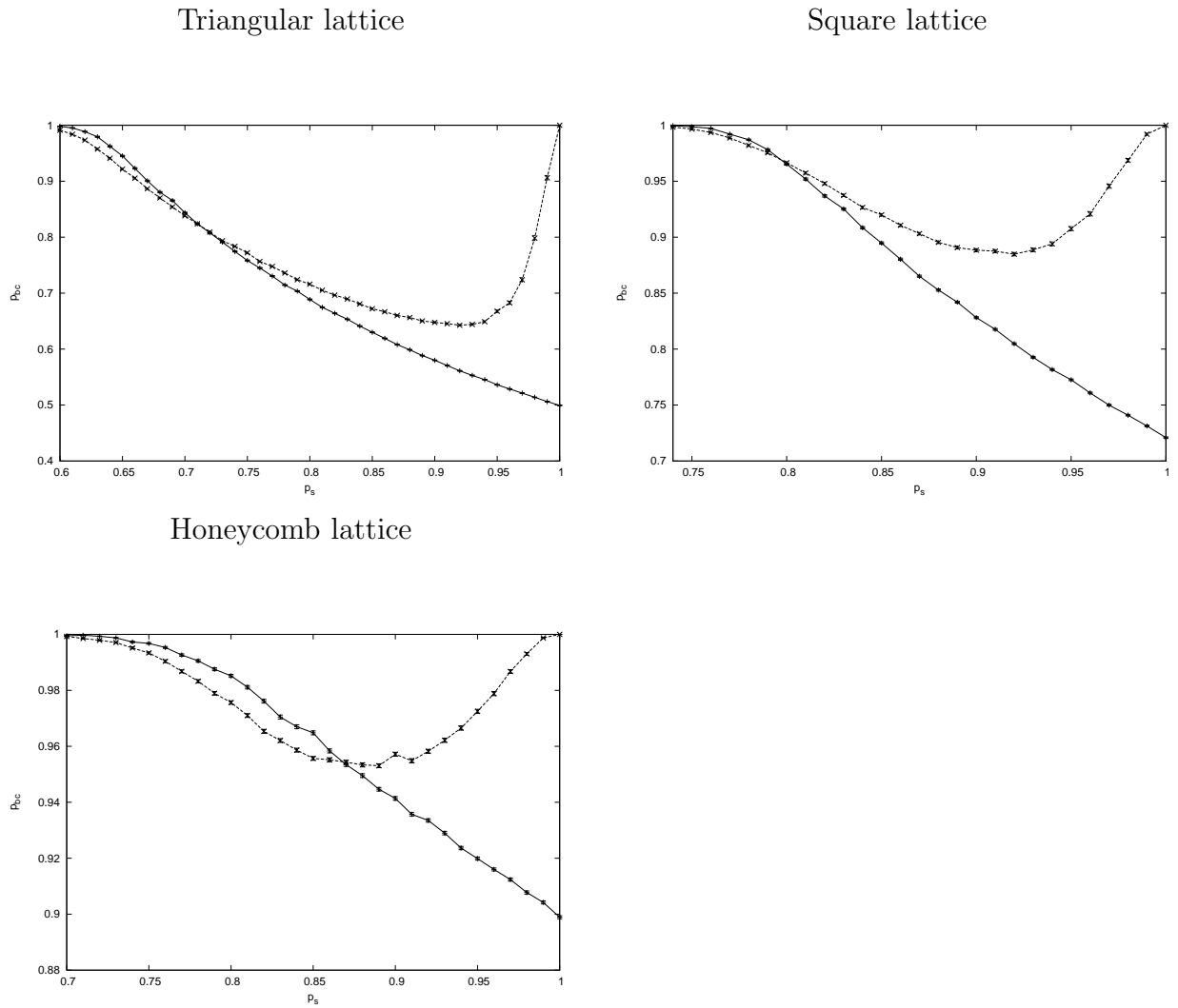
From Figure 5.5 to Figure 5.8, mean cluster sizes S_s and S_b are plotted as functions of p_b in particular way for both models when γ is maintained equal to 0.85, the fraction of occupied sites p_s is 0.85, and in model 1 α is 1 while in model 2 β

Figure 5.1: Variation of p_{bc} versus p_s for three values of γ



takes values $\frac{3}{6}$, $\frac{3}{4}$, and $\frac{5}{6}$ for triangular, square, and honeycomb lattices respectively. Through these graphs, one can determine in which range of values of p_b is the critical concentration of a given system.

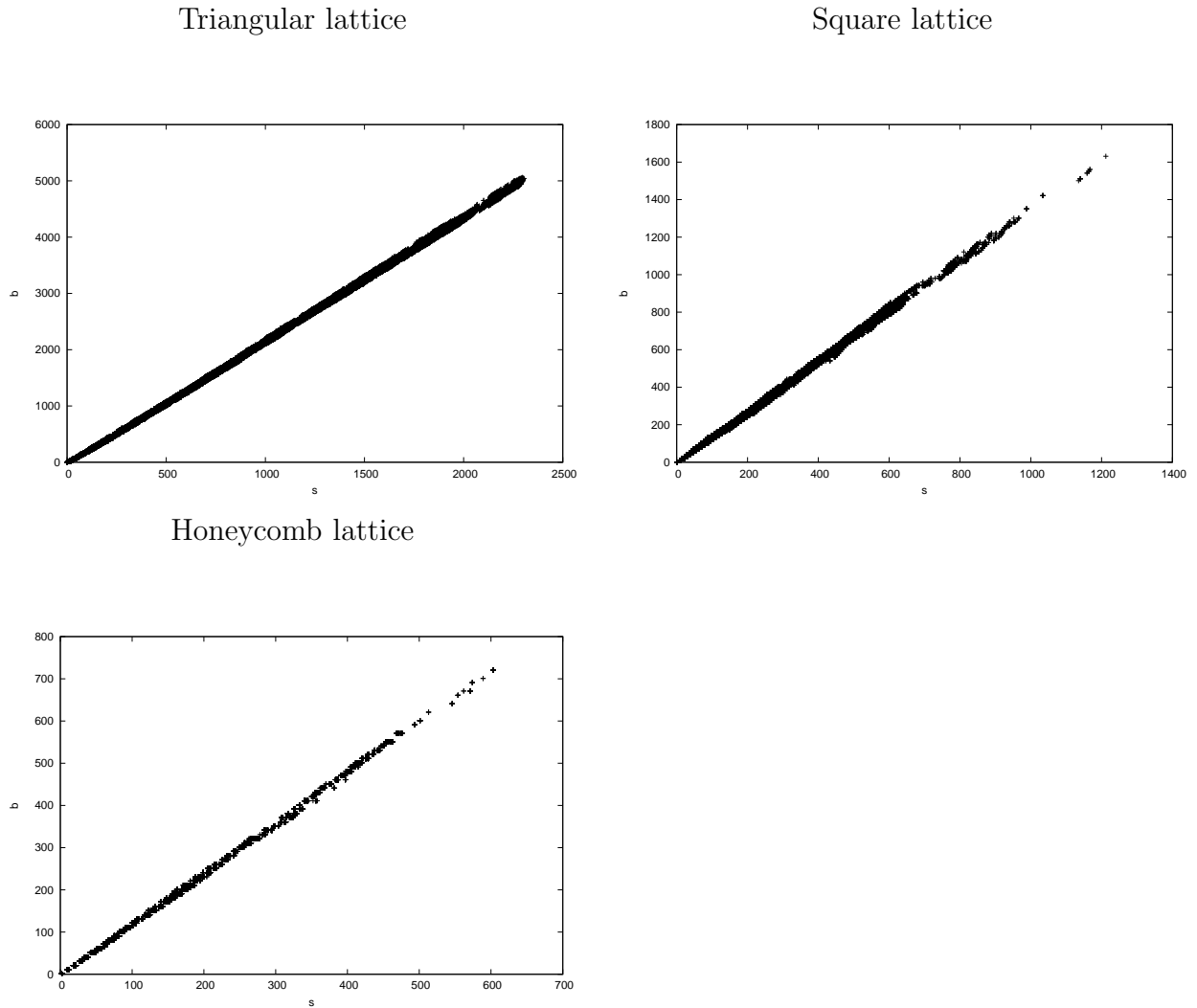
Figure 5.2: Variation of p_{bc} versus p_s in models 1 and 2 for $\gamma = 0.85$. Solid curve is model 1, dashed curve is model 2



5.3 Gyration radius and correlation length

Figures 5.9 and 5.10 show the lost of linearity between R_{gs} and R_{gb} due to the fact that a site may belong to multiple different clusters. Under these circumstances, the systems do not contain loops due to the directivity of bonds. The magnitude of R_{gs} or R_{gb} compared to the quantity Δ defined in Chapter 2 is always less than a

Figure 5.3: Model 1: Cluster distribution in sizes

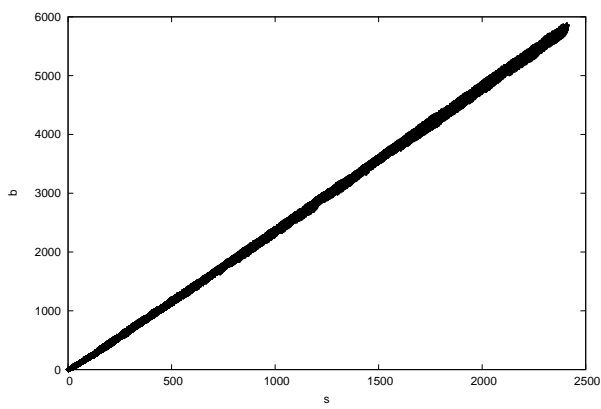


half of this.

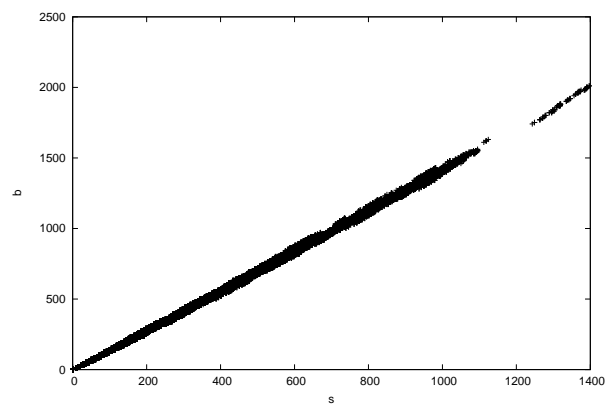
In Figures 5.11 and 5.12 we compared correlation lengths ξ_s and ξ_b for the whole range of values of p_b . The same quantities are also plotted as functions of p_b from Figure 5.13 to Figure 5.16. As found before, these curves allow to localise the critical concentration for each system.

Figure 5.4: Model 2: Cluster distribution in sizes

Triangular lattice



Square lattice



Honeycomb lattice

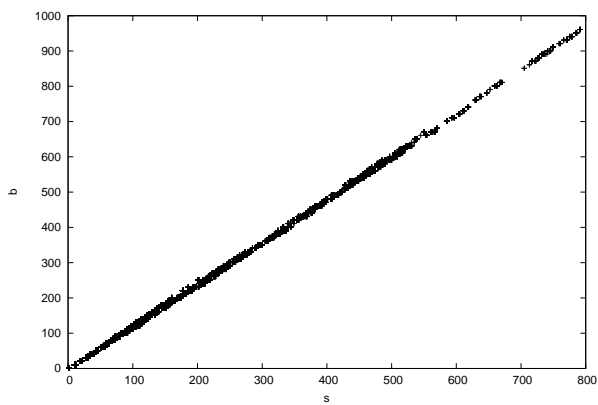
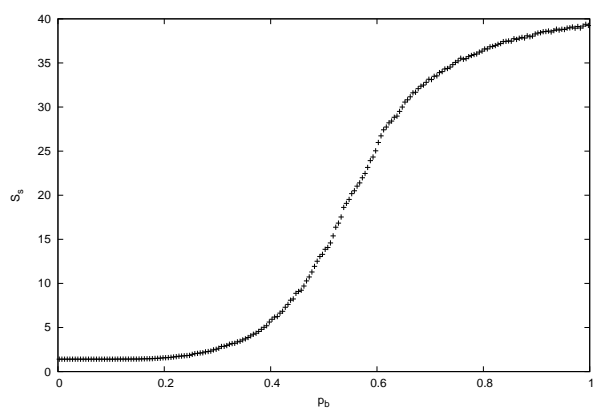
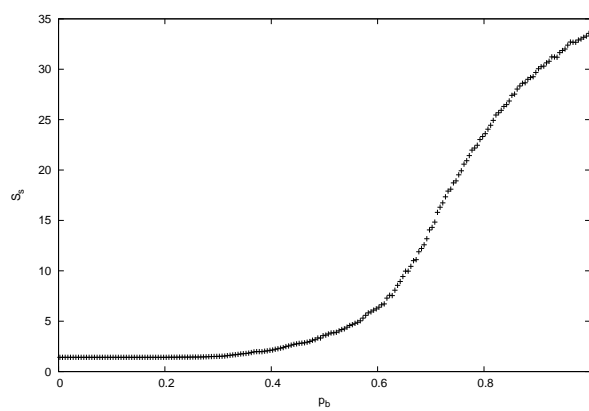


Figure 5.5: Model 1: Mean cluster size S_s

Triangular lattice



Square lattice



Honeycomb lattice

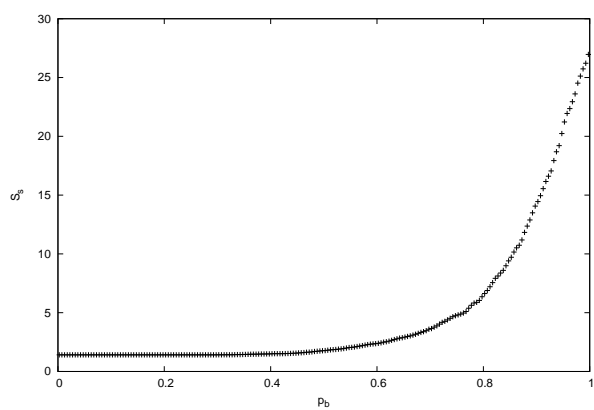
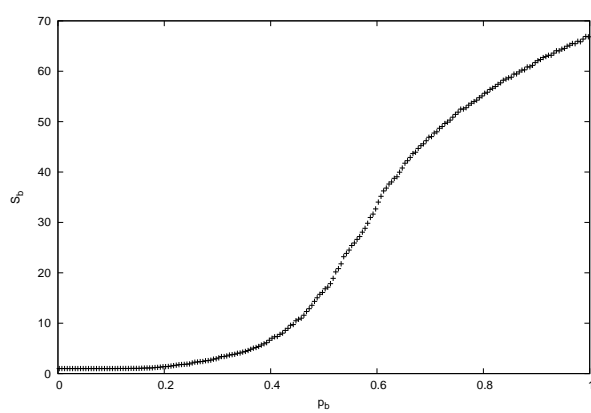
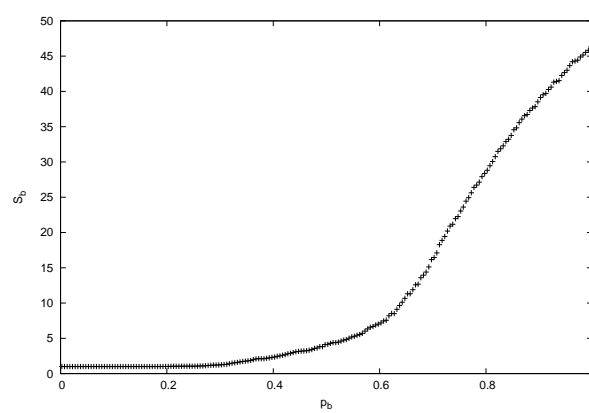


Figure 5.6: Model 1: Mean cluster size S_b

Triangular lattice



Square lattice



Honeycomb lattice

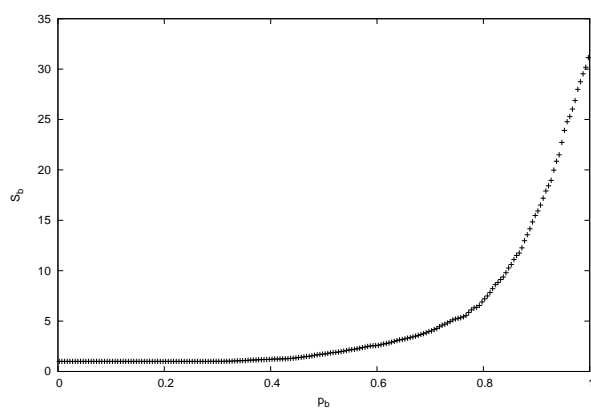
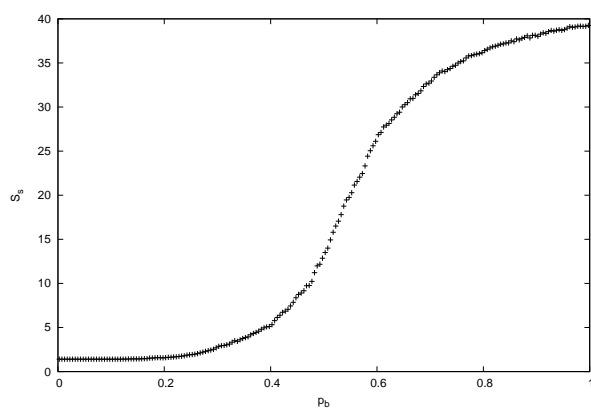
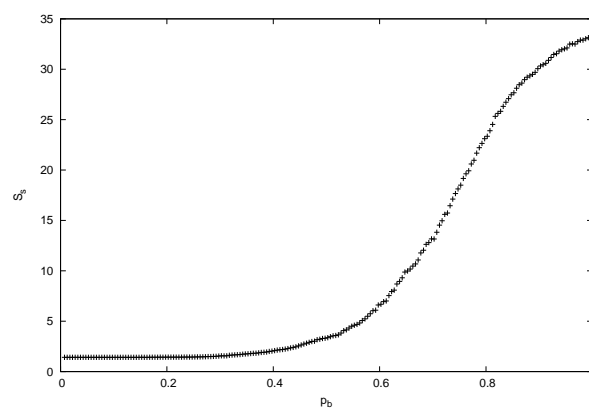


Figure 5.7: Model 2: Mean cluster size S_s

Triangular lattice



Square lattice



Honeycomb lattice

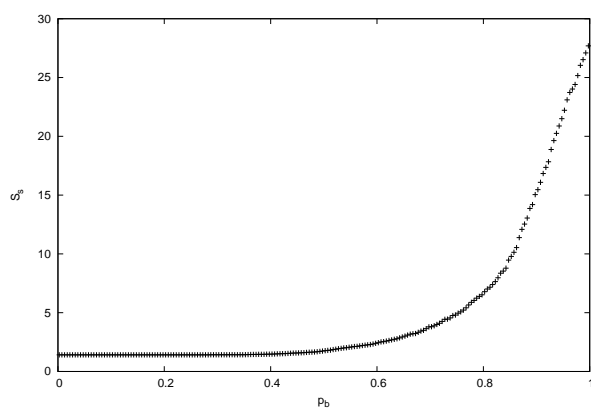
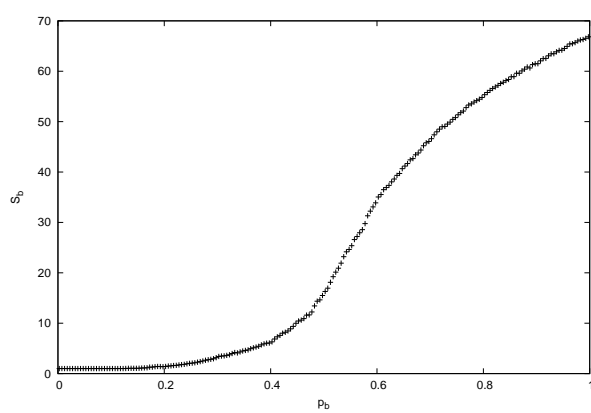
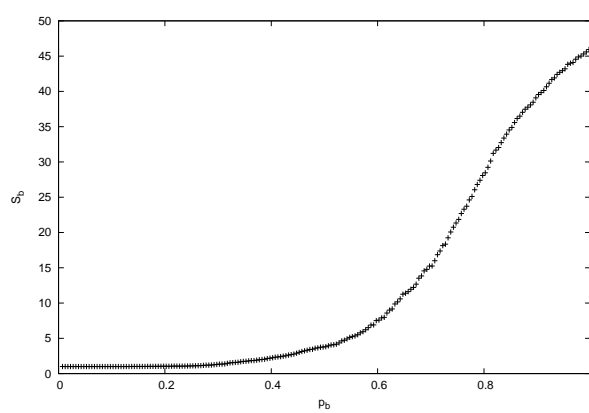


Figure 5.8: Model 2: Mean cluster size S_b

Triangular lattice



Square lattice



Honeycomb lattice

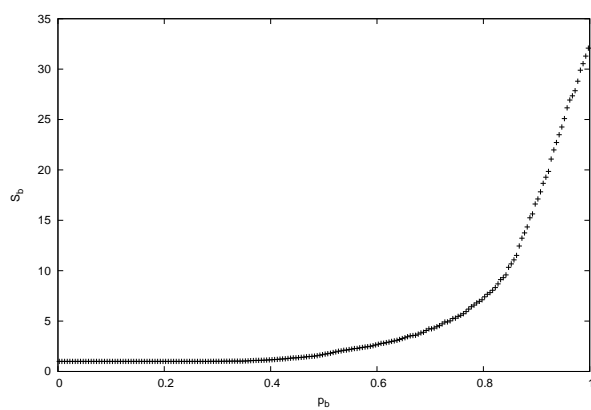
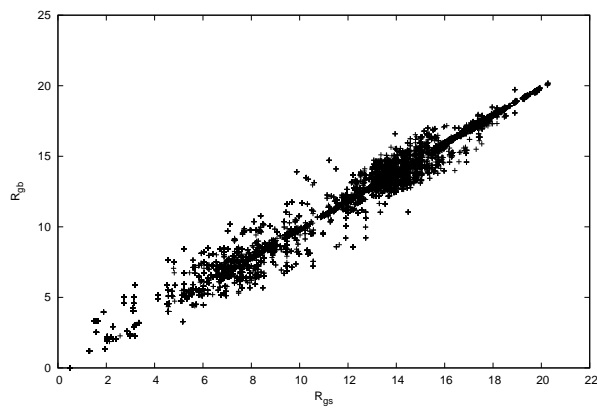
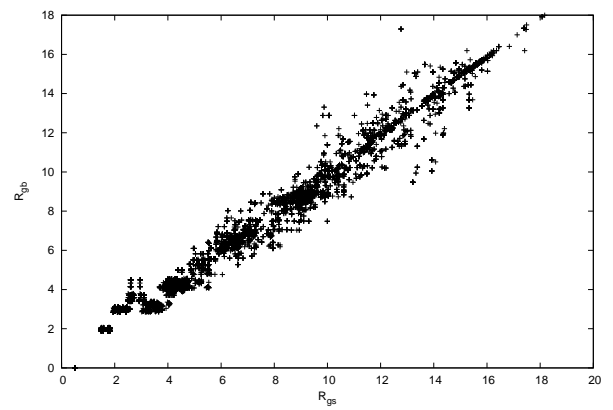


Figure 5.9: Model 1: Cluster distribution in gyration radii around critical concentration

Triangular lattice



Square lattice



Honeycomb lattice

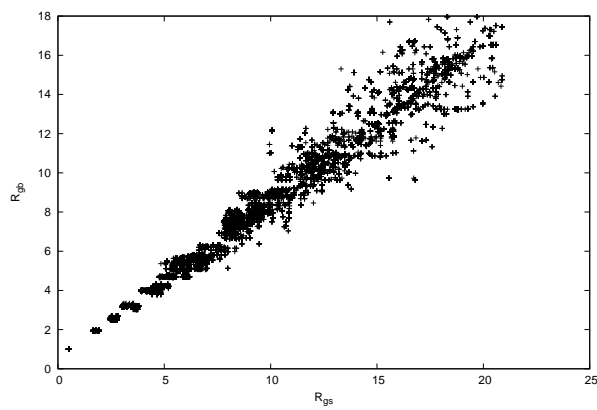
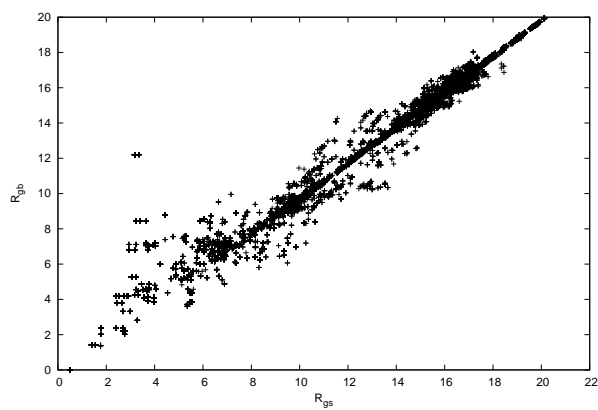
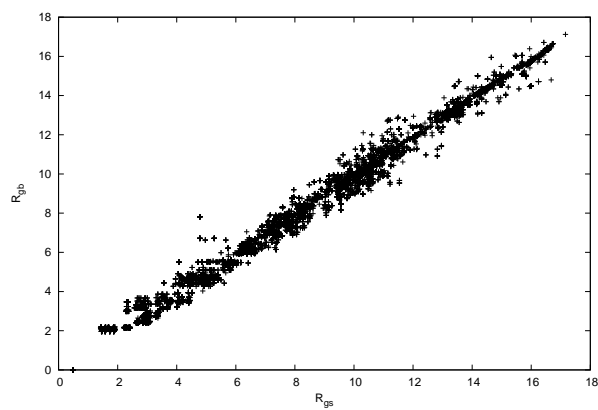


Figure 5.10: Model 2: Cluster distribution in gyration radii around critical concentration

Triangular lattice



Square lattice



Honeycomb lattice

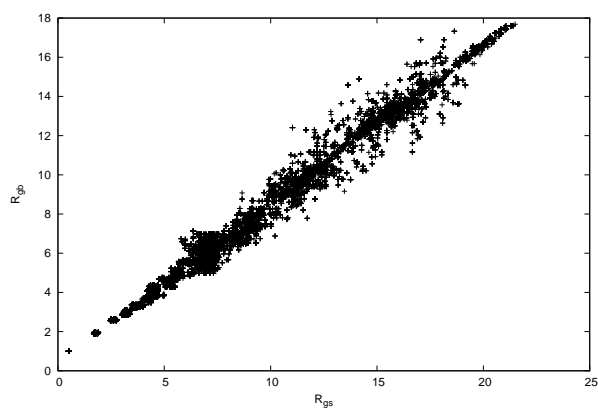
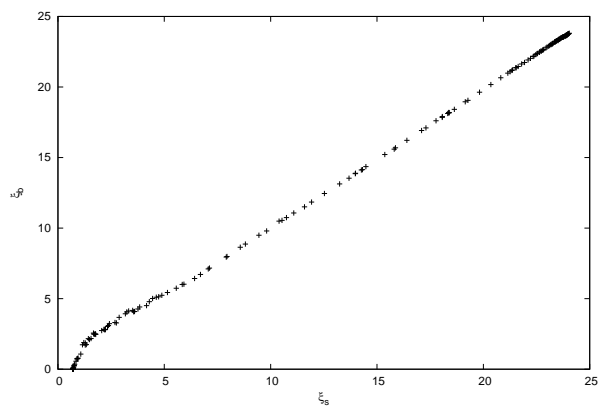
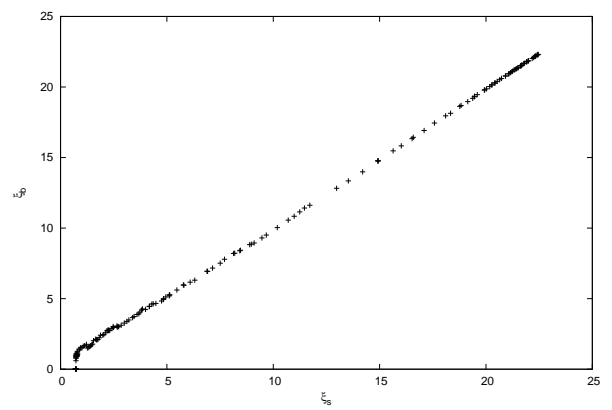


Figure 5.11: Model 1: Comparison between ξ_s and ξ_b

Triangular lattice



Square lattice



Honeycomb lattice

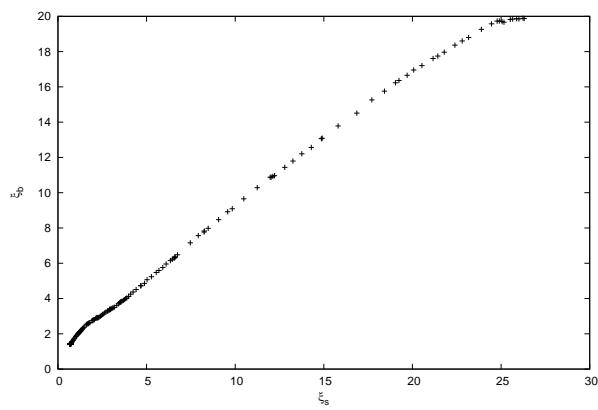
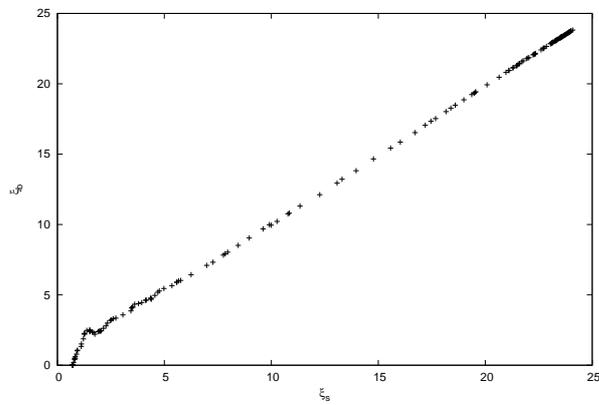
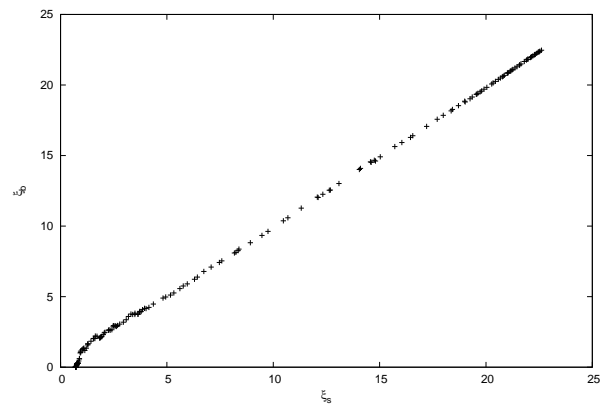


Figure 5.12: Model 2: Comparison between ξ_s and ξ_b

Triangular lattice



Square lattice



Honeycomb lattice

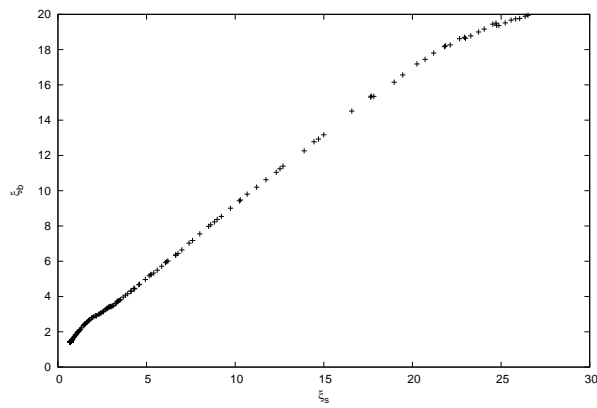
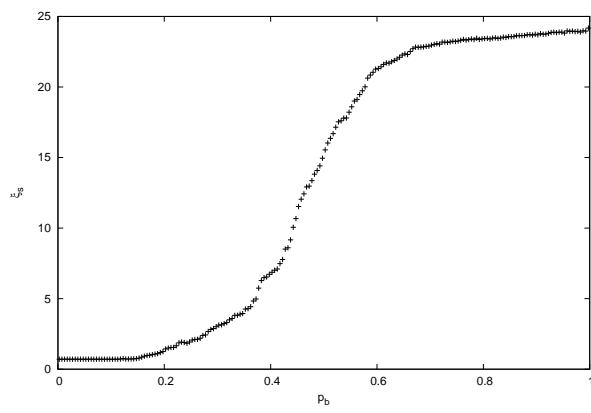
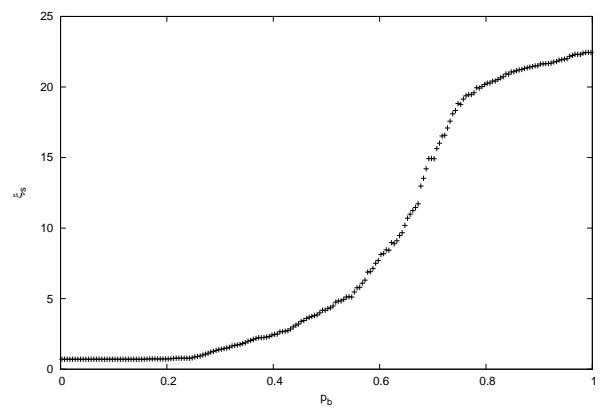


Figure 5.13: Model 1: Variation of ξ_s with p_b

Triangular lattice



Square lattice



Honeycomb lattice

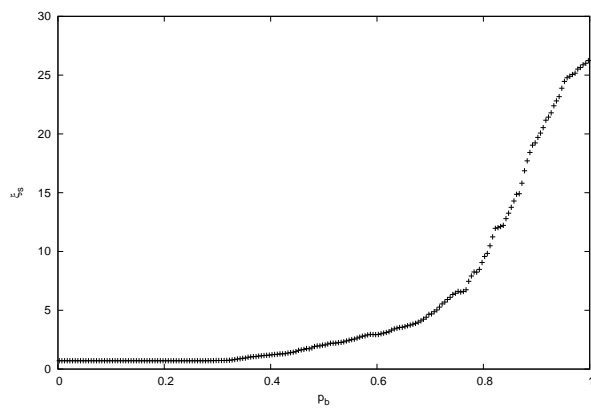
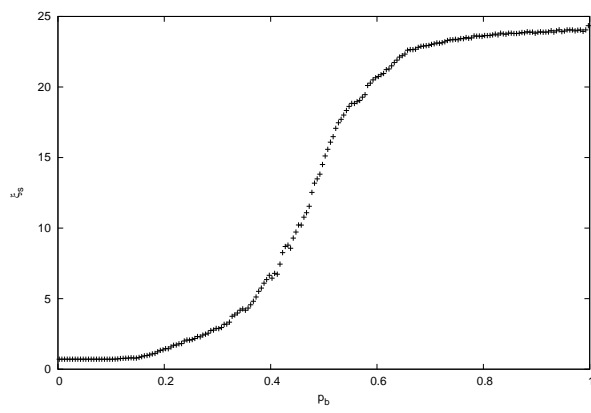
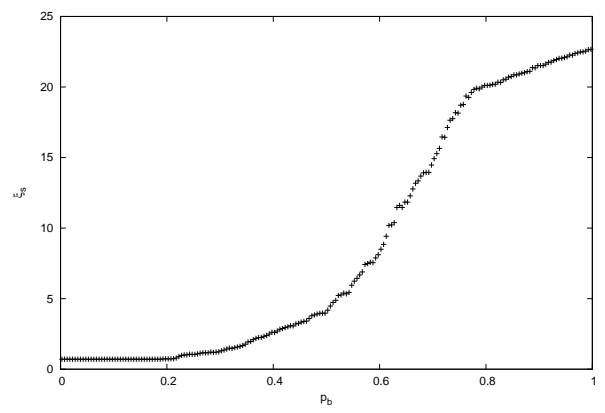


Figure 5.14: Model 2: Variation of ξ_s with p_b

Triangular lattice



Square lattice



Honeycomb lattice

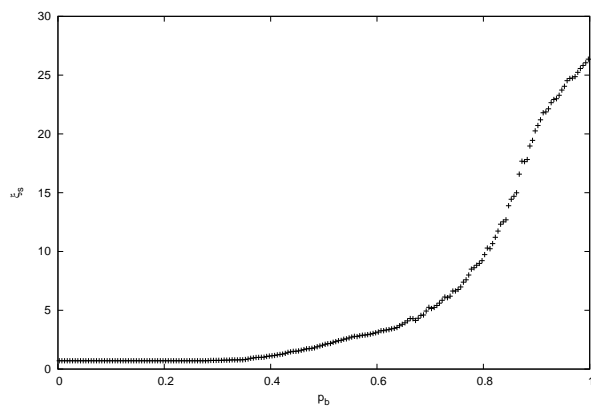
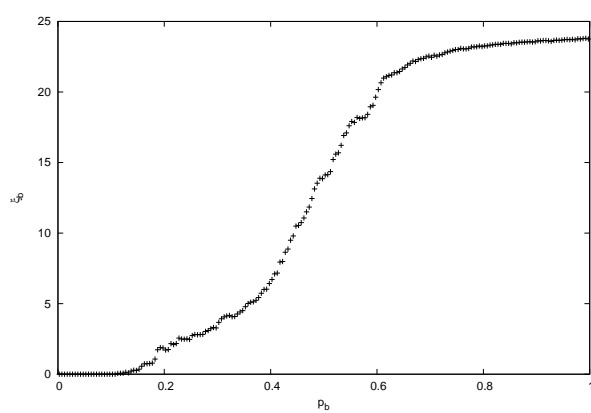
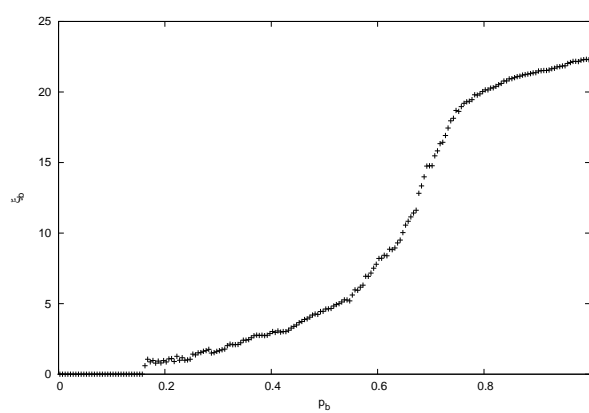


Figure 5.15: Model 1: Variation of ξ_b with p_b

Triangular lattice



Square lattice



Honeycomb lattice

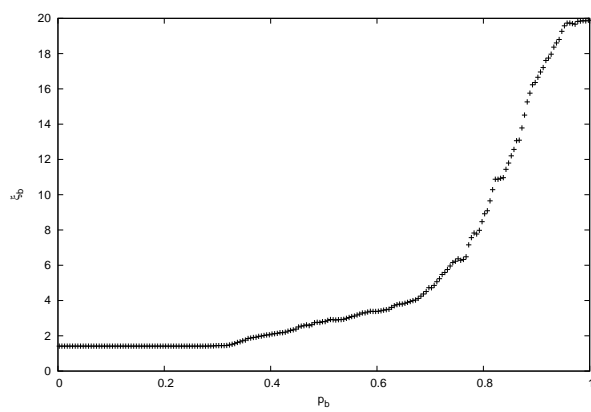
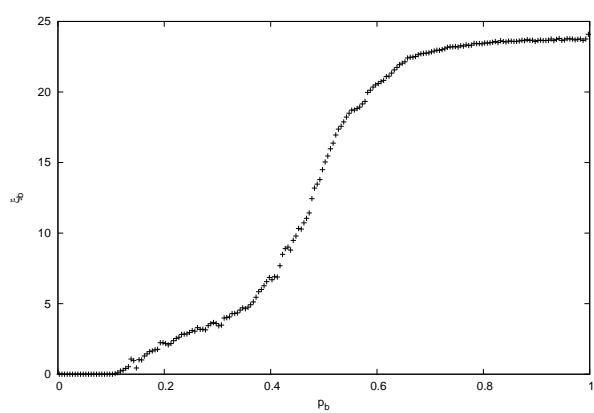
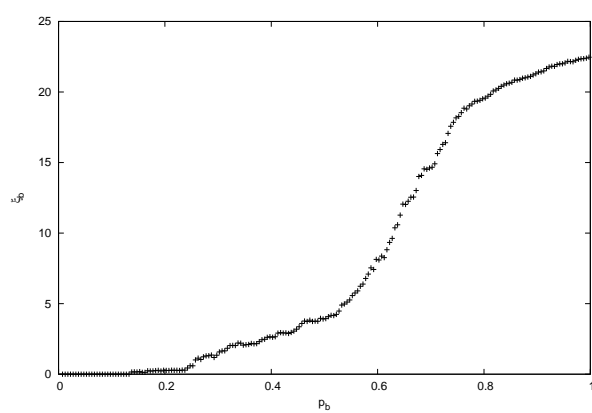


Figure 5.16: Model 2: Variation of ξ_b with p_b

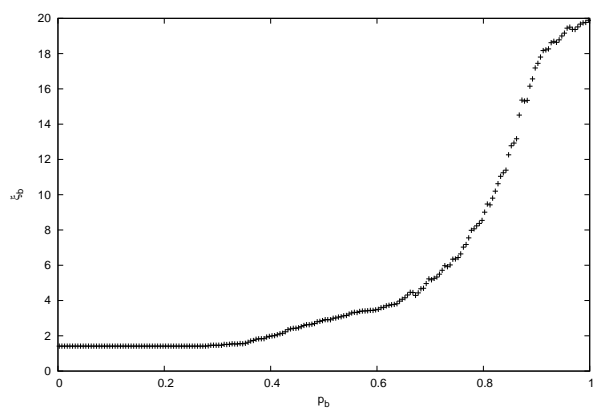
Triangular lattice



Square lattice



Honeycomb lattice



Chapter 6

Conclusions

In the introductory chapter we developed basic known notions of percolation theory and most of its applications. This work constitutes an extension of a MSc study on some numerical aspects of percolation theory in which we determined the cluster number scaling function and its associated critical exponents for lattices in 2-dimensions.

The standard pure bond-site percolation has been analyzed by counting up simultaneously the number of sites and bonds in a cluster. Once a bond is chosen, its end sites are occupied with probability 1. Useful quantities to describe the geometrical structure of clusters are determined for three 2-dimensional lattices (triangular, square, and honeycomb). Referred simultaneously to the number of bonds and sites that each cluster contains, these quantities are cluster size, mean cluster size, radius of gyration, and correlation length.

From Figures 2.2, 3.2, 4.5, 4.6, 5.4 and 5.5, where we compared the number of sites and bonds inside clusters when a system is around critical concentration, the numbers of sites and bonds are comparable. The boundary effects do not seem to

affect this feature.

We observed a similar behaviour on other determined quantities such as mean cluster size, gyration radius, and correlation length. The only changes observed are in the ranges of probabilities of opening bonds in which systems percolate and in the magnitudes of quantities. Clusters of low size contain more inside loops compared to those of large size.

For each system (related to N and the type of lattice), around critical concentration, the percolating cluster (i.e. the largest cluster in the system) seems to be an intrinsic property of the system. Its gyration radius and size are practically the same for both considered models (suppressed bond-site percolation and directed suppressed bond-site percolation) in the limit of a numerical simulation using Monte Carlo methods. The study of the mean cluster and correlation lengths as functions of the probability of opening a bond p_b shows that these quantities present a phase transition around critical concentration. Their magnitudes are modulated by the relation between fraction of occupied sites p_s and p_b , and by the probability of taking one of the two directions of a bond γ . Around critical concentration, the ratio between the number of bonds and the number of sites inside a cluster increases from the case of pure bond percolation to that of directed suppressed bond percolation.

The relationship between f_s and p_{bl} moves the critical curve in the (p_s, p_b) plane separating the percolating area to the non-percolating zone. In other words, the details of the percolation threshold depend on whether site distribution is related or not to the occupation of bonds[78]. In bond-site percolation, the critical concentration p_{bc} depends upon the macroscopic structure of the system and varies from one configuration of the system to another configuration[79]. There is a minimum percentage

of occupied sites in a lattice sample for which a system can reach percolation. That fraction of occupied sites, as shown in Tables 3.2, 4.1, 4.2, 5.1 and 5.2, is greater than the corresponding critical concentration for pure site percolation as given in Table 3.1 and the percentage increases as a relationship is established between f_s and p_{bl} . This change is more pronounced by the introduction of the directivity of bonds.

In model 2 the system reaches percolation when the fraction of occupied sites is in the range of β . Through figures representing the partition of (p_s, p_b) plane into percolating and non-percolating zone, one may understand that a value of p_{bc} close to 1 means that the system has less chance to reach percolation. For two systems with the same occupied site fraction and with the same value of p_b , that which reaches percolation has a higher mean cluster size and correlation length than one which does not.

The suppressed directed bond site percolation in the physical world can be symbolized by a ground soil having a kind of porosity, since the water may flow through it by gravity. However, the water may also be retained in the ground by capillarity. This has an impact on the wettability of the surface of soil and on water penetration. Working soils and use of organic material as fertilizer act on the porosity and hydraulic conductivity[30].

Some cluster properties are defined in the limit of infinitely large clusters. Consideration of both sites and bonds of percolation systems suggests the following further future investigation:

- the *cluster dimension* D known as a fractal (D not an integer)[80], and defined by a scaling relation of the form $s \propto l^D$ or $b \propto l^D$. Here s and b are the

number of sites and bonds located at the distance l relative to a reference point over which the averages are determined.

- the *spectral dimension of a cluster* which is related to the probability of reversal of a diffusion process.
- the *cluster strength* termed also as the probability that a cluster is a part of the infinite cluster. One may understand that this is an extrinsic property of clusters.

The above quantities (cluster dimension, spectral dimension and cluster strength) are properties of a single connected cluster. The determination that we did for S_s (or S_b) and ξ_s (or ξ_b) corresponds to the configuration of a collection of clusters. The cluster size or its mass and the radius of gyration are defined only for a finite cluster and do not have a meaning for an infinite cluster.

Appendix

This appendix gives an introduction to the use of the attached CD containing all codes in fortran 90, and templates for graphs in gnuplot that we used in this research. Codes are grouped by chapter topics and lattice type, while templates are set per chapter.

In our codes we use a random number generator found on the web site <http://www.math.keio.ac.jp/matsumoto/emt.html> coded in C by Takuji Nishimura and Makoto Matsumoto and converted in Fortran by Josi Rui Faustino de Sousa.

Programs with extension *11.f90 or *12.f90

It is in the main program where the size of the lattice and the number of iterations are set, and where the random number generator is initialized. We also specify in the files where we store data to be treated. The main uses a module containing a set of subroutines with the follow duties:

- Set up the fraction of open sites. This step is not needed for the case of pure bond percolation because all sites are opened with probability one.

- Treat aspects of different types of bond percolation: pure bond percolation, uncorrelated bond-site percolation, suppressed bond-site percolation, and directed suppressed bond site percolation. The decision of opening a bond with an appropriate probability (1, randomly, or correlated) is made at this stage.
- Identify the occupied nearest-neighbour sites of an occupied site.
- Update recursively the connectivity of clusters once an opened bond joins two clusters or a site and an existing cluster.

Other programs

Some programs allow the determination of the critical concentration, and the calculation of the mean cluster size and the correlation length. With gnuplot, it was difficult to handle a large file bigger than 8 GB to plot the distribution of clusters in sizes or in gyration radii around critical concentration. The program *cut.f90* was used to solve the problem.

Codes used may be improved in order to store exclusively or calculate systematically the needed quantities. I'm not able to count how many calculations stopped due to the shortage of enough space for storage. The big file produced was in the range of 48 GB after a week. For any body whose interest is to compile and run such codes, it is very important at anytime to verify the efficiency of the compiler and the random number generator, and be sure that resources are capable to handle data or to produce these data at the allotted time. Sometimes, you can wait days and weeks for unhelpful results.

References

- [1] R. Zallen, *Polychromatic percolation: Coexistence of percolating species in highly connected lattices*, Physical Review B **16** (1977), 1426.
- [2] D. Stauffer, *Scaling theory of percolation clusters*, Physics Reports **54** (1979), 1.
- [3] S. Kirkpatrick, *Percolation and conduction*, Review of Modern Physics **45** (1973), 574.
- [4] J. W. Essam, *Percolation theory*, Reports on Progress in Physics **43** (1980), 833.
- [5] D.J. Amit, *Field theory, the renormalization group, and critical phenomena*, World Scientific Publishing, Singapore, 1984.
- [6] R. Sahara, K. Ohno, and Y. Kawazoe, *Weak universality of a site percolation model with two different sizes of particles on a square lattice*, Journal of the Physical Society of Japan **68** (1999), 3755.
- [7] J.C. Wierman, *Mixed percolation on the square lattice*, Journal of Applied Probabilities **21** (1984), 247.
- [8] N. Chabot, *La percolation, un modèle des phénomènes de porosité*, Le journal de Maths des élèves **1** (1994), 26.

- [9] J. C. Wierman, *Bond percolation on honeycomb and triangular lattices*, *Advanced Applied Probabilities* **13** (1981), 298.
- [10] http://en.wikipedia.org/wiki/Percolation_theory.
- [11] M. Dolz, F. Nieto, and A. J. Ramirez-Pastor, *Dimer site-bond percolation on a square lattice*, *The European Physical Journal B* **43** (2005), 363.
- [12] G.H. Weiss, *Contemporary problems in statistical physics*, Society for Industrial and Applied Mathematics, Philadelphia, 1994.
- [13] A. Aharony, *Universal critical amplitude ratios for percolation*, *Physical Review B* **22** (1980), 400.
- [14] J. Kurkijärvi and T. C. Padmore, *Percolation in two-dimensional lattices*, *Journal of Physics A: Mathematical and General* **8** (1975), 683.
- [15] P. Agrawal, S. Redner, P. J. Reynolds, and H. E. Stanley, *Site-bond percolation: a low-density series study of the uncorrelated limit*, *Journal of Physics A: Mathematical and General* **12** (1979), 2073.
- [16] R. M. Ziff, X. P. Kong, and E. G. D. Cohen, *Lorentz lattice-gas and kinetic-walk model*, *Physical Review A* **44** (1991), 2410.
- [17] J. S. Andrade, A. D. Araújo, S. V. Buldrev, S. Havlin, and H. E. Stanley, *Dynamics of viscous penetration in percolation porous media*, *Physical Review E* **63** (2001), 51403.
- [18] Academic Press, *Dictionary of science and technology*, 1992.
- [19] H. Nakanishi and H. E. Stanley, *A test of scaling near the bond percolation threshold*, *Journal of Physics A: Mathematical and General* **11** (1978), L190.

- [20] M. F. Sykes, M. Glen, and D. S. Gaunt, *The percolation probability for site problem on the triangular lattice*, Journal of Physics A: Mathematical, Nuclear and General **7** (1974), L105.
- [21] G. Kortemeyer, W. Bauer, and G. J. Kunde, *Isospin dependent multifragmentation in $^{112}\text{Sn} + ^{112}\text{Sn}$ and $^{124}\text{Sn} + ^{124}\text{Sn}$ collisions*, Physical Review C **55** (1997), 2730.
- [22] M. Sahimi, *Applications of percolation theory*, Taylor & Francis, London, 1994.
- [23] M. Yanuka and R. Engelman, *Bond-site percolation: empirical representation of critical probabilities*, Journal of Physics A: Mathematical and General **23** (1990), L339.
- [24] J. C. Gimel, T. Nicolai, and D. Durand, *Relation between aggregation and phase separation: Three-dimensional Monte Carlo simulations*, Physics Review E **66** (2002), 061405.
- [25] J. Goldenberg, B. Libai, S. Solomon, N. Jan, and D. Stauffer, *Marketing percolation*, Physica A **284** (2000), 335.
- [26] D.J. Jacobs and M.F. Thorpe, *Generic rigidity percolation in two dimensions*, Physical Review E **53** (1996), 3682.
- [27] A. Coniglio, *Some cluster size and percolation problems for interacting spins*, Physical Review B **13** (1976), 2194.
- [28] M. Kotori, *Percolation transitions and wetting transitions in stochastic models*, Brazilian Journal of Physics **30** (2000), 83.
- [29] E. Ben-Naim and P. L. Krapivsky, *Cluster approximation for the contact process*, Journal of Physics A: Mathematical and General **27** (1994), L481.

- [30] L. Vidal-Beaudet and S. Charpentier, *Percolation theory and thermodynamics of soil-peat mixtures*, Soil Science Society of America Journal **64** (2000), 827.
- [31] R. G. Lerner and G. L. Trigg, *Encyclopedia of physics*, Second ed., 1991.
- [32] J. Hoshen and R. Kopelman, *Percolation and cluster distribution, cluster multiple labelling technique and critical concentration algorithm*, Physical Review B **14** (1976), 3438.
- [33] G. Deutscher, R. Zallen, and J. Adler, *Percolation structures and processes*, Annals of the Israël Physical Society, Jerusalem, 1983.
- [34] A. Coniglio, H.E. Stanley, and W. Klein, *Solvent effects on polymer gels: A statistical-mechanical model*, Physical Review B **11** (1982), 6805.
- [35] A. Y. Tretyakov and N. Inui, *Critical behaviour for fixed site-bond directed percolation*, Journal of Physics A: Mathematical and General **28** (1995), 3985.
- [36] F. di Liberto, G. Monroy, and C. Palmieri, *Site-bond correlated percolation in a ferromagnetic and antiferromagnetic lattice gas: the Bethe cluster approximation*, Journal of Physics A: Mathematical and General **16** (1982), 405.
- [37] A. Coniglio, H.E. Stanley, and W. Klein, *Site-bond correlated percolation problem: A statistical mechanical model of polymer gelation*, Physical Review Letters **42** (1979), 518.
- [38] E.D. Gado, L. de Arcangelis, and A. Coniglio, *A percolation dynamic approach to the sol-gel transition*, Journal of Physics A: Mathematical and General **31** (1998), 1901.
- [39] A. J. Guttmann and S. G. Whittington, *Real space renormalisation group study of bond-site percolation on an anisotropic triangular lattice*, Journal of Physics A: Mathematical and General **15** (1981), 2267.

- [40] H. M. Harreis and W. Bauer, *Phase transitions in two-component site-bond percolation model*, Physical Review B **62** (2000), 8719.
- [41] F. Mandl, *Statistical physics*, Second ed., Wiley & Sons, New York, 1988.
- [42] M.E.J. Newman and R.M. Ziff, *Fast Monte Carlo algorithm for site or bond percolation*, Physical Review E **64** (2001), 016706.
- [43] P. R. A. Campos and R. N. Onody, *Single-cluster algorithm for the site-bond correlated Ising model*, Physical Review B **52** (1997), 14529.
- [44] S. Redner and A. Coniglio, *Flory theory for directed lattice animals and directed percolation*, Journal of Physics A: Mathematical and General **15** (1982), L273.
- [45] C. Tsallis and S. Redner, *New approach for multicriticality in directed and diode percolation*, Physical Review B **28** (1983), 6603.
- [46] P. Grassberg, *Directed percolation in 2 + 1 dimensions*, Journal of Physics A: Mathematical and General **22** (1989), 3673.
- [47] A. Chame, S.L.A. de Queiroz, and R.R. dos Santos, *Finite-size scaling for directed bond percolation with and without cycles on a triangular lattice*, Journal of Physics A: Mathematical and General **19** (1986), L527.
- [48] Y. Pomeau, *Front motion, metastability and subcritical bifurcations in hydrodynamics*, Physica D **23** (1986), 3.
- [49] P. Rupp, R. Richter, and I. Rehberg, *Critical exponents of directed percolation measured in spatiotemporal intermittency*, Physical Review E **67** (2003), 036209.
- [50] T. Ohtsuki and T. Keyes, *Biased percolation: forest fires with wind*, Journal of Physics A: Mathematical and General **19** (1986), L281.

- [51] I. Jensen, *Low-density series expansions for directed percolation on square and triangular lattices*, Journal of Physics A: Mathematical and General **29** (1996), 7013.
- [52] Z. Gingl, C. Pennetta, L.B. Kiss, and L. Reggiani, *Biased percolation and abrupt failure of electronic devices*, Semiconductor Science and Technology **11** (1996), 1770.
- [53] T. C. Li and Z. Q. Zhang, *A long-range Domany-Kinzel model of directed percolation*, Journal of Physics A: Mathematical and General **16** (1983), L401.
- [54] C. C. Chen, H. Park, and M. den Nijs, *Active width at a slanted active boundary in directed percolation*, Physical Review E **60** (1999), 2496.
- [55] G. Pruessner and O. Peters, *Self-organized criticality and absorbing states: Lessons from the Ising model*, Physical Review E **73(2)** (2006), 025106.
- [56] D. Wilkinson and J. F. Willemsen, *Invasion percolation: a new form of the percolation theory*, Journal of Physics A: Mathematical and General **16** (1983), 3365.
- [57] M. Porto, S. Havlin, S. Schwarzer, and A. Bunde, *Optimal path in strong disorder and shortest path in invasion percolation with trapping*, Physical Review Letters **79** (1997), 4060.
- [58] T. J. Perham, D. C. Chrzan, and L. C. De Jonghe, *Invasion percolation model of co-interpenetrating ceramic-metal composites*, Modelling and Simulation in Materials Science and Engineering **10** (2002), 103.
- [59] M. Cieplak, A. Maritan, and J. R. Banavar, *Optimal paths and domain walls in strong disorder limit*, Physical Review Letters **72** (1994), 2320.

- [60] A. P. Sheppard, M. A. Knacksted, W. V. Pinczewski, and M. Sahimi, *Invasion percolation: new algorithms and universality classes*, Journal of Physics A: Mathematical and General **32** (1999), L521.
- [61] M. Cieplak, A. Maritan, and J. R. Banavar, *Invasion percolation and Eden growth: geometry and universality*, Physical Review Letters **76** (1996), 3754.
- [62] L. Nduwayo, *Computational studies of percolation: Determination of the cluster number scaling function for lattices in 2 dimensions*, Master's thesis, School of Chemical and Physical Science, University of Natal, Pietermaritzburg, South Africa, 2002.
- [63] H. Nakanishi and H. E. Stanley, *Scaling studies of percolation phenomena in systems of dimensionality two to seven: cluster numbers*, Physics Review B **22** (1980), 2466.
- [64] M. E. J. Newman and R. M. Ziff, *Efficient Monte Carlo algorithm and high-precision for percolation*, Physical Review Letters **85** (2000), 4104.
- [65] W. Klein, H. E. Stanley, S. Redner, and P.J. Reynolds, *Exact solution of one-dimensional percolation problem with further neighbor bonds*, Journal of Physics A: Mathematical and General **11** (1978), L17.
- [66] M. F. Sykes and J. W. Essam, *Critical percolation probabilities by series methods*, Physical Review **133** (1964), A310.
- [67] K. De Bell and J. W. Essam, *Directed percolation: mean field theory and series expansions for some two-dimensional lattices*, Journal of Physics A: Mathematical and General **16** (1983), 385.
- [68] A. Margolina, H. Nakanishi, D. Stauffer, and H. E. Stanley, *Monte Carlo and*

- series study of corrections to scaling in two-dimensional percolation*, Journal of Physics A: Mathematical and General **17** (1984), 1683.
- [69] J. P. Hovi and A. Aharony, *Renormalization group calculation of distribution functions: Structure properties for percolation clusters*, Physics Review E **56** (1997), 172.
- [70] D. Stauffer and A. Aharony, *Introduction to percolation theory*, Second ed., Taylor & Francis, London, 1994.
- [71] G. Grimmett, *Percolation*, Second ed., Springer, Berlin, 1999.
- [72] Academic Press, *Dictionary of physics*, 2004.
- [73] D.F. Groebner, P. W. Shannon, P. C. Fry, and K. D. Smith, *Business: A Decision-Making Approach*, 5th ed., Pentice Hall, New Jersey, 2001.
- [74] Y.Y. Tarasevich and S. C. van der Marck, *An investigation of site-bond percolation on many lattices*, International Journal of Modern Physics C **10** (1999), 1193.
- [75] R. M. Ziff and B. Sapoval, *The efficient determination of the percolation threshold by a frontier generating walk in a gradient*, Journal of Physics A: Mathematical and General **19** (1986), L1169.
- [76] [http://www.answers.com/topic/steric factor](http://www.answers.com/topic/steric-factor).
- [77] S. Chatterjee, S. D. Choudhury, S. Basu, N. Ghosh, and Chakrabarty, *Influence of steric factor on exciplex energy and magnetic field effect*, Spectrochimica Acta Part A, Molecular and Biomolecular Spectroscopy **60** (2004), 97.
- [78] D. Stauffer and A. Aharony, *Universality at the three-dimensional percolation threshold*, Journal of Physics A: Mathematical and General **27** (1994), L475.

[79] R. M. Ziff, S. R. Finch, and V. S. Adamchick, *Universality of finite size corrections to the number of critical percolation clusters*, Physical Review Letters **79** (1997), 3447.

[80] N. J. Giordano, *Computational Physics*, Pentice Hall, New Jersey, 1997.

Résumé

Born at Kiyange, Burundi in November 12, 1961, I graduated from high school in 1980 and entered directly into the University of Burundi, where I graduated with a Bachelor of Science degree in Physics (Licencié en Sciences Physiques) in September 1985.

From that period until June 1994, I was employed by the Burundi Government as a high school teacher of Mathematics and Physics, later as the headmaster of a high school, and then as a pedagogical adviser to the National Curriculum Development Office for high schools (Bureau d'Etudes et des Programmes de l'Enseignement Secondaire – BEPES). In 1990-1991, I was on service training at Leuven Catholic University (Louvain-La-Neuve) in Belgium. In June 1994, I was appointed by the University of Burundi as an assistant lecturer.

Since August 2000, I have been a postgraduate physics student at the University of KwaZulu-Natal - Pietermaritzburg, South Africa. I graduated with a Master's degree with distinction in April 2003. As a senior demonstrator and tutor, I was at various times in charge of physics practical classes in the Science Foundation Program and the first year physics laboratories.

June, 2007

Léonard NDUWAYO

Summary in French

Le présent travail est une extension d'une recherche entamée dans le cadre d'un doctorat. Cette recherche est du ressort de la physique statistique. Elle s'appuie sur la simulation sur ordinateur des aspects de la théorie de percolation en exploitant une argumentation probabilistique. Cette théorie illustre parfaitement des phénomènes transitoires présentant une criticalité. Une étude a été menée sur la théorie de percolation sur des réseaux réguliers en vue de déterminer la fonction pondérée du nombre d'amas par site ou lien du réseau. Cette détermination numérique a été accompagnée par le calcul des exposants critiques liés à cette fonction.

Les valeurs seuils obtenues pour les probabilités d'occupation des sites et d'ouverture des liens sont proches de celles connues de la littérature scientifique. Indépendamment de la nature du réseau utilisé et bien que la percolation de sites et celle des liens soient différentes, la fonction pondérée du nombre d'amas par site ou lien du réseau affiche un caractère universel dans les limites d'une simulation numérique recourant à l'usage des méthodes de Monté Carlo.

Cette seconde phase a consisté à étudier sur un réseau donné la percolation des liens tout en tenant compte de l'état des sites. Un site se trouve dans l'une des deux situations: il est vide ou occupé. De même, un lien est fermé ou ouvert. Cette considération conduit à la notion d'amas et de la connectivité des sites. Ainsi, un

amas est un ensemble de sites occupés connectés par des liens ouverts. Il possède un nombre donné de sites occupés et de liens ouverts. La connectivité est liée au fait que deux plus proches sites sont connectés ou rattachés si ils sont d'abord occupés et ensuite reliés par un lien ouvert.

Aux probabilités d'ouverture et d'occupation des liens et des sites, on associe les valeurs p_b et p_s . La taille d'un amas, aussi appelée sa masse, est définie en termes du nombre de sites occupés et de liens ouverts que cet amas contient.

Pour différents modèles étudiés, on a déterminé des grandeurs liées à la structure globale des amas (telles sont la taille moyenne et la longueur de corrélation) et aux amas individuels (comme le rayon de giration et la taille d'un amas) en se référant systématiquement aux sites et aux liens. Ici un lien est considéré comme un point qui est milieu des extrémités de ce lien. L'usage d'une relation de dépendance de p_b vis-à-vis de p_s (exprimée en termes des paramètres α , β et γ aux chapitres 4 et 5) affecte la structure non seulement des grandeurs calculées mais aussi les valeurs seuils de percolation. Ces valeurs seuils sont localisées sur une courbe critique partageant le plan (p_s, p_b) en deux régions : l'une pour la percolation et l'autre pour la non percolation.